

M.A.ILGAMOV

**STATIC PROBLEMS
OF HYDROELASTICITY**



Moscow
Nauka. Fizmatlit
1998

UDK 539.3
BBK 22.251
I 45



*The publication was supported by the
Russian Foundation of Basic Research
Grant 98-01-14013*

ILGAMOV M.A. Static Problems of Hydroelasticity. — Moscow:
Nauka. Fizmatlit, 1998. — 208 p. — ISBN 5-02-015122-X

The formulation of the static problems of hydroelasticity is based on hydrostatics and the static theory of elasticity, the strength of materials, and plate and shell theory. The greatest interest is the interaction of a fluid with thin-walled structures such as a rod, membrane, plate, or shell. In the listed order, the equilibrium and deformation of various elastic thin-walled elements under the action of fluid forces is considered in this book.

The book is intended for the specialists dealing with the problems on strength of construction elements, and the reliable functioning of separate assemblies of machinery and devices. It may also be used by students for the comprehensive study of certain questions in courses on engineering subjects.

Il. 106. Tabl. 1. Bibl. 72.

TP-98. Without announcement

ISBN 5-02-015122-X

© M.A.Ilgamov, 1998

PREFACE

The book is devoted to problems in which the interaction between an elastic solid and an incompressible fluid plays an essential role, both media being considered at rest.

The formulation of the static problems of hydroelasticity is based on hydrostatics and the static theory of elasticity, the strength of materials, and plate and shell theory. The greatest interest is the interaction of a fluid with thin-walled structures such as a rod, membrane, plate, or shell. In the listed order, the equilibrium and deformation of various elastic thin-walled elements under the action of fluid forces is considered in this book.

In the introduction, the statement of static problems of interaction is given, and some information from hydrostatics necessary for later use is presented. Several examples are noted in which the effect of two-media interaction leads to qualitatively new results.

The first chapter includes characteristic problems concerning a vertically placed thin rod and a thin-walled tube. The axial and lateral forces resulting from the action of their own weight and a hydrostatic force are determined. The stability of the elastic element is considered.

The second chapter is devoted to the consideration of elastic membrane behaviour. The membrane may be the bottom of a cavity or it may cover a container with fluid. The cases of a circular cavity and a cavity extended in one direction are considered.

In the third chapter, bending and stability of a plate contacting a fluid are considered under the action of different forces. In all these three chapters, problems are mainly stated and solved in a linear approximation.

Nonlinear problems of bending of a plate and buckling of shallow cylindrical panels under the hydrostatic pressure are studied in the fourth chapter. To simplify the analysis, the models of plane deformation for a plate or panel and consistent fluid behaviour are taken.

The fifth and sixth chapters are devoted to the consideration of equilibrium of a membrane shell and a film in the presence of fluid forces. Out of the wide range of possible problems, results concerning two problems are presented here. They deal with the soft containers for storing and transportation of fluids and displacing equipment. These problems are essentially nonlinear.

The references are given separately for each chapter. The list of literature is not complete, but is representative.

The statement and solution of some of the problems presented here have been known previously. Other problems are described for the first time. Their choice has been made according to the author's scientific interests and his knowledge of the extensive literature. Preference has been given to problems with simple and clear solutions. That is why some problems are mainly of a model character. They may be used for the simplest presentation of the principal features of hydroelastic systems, namely, the dependence of hydrodynamic forces, acting on deformable body, on the body deformations themselves. Because of this choice, the main direction of the book is related to the analytical solutions of boundary value problems. Results of numerical simulation are rarely used.

Different chapters and paragraphs are written in different styles. Those problems which have relatively simple mathematical representation, are discussed quite comprehensively. As for problems complicated to calculate, their formulation and results of practical importance are mainly given. In doing so, attention is drawn to the dependences of system behaviour, of forces arising

in the system, on the mass properties of media, dimensions and other input parameters. Essential problem features are pointed out. If necessary, the details of solution may be found in the original references.

The book is intended for the specialists dealing with the problems on strength of construction elements, and the reliable functioning of separate assemblies of machinery and devices. It may also be used by students for the comprehensive study of certain questions in courses on strength of materials, hydrostatics, plate and shell theory.

The author is obliged to doctor A.A.Aganin for his help in translation and L.B.Gaseeva for her assistance in preparing the manuscript. Prof. M.S.Ganeeva and Prof. V.I.Usyukin have introduced many suggestions for improving the arrangement of the material. The author gratefully acknowledges Prof. Earl H. Dowell, Dean of the School of Engineering at Duke University, for his close support while editing and issuing the book. Without his generous participation the publication of the book would not have been possible.

The research described in this publication was made possible in part by Grant No RH4000 from the International Science Foundation and by Grant No 93-013-17940 from the Russian Foundation of Basic Research.

CONTENTS

Static Problems of Hydroelasticity

INTRODUCTION	1
------------------------	---

CHAPTER I

EQUILIBRIUM OF A THIN ROD AND TUBE IN LIQUID

§1. Equilibrium of a vertical rod in a liquid	10
§2. Stability of the vertical position of a rod in a liquid	15
§3. Some general features of problem of stability of vertical rod	20
§4. Two special cases of load	23
§5. Stability of rod under various fastening conditions. Mine shaft	27
§6. Stability of vertical pipe with liquid. Buckling of pipe in tension	31
§7. Stability of drilling and producing oil column tubes	37
§8. Stability of pipes fastened on movable supports	44

CHAPTER II

EQUILIBRIUM OF A MEMBRANE CONTACTING A LIQUID

§1. Linear theory of equilibrium of a membrane under liquid weight	48
§2. Nonlinear theory of the equilibrium of a membrane under a liquid layer	53
§3. The circular membrane under hydrostatic load	56
§4. Interaction of membrane with liquid in closed vessel	59
§5. Stability of membrane between liquids of different density	63
§6. Determination of membrane deflection in stability problem	67
§7. Nonlinear deflection of membrane under concentrated action	71

CHAPTER III

EQUILIBRIUM OF A PLATE CONTACTING A LIQUID

§ 1. Bending of a beam resting on a water surface	75
§ 2. Bending of a circular plate under liquid weight	78
§ 3. Bending of a circular plate covering cavity with liquid	81
§ 4. Hertz's problem of a floating plate	83
§ 5. Bending of a circular plate under concentrated load	88
§ 6. Circular plate under the action of a noncentral concentrated load	93
§ 7. Cylindrical bending of a vertical plate contacting a liquid of limited volume	97
§ 8. Stability of a vertical plate in a liquid	101
§ 9. Influence of medium compressibility on plate bending	105
§ 10. Influence of medium compressibility on plate stability	110

CHAPTER IV

SOME EXAMPLES OF NONLINEAR PROBLEMS

§ 1. Flexible plate on liquid surface under load distributed along line	114
§ 2. Cylindrical panel under the action of a load distributed along line	120
§ 3. Cylindrical shell in a liquid under load distributed along a line	126
§ 4. Stability of a shallow panel under a liquid layer	131
§ 5. Stability of a cylindrical panel loaded by pressure of a compressible fluid .	143
§ 6. Appendix. Rigid cylindrical shell being in liquid or containing liquid .	151

CHAPTER V

EQUILIBRIUM OF MEMBRANE SHELLS CONTACTING
LIQUIDS IN CONTAINERS

§ 1. A long cylindrical shell containing liquid	156
§ 2. Volume of liquid in a rectangular cushion-shaped container	161
§ 3. Equilibrium of a cylindrical shell under total hydrostatic pressure	164
§ 4. Analysis of partitions separating compartments with liquid	168

§5. Freely lying containers	171
§6. Insertable vessel containers	174
§7. Soft floating containers	177
§8. Containers for load lifting	180

CHAPTER VI

EQUILIBRIUM OF FILMS CONTACTING A LIQUID IN DISPLACING DEVICES

§1. Plane problem of film equilibrium	186
§2. Equilibrium of a spherical and semispherical film	191
§3. Equilibrium of a cylindrical film	196
§4. Finite strains of a membrane	198

CONCLUSION	201
----------------------	-----

REFERENCES	203
----------------------	-----

INTRODUCTION

The problems of aerohydroelasticity may be divided into dynamics and statics. In the first, both interacting media are subjected to changes in time. The transition process (for example, response of structure in fluid to incident shock wave), the steady motion (oscillations with constant amplitude and period etc.) are considered. Such a well known aeroelastic phenomenon as flutter of a lifting thin surface (wing, blade) in fluid flow belongs to the first class while divergence of the same system falls to the second one. In the simplest static problems, it is assumed that both media are at rest.

Overwhelming majority of original investigations, reviews and monographs are devoted to dynamic problems, which can be explained by their great practical significance and complexity in analysis of the physical processes under consideration. Since the appearance of the first substantial publications e.g. [1,2], which have already become classical, several dozens of monographs and reviews have been published on various problems. They also touch upon static problems with steady fluid flow. A brief review and quite complete list of monographs are given in the books [3-5].

With respect to the classical problems for both interacting media at rest, there are no previous texts on the subject. To some extent this work fills the gap. But it does not pretend to cover the subject completely.

It should be noted that the absence of such books does not indicate that the static problems of hydroelasticity are of little importance. First, analysis of equilibrium of hydroelastic system is a component part of total structure analysis. Secondly, statics calculations are of great independent significance. Long before

the appearance of constructions in which hydroelastic effects were essential (air and water transport, various reactors and tubing systems, sensors in instruments etc.), there had been objects in which static interaction of a structure with a fluid medium was the most substantial factor. The origin and application of some of these has been lost with time. Perhaps the first objects were the closed shells made out of skin and hollow organs of animals. They were used for storing fluids (wineskin) and flotation (balloons, pneumatic rafts). The subsequent development of weaving introduced air balloons, pneumatic boats, etc.

More recently it became possible to use new hydroelastic devices due to the appearance of modern synthetic tissues and films possessing large strength. These include a pneumatic cylindrical shell (airbeam), pneumatic structures, air supporting building constructions (domes of sport and storage buildings with large bays), ship's containers for transportation of fluid cargo, displacing equipment in aerospace engineering and many other objects.

Another reason has been the development of new energy technologies. For example, sea-oil extraction is related to building and exploitation of various platforms, as well as vertical boring and extracting tubes. Many hundred meters long, these tubes even in a stretched state may be subjected to undesirable longitudinal bending. For their proper strength and reliability analysis the fluid inside the tube and the water surrounding it should necessarily be taken into account.

The general statement of the fluid-structure interaction problem includes a choice of model of motion or equilibrium of the deformable solid and liquid (gas) and formulation of conditions on their contact surface.

To describe the behaviour of a deformable body, we shall use the equations of the bending theory of rods, membranes, plates and shells based on the hypotheses valid for the case of a small thickness as compared to the length and radius. The choice of the

corresponding equations and conditions of fastening will be determined by the physical statement of a problem.

Fluid is considered to be inviscid. Standard assumptions of hydrostatics are taken. Their brief representation is given below.

Slow fluid deformation without change in volume may be caused by action of some small force. In a gravitational field, the fluid takes the shape of the vessel. Its free surface is perpendicular to the direction of the gravitational force. In communicating vessels the liquid if homogeneous in density is set to the same level.

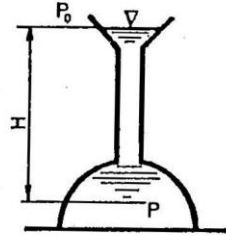


Fig. 0.1. Hydrostatic pressure is independent of vessel shape

Pressure in a liquid does not depend on the orientation of the area under consideration and acts equally in all directions (Pascal's law).

In a gravitational field, pressure in the fluid increases with the depth of submergence due to the liquid weight itself. If the fluid is incompressible, the total pressure p (hydrostatic pressure) consists of pressure p_0 on the fluid surface and weight of fluid column (of height H , Fig. 0.1) with density ρ , and free fall acceleration g

$$p = p_0 + \rho g H. \quad (0.1)$$

Pressure force $\rho g H S$ acting on the bottom of a volume with the area S does not generally coincide with the weight of fluid contained in the volume. If the height H is the same for the volumes of different shape but with the equal bottom area S (Fig. 0.2), then, in spite of the difference in weight, the pressure force on the bottom is the same for any volume and is equal to the weight of the liquid in cylindrical vessel. This "hydrostatic paradox" is due to the fact that the fluid pressure force on inclined walls has a

vertical component with the upward and downward direction depending on the orientation of wall element.

In the general case, equal pressure p_0 over all the volume results from the fact that the volume is subjected to the action of external forces. For the example in Fig. 0.3, we have $p_0 = P/S$. But the pressure can not always be determined so easily. In the

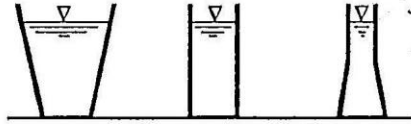


Fig. 0.2. "Hydrostatic paradox" – pressure force on the bottom of a vessel is independent of the shape of the vessel

case of loading of a flexible plate with freely slipping edges (without separation) along the vessel wall (Fig. 0.4a) it is again equal to the same value P/S , whereas for the case of the edges clamped in the wall (Fig. 0.4b) it may be found only by solving the corresponding problem of plate bending.

In fact, the first example does not belong to hydroelasticity, because the problems of hydrostatics and elasticity are decoupled here (when the value of ρgH is small as compared with p_0). This may be valid for the small size of a vessel along the vertical and in some other cases. Parameters of plate bending are determined from the known values P and p_0 . The second example leads to a coupled hydroelastic problem. Only the uniform distribution of pressure p_0 can be known beforehand. It should be noted that the necessity of taking into account of p_0 always arises in the case of closed cavities totally filled with fluid.

In a fluid, a body with the volume V is subjected to a buo-

yancy force P , directed upwards and equal to the weight of fluid displaced by the body (Archimede's law).

$$P = \rho g V. \quad (0.2)$$

It is independent of the body submergence depth. Mass center of a uniform body (the center of displacement) is taken as the load

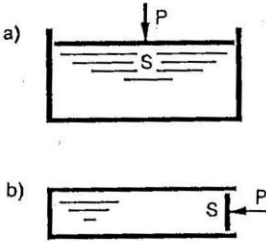


Fig. 0.3. Rigid piston freely slipping along the vessel walls

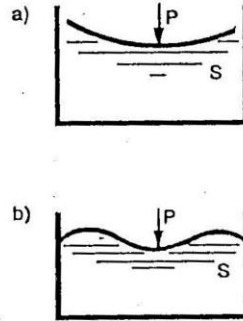


Fig. 0.4. Flexible plate with freely slipping (a) and fixed (b) edges

point. When the body is not uniform the point does not coincide with the mass center of its submerged part. If for the total submergence of the body the buoyancy force is greater than its weight, the body only partly submerges into the fluid. Clearly, in equilibrium, the point of buoyancy force application and body mass center are located on the same vertical line.

Let the deformable body A be bounded by a contour Γ (Fig. 0.5). According to the assumption of an incompressible fluid, the normal displacement ω of Γ and liquid surface deflection h after deformation will be related by

$$\int_{\Gamma} \omega d\Gamma = \int_{\Gamma_0} h d\Gamma_0. \quad (0.3)$$

Here the kinematic condition for the equality of the normal deflections of elastic body and liquid has already been taken into account. Static condition for pressure equality on contact surface should also be satisfied.

If even only one dimension of the volume occupied by fluid is of order 1cm, it is equally important to take into account gravity and surface tension forces. In the case of large dimensions, the gravitational effects dominate while capillary ones become predominant when the dimensions are small. The same estimations are valid for the dimensions of a rigid body contacting fluid.

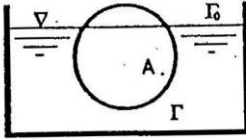


Fig. 0.5. Elastic body *A* partly submerged into incompressible fluid

In this book, no consideration is given to the problems in which surface tension forces have to be taken into account.

In what follows we shall also use the notion of specific weight $\gamma = \rho g$. In the general case we also introduce into consideration the overload factor n and the gravitational field vector \bar{g} . Then $\bar{\gamma} = n\rho\bar{g}$. What was mentioned above together with relations (0.1)–(0.3) cover almost all the knowledge from hydroelasticity which will be necessary for further consideration. The particular related questions will be discussed below in connection with the formulation of concrete problems.

At first sight it may seem that the hydroelastic forces acting on an elastic element will not produce any effects leading to qualitatively differing results as compared with the case of prescribed "dead" load. But this is not always the case.

A metallic circular plate cannot float on the water surface. It goes down. But at certain values of the plate radius and load in its center it will be floating. Clearly, this phenomenon may be described only on the basis of hydroelasticity.

The value of the internal pressure in incompressible liquid seems to be unexpected in the problem shown above in Fig. 0.4*b*. Under some conditions one has $p_0 = 3P/S$ in the case of circular plate, i.e. the pressure is three times as much as in the problem of Fig. 0.4*a*. Hence, the plate is also subjected to the trebled pressure from below.

A vertical plate separating an incompressible fluid in a closed vessel and subjected to compression in the direction of the shorter part, loses stability of the plane shape forming two half waves. Under the usual conditions, only a one half wave is known to arise. Certainly, corresponding critical values of compressive loads will also be different.

The list of such examples may be continued. In more detail, we consider the following simple example. Let the bottom of a long vessel with the width $2L$ and height H be a membrane (Fig. 0.6*a*). The latter, being fastened to the walls ($x = \pm L$), is in tension with the initial strength T_0 . The vessel is filled up to its edges with fluid with the specific weight γ . The equation which describes the deflection w of a membrane from its plane position is known to have the form $T_0 d^2w/dx^2 + p_* = 0$, where p_* is the fluid pressure. The downward direction of w is taken to be positive.

Let H be approximately the height of the fluid column. Then the pressure will be known beforehand: $p_* = \gamma H$. The membrane weight is assumed neglected as compared with the γH .

Then the equation

$$d^2w/dx^2 = -\alpha^2 H \quad (\alpha^2 = \gamma/T_0) \quad (0.4)$$

has a solution

$$w = A + Bx - \alpha^2 H x^2/2.$$

Satisfying the boundary conditions $w = 0$ ($x = \pm L$), we find

$$\frac{w}{A} = \frac{\alpha^2 L^2}{2} \left(1 - \frac{x^2}{L^2} \right). \quad (0.5)$$

If we take into account the exact value of fluid column $A + w(x)$ then $p_* = \gamma(H + w)$ and, instead of (0.4) and (0.5), we shall have

$$d^2 w / dx^2 + \alpha^2 w = -\alpha^2 H, \quad (0.6)$$

$$\frac{w}{A} = \frac{\cos \alpha x}{\cos \alpha L} - 1. \quad (0.7)$$

For small values of αL as compared with unity, (0.5) may be derived from (0.7) by expanding the functions $\cos \alpha x$ and $\cos \alpha L$ into power series. Thus, for small values of αL , both solutions give the same result. Relative deflection of membrane is

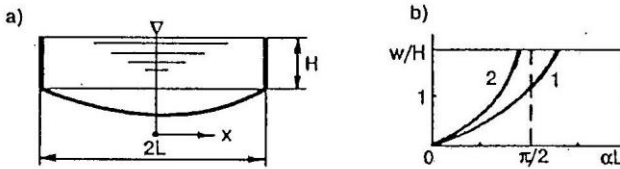


Fig. 0.6. a) Membrane under action of liquid weight. b) Relative membrane deflection versus the parameter $\alpha L = L\sqrt{\gamma/T_0}$

directly proportional to the specific weight of fluid and the square of membrane width and is inversely proportional to its tension ($\alpha^2 L^2 = \gamma L^2 / T_0$).

With increasing αL , the solution (0.5) remains formally valid whereas, according to (0.7), the solution increases indefinitely when $\alpha L \rightarrow \pi/2$ (the curves 1 and 2 in Fig. 0.6b correspond to the solution (0.5) and (0.7), respectively). For $\alpha L > \pi/2$ the deflection w becomes negative, but this does not correlate with the real physical phenomenon. For its proper description the model

of membrane deformation should be changed. This question is considered later in the relevant section of the book.

For $H = 0$ and for finite values of αL , expressions (0.4), (0.5) give $w = 0$. In this solution there is a membrane deflection from the plane form and there is no liquid over the membrane. But (0.6), (0.7) together with the boundary conditions $w = 0$ ($x = \pm L$) become an eigenvalue problem. Nonzero solution for w (when $H = 0$) exists for $\cos \alpha L = 0$, that is when $\alpha L = n\pi/2$ ($n=1,3,\dots$). So, when $\alpha L = \pi/2$ (or $\gamma L^2/T_0 = \pi^2/4$) the equilibrium state of fluid meniscus over membrane is possible together with membrane deflection for $H = 0$.

Thus, this example also demonstrates the possibility of qualitative differences of solutions for one and the same problem formulated with or without taking into account the interaction of the media.

The property of compressibility of fluids has an appreciable effect on the process of their interaction with elastic elements, especially when the medium is compressed in closed cavity. Let there be initially in the volume V_0 a weightless fluid with the mass M_0 , density $\rho_0 = M_0/V_0$ and pressure p_0 . After boundary deformations and mass inflow (outflow) these parameters become equal to V , M , $\rho = M/V$ and p , respectively. Then

$$p/p_0 = (\rho/\rho_0)^\kappa. \quad (0.8)$$

If the process of interaction goes on isothermally (at constant temperature due to the heat removal), $\kappa = 1$. In the adiabatic process (without the heat removal) $\kappa = 1.4$ for gases and $\kappa \approx 7$ for liquids. Some other relations between these parameters are also used for liquids.

CHAPTER I

EQUILIBRIUM OF A THIN ROD AND TUBE IN A LIQUID

§1. Equilibrium of a vertical rod in a liquid

A thin elastic rod with ball tip is at rest in a liquid in a vertical position. On the fluid surface there is a rigid plate with a hole in which the upper end of the rod is clamped (Fig. 1.1*a*). We shall examine the axial forces in the rod when it is in an exactly vertical position, as a function of the size of the rod and ball as well as of specific weight of the rod γ_0 , ball γ_1 and liquid γ .

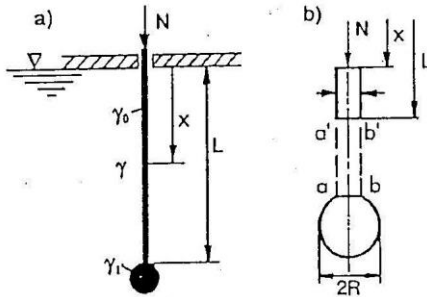


Fig. 1.1. The rod with ball tip lowered into the fluid; γ_0 , γ_1 , γ are the specific weights of material of the rod, ball and liquid, respectively

We assume that the ball radius R is small in comparison with the rod length L , the cross-section radius of which is r . The ball is supposed to be rigid.

Weight of the ball and the rod element $(L-x)$ is equal to $(4/3)\pi R^3 \gamma_1 + \pi r^2(L-x)\gamma_0$. According to (0.2) the buoyancy force of the fluid on the ball, not attached to the rod over the area ab (Fig. 1.1, *b*), is equal to $(4/3)\pi R^3 \gamma$. In order to exclude in the system the effect of pressure on the area ab it is necessary to apply the same pressure, but with the opposite sign, on the rod section $a'b'$. Then the buoyancy force on the rod (without the ball) will be $\pi r^2 L \gamma$. Consequently, from the equilibrium condition the axial force N in the rod, with the x -coordinate calculated from the clamped end, is

$$N = \pi r^2 [\gamma L - \gamma_0(L-x)] + \frac{4}{3} \pi R^3 (\gamma - \gamma_1). \quad (1.1)$$

Positive values of N correspond here to the compression. The reaction force is found from (1.1) by setting $x=0$.

Consider some consequences from (1.1) as a function of specific weight and size of the rod and tip.

1. The inequality $N(x=L) < 0$ or

$$\gamma \left(1 + \frac{4R^3}{3r^2L} \right) < \gamma_1 \frac{4R^3}{3r^2L} \quad (1.2)$$

gives the condition under which the rod is stretched everywhere, maximum tension being near the support ($x=0$). When $R^3/r^2L \gg 1$ this condition reduces to the inequality $\gamma < \gamma_1$.

2. If the parameters of the problem fulfill the condition $N(x=0) > 0$ or

$$\gamma \left(1 + \frac{4R^3}{3r^2L} \right) > \gamma_0 + \gamma_1 \frac{4R^3}{3r^2L}, \quad (1.3)$$

the rod is compressed everywhere. The section near the tip

($x = L$) is subjected to the maximum compression. When $\gamma_0 = \gamma_1$, condition (1.3) is reduced to an obvious inequality $\gamma_0 > \gamma_1$. The same is true if $R^3/r^3L \ll 1$, and γ_1 is not much greater than γ_0 .

3. The case of stretched upper and compressed lower parts of the rod arises when the total weight of the rod with the tip is greater than the weight of displaced fluid and the weight of the ball is less than the weight of fluid displaced by the ball. This is the case if $\gamma_1 < \gamma$, $\gamma_0 > \gamma$. The boundary x_0 between these zones is determined by taking the force in (1.1) to be equal to zero. Then

$$x_0 = L - L_*, \quad L_* = L \frac{\gamma}{\gamma_0} + \frac{4R^3(\gamma - \gamma_1)}{3r^2\gamma_0} \quad (0 < L_* < L). \quad (1.4)$$

The stressed state is also strongly dependent on the geometric parameters L , r , R .

When the rod is compressed along all its length (the case 2) some force is necessary to apply to its upper end (if the rod can be moved in the hole without friction) in order to confine it in fluid. Under conditions 2 and 3 the rod is in equilibrium and does not move downward only if its upper end is held. For the latter condition the upper part of the rod is in tension while the lower one is compressed.

The analysis given above may be simplified if there is no ball tip (or if $R \leq r$). According to the assumption of r to be small as compared with L , (1.1) reduces to the expression

$$N = \pi r^2 [\gamma L - \gamma_0(L - x)].$$

This means that only second and third states are possible. Either there is compression along all the length ($\gamma > \gamma_0$) or we have partial compression and tension ($\gamma < \gamma_0$). In both cases the

compression force has its maximum at the lower end and the tension force at the support.

Now consider the values of L_* for the typical densities. For an aluminum rod with radius $r = 1.5 \cdot 10^{-3}$ m ($\gamma_0 = g\rho_0 = 2.7$ g kg/(m²s²)), plastic tip with radius $R = 10^{-2}$ m ($\gamma_1 = g\rho_1 = 0.5$ g kg/(m²s²)) and water ($\gamma = g\rho = 1$ g kg/(m²s²)), it follows from (1.4) that $L_* = (0.37L + 0.11)$ m. The lower part of the rod with the length L_* is compressed while the upper one with the length $x_0 = (0.63L - 0.11)$ m is stretched.

If mercury with specific weight $\gamma = 13.55$ g kg/(m²s²) is chosen instead of water the value of L_* becomes equal to $(5L + 2.86)$ m. Consequently, independently of the length L , there is only compression force in the rod. This also results from the condition $\gamma > \gamma_0$ mentioned above. Note that the size of the compression and tension zones are not affected by acceleration g . Different overloads lead to corresponding changes in forces in a rod.

In the case of a hollow ball and rod (tube) the influence of fluid density increases in comparison with the examples considered above. Assume that there is no liquid inside (Fig. 1.2a).

If the wall thickness h is small as compared with radii R and r ($R = R_0 + h$, $r = r_0 + h$, $h \ll R$, $h \ll r$), then instead of (1.1) we have

$$\begin{aligned} N &= \pi r^2 L \gamma - \pi (r^2 - r_0^2) (L - x) \gamma_0 + \\ &+ \frac{4}{3} \pi R^3 \gamma - \frac{4}{3} \pi (R^3 - R_0^3) \gamma_1 = \\ &= \pi r [r L \gamma - 2h(L - x) \gamma_0] + \frac{4}{3} \pi R^2 (R \gamma - 3h \gamma_1). \end{aligned} \quad (1.5)$$

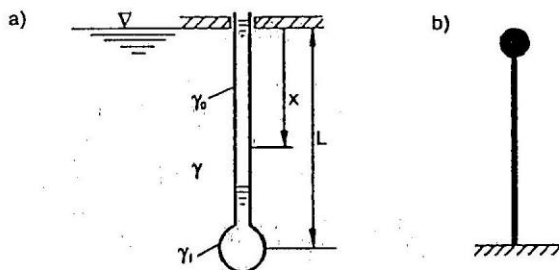


Fig. 1.2. a) The hollow rod and spherical ball in fluid. b) The column under own weight

All the discussion above can be fully transferred, with some small changes, to the system directed upwards (Fig. 1.2b). It may be a bearing column, support of a sea construction, a rubber ball filled with a light gas and held by a thread, etc.

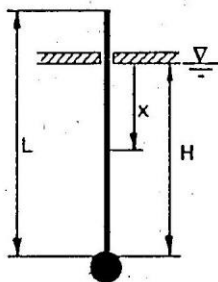


Fig. 1.3. A rod freely slipping in the orifice of the plate

If we assume that there is no friction between the rod and the orifice of the plate, and that the length L is greater than the submergence depth H (Fig. 1.3), then the expression for the force will have, instead of (1.1), the following form

$$N = \pi r^2 [\gamma H - \gamma_0 (H - x)] + \frac{4}{3} \pi R^3 (\gamma - \gamma_1). \quad (1.6)$$

The force N is only compressive. The value H is determined from the condition of equilibrium of the whole system

$$H = L \frac{\gamma_0}{\gamma} - \frac{4R^3 (\gamma - \gamma_1)}{3r^2 \gamma} \quad (H \leq L). \quad (1.7)$$

For $R \leq r$ and $r \ll L$ it follows from (1.7) that $H/L = \gamma_0/\gamma$. The submerged depth of the rod is to its length as the specific

weight of the rod to that of the fluid.

Substituting (1.7) into (1.6), we have

$$N = \pi r^2 \left[\gamma_0 L \left(1 - \frac{\gamma_0}{\gamma} + \frac{x}{L} \right) - \frac{4R^3(\gamma - \gamma_1)}{3r^2} \left(1 - \frac{\gamma_0}{\gamma} \right) \right] + \frac{4}{3} R^3 (\gamma - \gamma_1). \quad (1.8)$$

When $R \leq r$ we obtain

$$N = \pi r^2 \gamma_0 L \left(1 - \frac{\gamma_0}{\gamma} + \frac{x}{L} \right).$$

Maximum compression is at $x = H$. Since now $H = L\gamma_0/\gamma$, it is equal to $N = \pi r^2 \gamma_0 L$. At the upper end of the rod $x = H - L$ and $N = 0$.

It is known that when the rod is stretched along its full length, the corresponding strains and displacements can be easily found. The case becomes more complicated if the rod is compressed. For certain system parameters, other equilibrium states are possible, namely the elastic line can deflect from a strictly vertical position. It causes the appearance of bending moments. This question will be considered in the following paragraphs.

§2. Stability of the vertical position of a rod in a liquid

To determine the conditions under which equilibrium states of a compressed rod with deflection from the vertical line are possible, we make some simplifying assumptions.

Suppose that the rod radius r is small as compared with the ball radius R , which, in turn, is assumed to be small in comparison with the rod length L ($L \gg R \gg r$). Because of this we consider L to be a distance from the ball center to the plate

(Fig. 1.4) and do not take into account the own weight of the rod and the action of the lifting force of fluid on the rod. In other words, we consider the case (1.3) along with additional condition $\gamma > \gamma_1$, $\Delta \ll 1$ where

$$\Delta = \frac{3}{4} \frac{L}{R} \left(\frac{r}{R} \right)^2 \left| \frac{\gamma - \gamma_0}{\gamma - \gamma_1} \right|. \quad (2.1)$$

Thus, the rod is subjected to the constant compression, along its length, by the end force equal to the difference between lifting force of the tip and its weight.

Assume the deflection from vertical line to be small. Conventional assumptions for considering the bending of a thin rod are taken. The depth of tip submergence will not be changed by such a bending. It will only lead to the appearance of some small angle between the elastic line at $x = L$ and weight forces and buoyancy forces of the liquid. Regarding the latter forces, the following remark should be made. Under deflection from the vertical and rotation of the ball in the plane of a figure, the resultant force of fluid pressure forms an angle with the vertical line. This angle

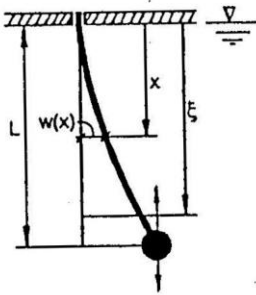


Fig. 1.4. Bent rod in fluid

depends on the relationship between constant and variable components of hydrostatic pressure (p_0 and γx). If there is only p_0 , it coincides with the angle of elastic line rotation dw/dx at the point $x = L$. Such a "tracing" force causes some difficulties in the investigation. The problem should be formulated as a dynamic one. Relevant questions are considered, for example, in the monograph [7]. In the given case it is necessary to pay attention to the lateral forces acting on the rod. Somewhat later we shall turn

back to this question. In the next paragraphs we take $p_0 = 0$. In doing so, the resultant $P = (4/3)\pi R^3(\gamma - \gamma_1)$, independently of axial line rotation $d\omega/dx$ ($x = L$), is directed along the vertical.

Thus, under assumptions mentioned above we come to the well-known Euler problem of rod stability. At the bearing cross-section, the deflection and rotation angles are zero:

$$\omega = d\omega/dx = 0, \quad (x = 0).$$

At the other end ($x = L$), the bending moment is zero, but the deflection is equal to some value W . These conditions are satisfied by the expression

$$\omega = W \left(1 - \cos \frac{\pi x}{2L} \right). \quad (2.2)$$

To continue our analysis we apply the strain energy method. Strain energy is known [21] to be related to the moment M as follows

$$U = \frac{1}{2EJ} \int_0^L M^2 dx, \quad (2.3)$$

where EJ is the bending stiffness. Bending moment of the elastic line from the concentrated force with respect to a point with coordinate x is

$$M = \frac{4}{3}\pi R^3(\gamma - \gamma_1)[\omega(L) - \omega(x)]. \quad (2.4)$$

Work A of the acting force is done on the axial deflection $u(L)$. With the assumptions taken above, it is related to the deflection ω by

$$u \approx \frac{1}{2} \int_0^L \left(\frac{d\omega}{dx} \right)^2 dx.$$

Therefore, we have

$$A = \frac{2}{3} \pi R^3 (\gamma - \gamma_1) \int_0^L \left(\frac{d\omega}{dx} \right)^2 dx. \quad (2.5)$$

The values of the parameters for which deflection of the rod from the vertical becomes possible, are determined by the equation [21]

$$U = A. \quad (2.6)$$

Substitution of (2.2) into (2.4) and (2.5) and the use of expressions (2.3) and (2.6) give the following critical value of the end force

$$P = \frac{4}{3} \pi R^3 (\gamma - \gamma_1) = \left(\frac{\pi}{2} \right)^2 \frac{EJ}{L^2}. \quad (2.7)$$

For the of rod of circular cross-section ($J = (\pi/4)r^4$) the critical difference between specific weights of fluid and tip materials is

$$\gamma - \gamma_1 = \frac{3\pi}{16} \frac{EJ}{R^3 L^2} = \frac{3\pi^2}{64} \frac{E}{R} \left(\frac{r}{R} \right)^2 \left(\frac{r}{L} \right)^2, \quad (2.8)$$

on exceeding which a new equilibrium state of the system, deflected from the vertical position, becomes possible.

For a tube-shaped section $J = (\pi/4)(r^4 - r_0^4)$. If the wall thickness is small so that we can take $h \ll r$ the mentioned critical value is

$$\gamma - \gamma_1 = \frac{3\pi^2}{16} \frac{E}{R} \frac{h}{L} \left(\frac{r}{R} \right)^3. \quad (2.9)$$

It is assumed here that there is no fluid in the inner space. Filling this space with fluid essentially changes the problem. This will be discussed further.

Now we consider the other critical case $\Delta \gg 1$ when the presence of the tip may be not taken into account. Changing signs of γ and γ_0 , we obtain the inverse system (Fig. 1.2*b*). Let $\gamma_0 \gg \gamma$. Therefore, the influence of the medium is not taken into consideration. This is a well-known stability problem of a column under its own weight [18, 19, 21, 22].

The solution can be presented by the series in which the first member is given by function (2.2), the next one is equal to $W_3(1 - \cos(3\pi x/2L))$, etc. The bending moment of elastic line from elementary force $(\pi r^2 d\xi)\gamma_0$ with respect to the point with coordinate x is

$$M = \pi r^2 \gamma_0 \int_x^L [\omega(\xi) - \omega(x)] d\xi. \quad (2.10)$$

Work of forces is

$$A = \pi r^2 \gamma_0 \int_0^L u(x) dx, \quad u(x) = \frac{1}{2} \int_0^x \left(\frac{d\omega(\xi)}{d\xi} \right)^2 d\xi. \quad (2.11)$$

From (2.10), (2.11), (2.3), (2.6) and taking into account the mentioned above, we obtain the critical value of the rod weight

$$\pi r^2 L \gamma_0 = 7.84 EJ/L^2. \quad (2.12)$$

It is important to note here the fast convergence of the series for ω . Taking only its first member (i.e. the function (2.2)) in (2.12), we obtain 7.89 in place of 7.84. The exact value of this factor is 7.83 [22]. Thus, the approximate value of the critical parameter somewhat exceeds the exact one. This is a distinguishing feature of the strain energy method used here. It is explained by the fact that, taking an approximate formula for elastic line, we impose some extra constraints on the system and, by doing so, we increase its rigidity.

ILGAMOV M.A. Static Problems of Hydroelasticity. — Moscow: Nauka. Fizmatlit, 1998. — 208 p. — ISBN 5-02-015122-X

§3. Some general features of problem of stability of vertical rod

We shall consider the stability of a vertical rod in a fluid under various fastening conditions on the basis of the buckling equation. Based on this equation, some general properties of rod stability problem will also be determined. We start from the usual assumption of the thin beam bending theory: the cross-section remains planar and its shape does not change. Changes in the length of the axial line are also neglected.

Fig. 1.5 presents an element of a deformed thin rod along with compression forces N , the own weight $F\gamma_0 dx$ and the resultant qdx of the fluid forces. To determine the latter, the Archimedes' law cannot be applied here in the form (0.2) because it is derived by summation of hydrostatic pressure over all the submerged surface of body. As a result of such a procedure, the buoyancy force of fluid does not depend on the shape of the body, on the depth of its submergence, and on the uniform pressure p_0 . Deformation of the body with its volume conservation does not

lead to any changes in the buoyancy force.

But the bending of the rod gives rise to the lateral force q acting on the rod (hydrostatic forces do not act on both cross-sections of the element). This is explained by the fact that, on buckling, a difference arises between areas of convex and concave sides of lateral surface of the rod as well as by the changes in hydrostatic pressure on rotating the element. These changes seem to be small as we consider small deformations and rotations. But in the given problem they should be taken into account [12, 15].

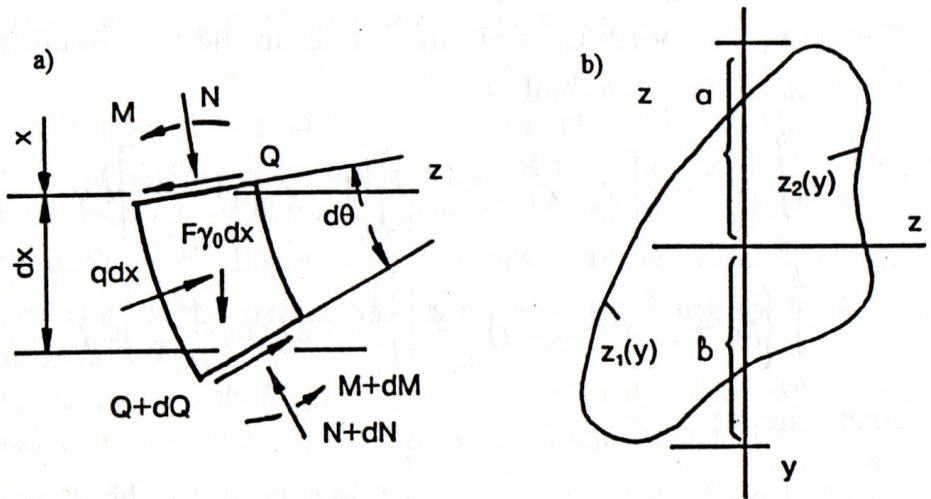


Fig. 1.5. a) Element of bent rod with length dx . b) Cross-section of rod of arbitrary shape

Let us put the origin of the axial coordinate x into the upper end of the rod. The bending takes place in the plane xz , the rod section rotates about axis y (the origin of coordinates y, z coincides with the gravity center of the section). For the sake of definiteness, we assume that the rod is borne by its lower end while the upper one may be in various conditions. Let the axial compression be $N = P + F\gamma_0 x$ where P is the vertical force applied to the upper end of the rod with cross-section area F .

From considering the equilibrium of the element in Fig. 1.5 we obtain the equation

$$-\frac{dQ}{dx} + \frac{d}{dx} \left(N \frac{dw}{dx} \right) - q = 0,$$

which, using equations $Q = dM/dx$, $M = -EJ d^2w/dx^2$, can be presented in the form

$$EJ \frac{d^4w}{dx^4} + \frac{d}{dx} \left[(P + F\gamma_0 x) \frac{dw}{dx} \right] = q. \quad (3.1)$$

Denoting the coordinates of lateral lines in the cross-section by $Z_1(y)$ and $Z_2(y)$, we shall have

$$q = \int_a^b \left\{ p_0 + \gamma \left[x - Z_1(y) \frac{dw}{dx} \right] \right\} \left[1 - Z_1(y) \frac{d^2w}{dx^2} \right] dy - \int_a^b \left\{ p_0 + \gamma \left[x - Z_2(y) \frac{dw}{dx} \right] \right\} \left[1 - Z_2(y) \frac{d^2w}{dx^2} \right] dy.$$

Using the integrals

$$\int_a^b [Z_2(y) - Z_1(y)] dy = F, \quad \int_a^b [Z_2^2(y) - Z_1^2(y)] dy = 0$$

we obtain

$$q = F(p_0 + \gamma x) \frac{d^2w}{dx^2} + F\gamma \frac{dw}{dx} = F \frac{d}{dx} \left[(p_0 + \gamma x) \frac{dw}{dx} \right]. \quad (3.2)$$

Thus, the distributed lateral force q on the rod from fluid depends on the curvature and slope of elastic line. Note that the rod, before deflection from the vertical, is subjected to only compression by a hydrostatic force on the end face and by its own weight, whereas the liquid does not have any influence on the lateral surface.

Using (3.2), the buckling equation can be written in the form

$$EJ \frac{d^4 w}{dx^4} + \frac{d}{dx} \left\{ [(P + F\gamma_0 x) - F(p_0 + \gamma x)] \frac{dw}{dx} \right\} = 0. \quad (3.3)$$

From equation (3.3) the following statement may be derived for the problem of stability of the rod. A rod under hydrostatic pressure bends with the same features as the rod without fluid action if the vertical end compressing force is presented in the form

$$P_e = P - Fp_0, \quad (3.4)$$

and the own weight of the rod is taken to be

$$\gamma_e = \gamma_0 - \gamma. \quad (3.5)$$

According to (3.4) and (3.5), the constant part of the pressure causes changes in the critical value of the end load P while its variable part in the critical value of the own weight of the rod of unit length $\gamma_0 F$. These critical values increase because the liquid acts on the lateral surface of the rod and, by doing so, leads to its stabilization.

For a tube with fluid inside these critical values significantly decrease because the sign of q in (3.2) should be changed. This corresponds to changing signs of p_0 and γ in (3.3)–(3.5) to the opposite ones. The behavior of the tube will be considered in the last paragraphs of this chapter. In the following two paragraphs we shall concentrate our attention on the problem stated above.

§4. Two special cases of load

Let us turn back to the problem of pillar stability under its own weight, considered at the end of § 2. It follows from (3.5) that the presence of surrounding fluid of depth L leads to changing the specific weight γ_0 in (2.12)–(2.14) to $\gamma_0 - \gamma$. For example, (2.12) will have the form

$$\pi r^2 L(\gamma_0 - \gamma) = 7.84 EJ/L^2. \quad (4.1)$$

When $\gamma_0 = \gamma$ the pillar is always stable.

This problem may seem to be equivalent to that of stability of a rod vertically lowered in fluid and clamped at the level of its free surface (Fig. 1.3). One need only to change the signs of γ_0 and γ . But it is well to bear in mind that in this case there is also the end tracing force equal to $FL\gamma$. The compression forces are significantly different even in their nondeflected state (§1).

Formulae like (4.1) are widely used. For example, they may be applied to estimating the stable length of the vertical position of the cable in liquid when its upper end is supported [9]. In spite of the relatively small flexural rigidity and specific weight exceeding the specific weight of the water ($\gamma_0 > \gamma$), there exists a length

$L = 1.25 \sqrt[3]{Er^2/(\gamma_0 - \gamma)}$ for which (and for lesser values) the lower part of the cable does not fall to the bottom. This formula shows what part of the cable can float in the vertical position.

In the process, some supporting influence on the cable is exerted by the pressure $p_0 = \gamma H$ where H is the depth of the upper end from the water surface. Of course, the last circumstance is not taken into account in (4.1).

Consider one more particular case: the action of the axial force P and the constant part p_0 of hydrostatic pressure on the rod the ends of which can freely slip in supports in longitudinal direction (Fig. 1.6), the weight of the rod being neglected.

Thus, we have $w = dw/dx = 0$ ($x = 0, L$) and the equation (3.3) takes the form

$$EJ \frac{d^4 w}{dx^4} + (P - Fp_0) \frac{d^2 w}{dx^2} = 0. \quad (4.2)$$

Its solution is

$$w = C_1 + C_2 x + C_3 \sin \alpha x + C_4 \cos \alpha x, \quad \alpha^2 = \frac{1}{EJ}(P - Fp_0) > 0,$$

$$w = C_1 + C_2 x + C_3 e^{\alpha x} + C_4 e^{-\alpha x}, \quad \alpha^2 = \frac{1}{EJ}(Fp_0 - P) > 0.$$

Satisfying the mentioned fastening conditions gives in the first case the equation

$$2(1 - \cos \alpha L) - \alpha L \sin \alpha L = 0,$$

when $C_k \neq 0$. The lowest nonzero root is $\alpha L = 2\pi$. Hence, the loss of stability takes place for

$$(P - Fp_0)_* = 4\pi^2 EJ/L^2. \quad (4.3)$$

Note that in the second case the coefficients C_k are equal to zero for all αL . Consequently, in the problem under consideration there is no stability loss for $Fp_0 > P$.

The question of interest is the rod behavior under all-sided pressure p_0 , i.e. when the end forces

are caused by fluid pressure $P = Fp_0$.

By special arrangement of supports, the force P does not change its direction in bending.

Using various assumptions and statements, this problem has been considered in many works, for example in [13, 14, 17]. It is assumed in [13] that the infinite elastic band ($-\infty \leq x \leq \infty$, $-h/2 \leq y \leq h/2$) is subjected to a uniform pressure p_0 along its boundaries $y = \pm h/2$. Moreover, the band is compressed in the longitudinal direc-

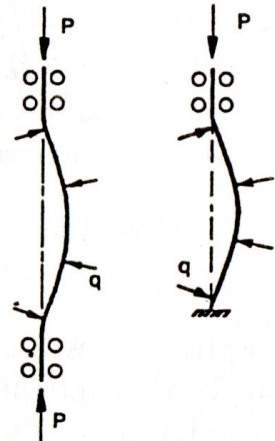


Fig. 1.6. Ends of rod can deflect in axial direction; their rotation is not allowed

tion x by the same pressure p_0 . Using equations of the plane elasticity theory, it was for the first time found in [13] that the band is always stable. There are also conclusions of an opposite character [14].

But these effects are beyond the range of the elementary bending theory (4.2). In the case under consideration we have $P = F p_0$ and equation (4.2) has the solution

$$w = C_1 + C_2 x + C_3 x^2 + C_4 x^3,$$

which, on satisfying the fastening conditions of the rod, gives $C_k \equiv 0$. The rod under all-sided uniform pressure is always stable.

This assertion is also valid for the cantilever rod when its own weight may be not taken into account (Fig. 1.7a). "For confirmation we may turn to our everyday observations. After all, the

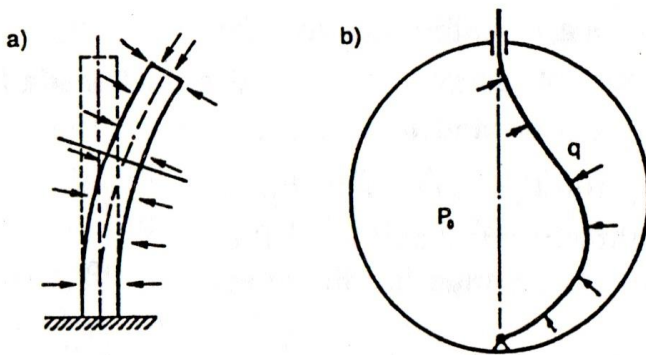


Fig. 1.7. a) The rod under uniform pressure. b) Behavior of flexible wire in container with high pressure

atmospheric pressure does not interfere with keeping the straight linear form by the thin straw of any length and rigidity" [8].

In conclusion let us underline again some features of the lateral forces (3.2). Unlike the buoyancy force which is the integral of the variable part of the hydrostatic pressure over the body surface, the expression (3.2) includes the total pressure $p_0 + \gamma x$.

Hence, q depends on the submergence depth of the object in liquid and on the mean part of the pressure p_0 . Since in a variety of technical devices p_0 may be much larger than the variable part of hydrostatic pressure, the influence of p_0 on the lateral force q should be taken into account in the general case.

Consider, for example, the behavior of a perfectly flexible wire in a vessel of high pressure [8]. One end of the wire is fastened while the other is passed through the orifice in the vessel wall (Fig. 1.7*b*). We assume that the wire can move in the orifice without friction. The bent wire will be pushed out until it becomes straight. Clearly, a wire of finite flexural rigidity will not be straightened out completely. Bending moments and transverse forces will arise in it.

§5. Stability of rod under various fastening conditions. Mine shaft

A vertical rod is fastened at its lower end, its upper one can be under various conditions. Liquid is assumed to exert only lateral pressure and not to produce axial forces, i.e. it does not act on the end sections of the rod. The liquid level coincides with the upper end of the rod.

Such a scheme may be used, for example, in studying mine tubes [15]. In contrast to usual practice, they need not be in the immediate contact with mining rock. Under conditions of alluvial layers, the mine tube along all its length (up to 500 m) is surrounded by a liquid bituminous mass filling the space between the outside wall and the mining rock. The tube bears up by its lower end against the circular concrete foundation. Mounted on the foundation, the thick lead plate provides the desirable hinge effect. In other cases it is necessary to fasten the lower end along its large

length, which is equivalent to clamping. The upper end can move in the horizontal direction or such displacement is eliminated by a plate made around the tube and firmly fixed in rock. In both these cases there is freedom of displacement in the vertical direction so that the weight of the tube is taken up by the lower support. The same scheme is used in sea-oil production, etc.

So, in the given case the equation (3.3) takes the form

$$\frac{d^4 \bar{w}}{d\xi^4} + t \left(\xi \frac{d^2 w}{d\xi^2} + \frac{dw}{d\xi} \right) = 0, \quad \xi = \frac{x}{L}, \quad t = \frac{FL^3(\gamma_0 - \gamma)}{EJ}. \quad (5.1)$$

The origin of the coordinate ξ coincides with the upper end of the rod. A solution in [15] is found in a series as

$$w = \sum_{k=0}^{\infty} C_k \xi^k. \quad (5.2)$$

Substitution of (5.2) into (5.1) gives the recurrent formula

$$(k+2)(k+3)(k+4)C_{k+4} + t(k+1)C_{k+1} = 0,$$

whence all the constants can be expressed in terms of C_0, C_1, C_2, C_3 . Finally, the solution is

$$w = C_0 + C_1 \xi \left(1 + \sum_{\nu=1} K_1^0(\nu) t^\nu \xi^{3\nu} \right) + C_2 \xi^2 \left(1 + \sum_{\nu=1} K_2^0(\nu) t^\nu \xi^{3\nu} \right) + C_3 \xi^3 \left(1 + \sum_{\nu=1} K_3^0(\nu) t^\nu \xi^{3\nu} \right). \quad (5.3)$$

Here the superscripts in K_k^m correspond to the subscripts of the constants and their subscripts to the order of derivative of w .

The values of K_k^m ,

$$K_1^0(\nu) = \frac{(-1)^\nu}{(3\nu+1)!} \prod_{n=0}^{\nu-1} (1+3n), \quad K_2^0(\nu) = \frac{(-1)^\nu \cdot 2!}{(3\nu+1)!} \prod_{n=0}^{\nu-1} (2+3n),$$

$$K_3^0(\nu) = \frac{(-1)^\nu \cdot 3!}{(3\nu+1)!} \prod_{n=0}^{\nu-1} (3+3n),$$

are tabulated [15]. As ν increases, they decrease rapidly. For example,

$$K_1^0(1) = -0.042, \quad K_1^0(2) = 0.079 \cdot 10^{-2}, \quad K_2^0(1) = -0.033,$$

$$K_2^0(2) = 0.049 \cdot 10^{-2}, \quad K_3^0(1) = -0.025, \quad K_3^0(2) = 0.030 \cdot 10^{-2}.$$

All $K_k^0(\nu)$ for $\nu = 3, 4, \dots$ decrease by two orders.

The first three derivatives of (5.3), which are necessary for determining the constants, are

$$\begin{aligned} \frac{dw}{d\xi} &= C_1 \left(1 + \sum_{\nu=1} K_1^1(\nu) t^\nu \xi^{3\nu} \right) + \\ &+ 2C_2 \xi \left(1 + \sum_{\nu=1} K_2^1(\nu) t^\nu \xi^{3\nu} \right) + 3C_3 \xi^2 \left(1 + \sum_{\nu=1} K_3^1(\nu) t^\nu \xi^{3\nu} \right), \\ \frac{d^2w}{d\xi^2} &= C_1 \sum_{\nu=1} K_1^2(\nu) t^\nu \xi^{3\nu-1} + \\ &+ 2C_2 \left(1 + \sum_{\nu=1} K_2^2(\nu) t^\nu \xi^{3\nu} \right) + 6C_3 \xi \left(1 + \sum_{\nu=1} K_3^2(\nu) t^\nu \xi^{3\nu} \right), \\ \frac{d^3w}{d\xi^3} &= C_1 \sum_{\nu=1} K_1^3(\nu) t^\nu \xi^{3\nu-2} + \\ &+ 2C_2 \sum_{\nu=1} K_2^3(\nu) t^\nu \xi^{3\nu-1} + 6C_3 \left(1 + \sum_{\nu=1} K_3^3(\nu) t^\nu \xi^{3\nu} \right). \end{aligned} \quad (5.4)$$

Using (5.3), let us consider different fastening conditions of the pillar ends.

a) In the previous paragraph, the critical value (4.1) was found for the case of free upper and fastened lower ends. Using the following conditions

$$\frac{d^2w}{d\xi^2} = \frac{d^3w}{d\xi^3} = 0 \quad (\xi = 0), \quad w = \frac{dw}{d\xi} = 0 \quad (\xi = 1),$$

for expressions (5.3), (5.4), we find $C_0 = C_2 = C_3 = 0$ and, for $C_1 \neq 0$, the equation

$$1 + \sum_{\nu=1} K_1^1(\nu)t^\nu = 0.$$

Therefore the lowest critical value of t is

$$t_* = 7.84, \quad (5.5)$$

which coincides with (4.1) and (2.12).

b) Both ends are hinged

$$w = \frac{d^2w}{d\xi^2} = 0 \quad (\xi = 0.1)$$

The critical value is

$$t_* = 18.58. \quad (5.6)$$

c) The upper end is hinged, the lower one clamped. From conditions

$$w = \frac{d^2w}{d\xi^2} = 0 \quad (\xi = 0), \quad w = \frac{dw}{d\xi} = 0 \quad (\xi = 1),$$

and from (5.3), (5.4) we obtain

$$t_* = 52.50. \quad (5.7)$$

d) The upper end is clamped, the lower one hinged

$$w = \frac{dw}{d\xi} = 0 \quad (\xi = 0), \quad w = \frac{d^2w}{d\xi^2} = 0 \quad (\xi = 1).$$

The critical value of the load parameter is

$$t_* = 30.01. \quad (5.8)$$

As is seen, the interchange of conditions in c) and d) leads to significant differences in critical values of load parameter (5.7) and (5.8).

e) Both ends are clamped. The critical parameter is

$$t_* = 74.62. \quad (5.9)$$

§6. Stability of vertical pipe with liquid.

Buckling of pipe in tension

Consider the same problem, as in §3, and corresponding equation (3.1). The difference is that the liquid of specific weight γ_i and mean pressure p_i fills the pipe of channel section area F_i . The outer surface is not in contact with liquid. Now F in (3.1) should be changed for the area of pipe cross-section F_0 . For a circular pipe $F_0 = \pi(r^2 - r_i^2)$ or if the wall thickness h is small $F_0 = 2\pi rh$. As in §3, the origin of the axis x is placed at the upper end of the tube.

Lateral distributed forces q are produced by liquid action on inner pipe walls and are $q = -q_i$, where $q_i dx$ is the lateral action of the wall on the liquid element of length dx (Fig. 1.8). Projecting forces on undeformed axes x and z , we obtain

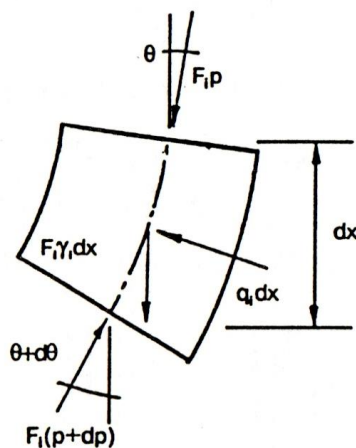


Fig. 1.8. Liquid element inside the tube of length dx

$$\begin{aligned} \gamma_i F_i dx + p F_i \cos \theta - (p + dp) F_i \cos(\theta + d\theta) - \\ - q_i dx \sin\left(\theta + \frac{d\theta}{2}\right) = 0, \end{aligned}$$

$$pF_i \sin \theta - (p + dp)F_i \sin(\theta + d\theta) + q_i dx \cos\left(\theta + \frac{d\theta}{2}\right) = 0.$$

Using $\cos \theta \approx 1$, $\sin \theta \approx \theta \approx d\omega/dx$, we have

$$\frac{dp}{dx} = \gamma_i, \quad q_i = F_i \frac{d}{dx} \left(p \frac{d\omega}{dx} \right). \quad (6.1)$$

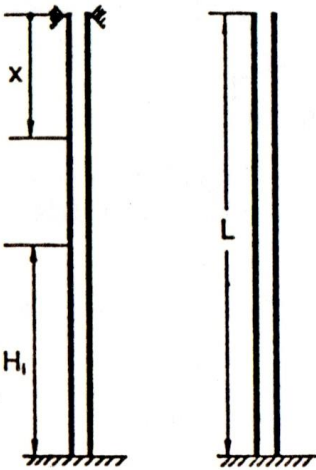
It follows from the first equation of (6.1) that $p = p_i + \gamma_i x$ while from the second one that

$$q = -q_i = -F_i \frac{d}{dx} \left((p_i + \gamma_i x) \frac{d\omega}{dx} \right). \quad (6.2)$$

Therefore, the equation (3.1) for the pipe takes the form

$$EJ \frac{d^4 \omega}{dx^4} + \frac{d}{dx} \left\{ [(P + F_0 \gamma_0 x) + F_i (p_i + \gamma_i x)] \frac{d\omega}{dx} \right\} = 0. \quad (6.3)$$

If the liquid fills the pipe only to height $H_i < L$ (Fig. 1.9), the term $p_i + \gamma_i x$ in (6.3) should be taken in the form $p_i + \gamma_i(x - H_i)$ and only in the interval $L - H_i \leq x \leq L$, putting $p_i + \gamma_i x \equiv 0$ for $0 \leq x < L - H_i$. The same is valid for the



term $(p_0 + \gamma x)$ in (3.3). If the upper part of the pipe with both ends closed is occupied by the light medium (gas) at the pressure p_i then p_i should be taken instead of $p_i + \gamma_i x$ in the interval $0 \leq x \leq L - H_i$ and $p_i + \gamma_i(x - H_i)$ in the interval $L - H_i \leq x \leq L$. Obviously, the force $P + F_0 \gamma_0 x$ is again taken along the entire length L . The height H_i can also be higher than L , for

Fig. 1.9. Pipes with liquid example, in the case of supplying liquid

through a flexible hose (Fig. 1.10). Then pressure $\gamma(H_i - L)$ is included in composition of mean pressure p_i .

As is seen from (6.3), bending of the pipe with liquid has the same features as in the case without liquid if the vertical compressing end force is presented in the form

$$P_e = P + F_i p_i, \quad (6.4)$$

and the own specific weight of rod γ_0 is changed for

$$\gamma_e = \gamma_0 + (F_i/F_0)\gamma_i. \quad (6.5)$$

Therefore, in contrast to (3.4), (3.5) the internal hydrostatic pressure leads here to a decrease of critical values of the end force and pipe weight.

Let us consider in more detail the case of a pipe with constant internal pressure, being under action only of the end force, neglecting own weights of the pipe and liquid [8].

Let a thin-walled pipe of internal radius r_1 and wall thickness h join together own containers under pressure p_i (Fig. 1.11a). If one end of the pipe can freely slip in the support, then $P = 0$. Also, the pipe presented in Fig. 1.11b is not subjected to axial compression. In this case, the equation (6.3) has the form

$$\frac{d^4 w}{d\xi^4} + \frac{p_i}{Ehr_1} \frac{d^2 w}{dx^2} = 0.$$

For clamped ends the critical value of internal pressure is $p_{i*} = 4\pi^2 Ehr_1/L^2$. If

the internal pressure exceeds this value, buckling of the pipe is possible as it is under axial compression. For the scheme in

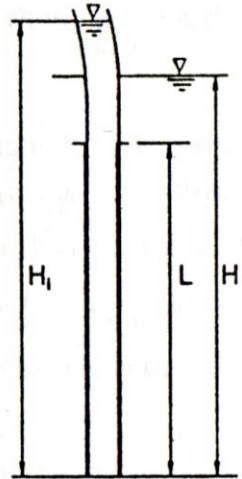


Fig. 1.10. Supply of liquid into pipe through a flexible hose. Different liquid levels in and out the pipe

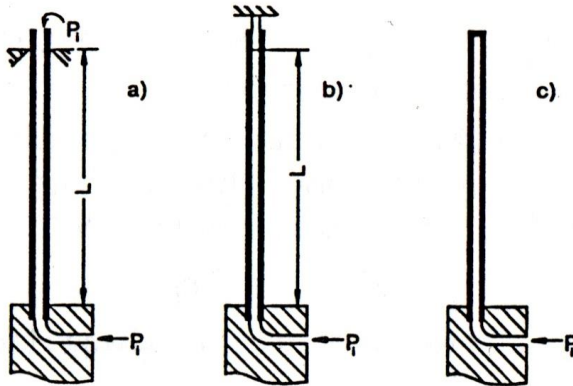


Fig. 1.11. Pipes with different conditions at one of their ends. Internal pressure exerts different action on the tubes

Fig. 1.12 considered in the book [8], the same result is valid when $p_i = \pi^2 E h r_i / L^2$ and the end force is $P = \pi^3 E h r_i^3 / L^2$.

Buckling of stretched pipe (by the force $-P$) is possible if

$$-P + F_i p_i \geq 4 \pi^2 E J / L^2. \quad (6.6)$$

When the stretching force $-P$ is produced by the internal pressure p_i acting on a circular diaphragm or a step (Fig. 1.13a) of orifice radius r_h at slipping end of the pipe, then

$$P = \pi (r_i^2 - r_h^2) p_i.$$

From (6.6) we derive the buckling condition

$$p_i \geq \frac{4 \pi^2 E h r_i^3}{L^2 r_h^2}. \quad (6.7)$$

If the step is absent ($r_h = r_i$), from (6.7) we derive the value of critical pressure mentioned above. If the diaphragm fully closes the slipping pipe end, a pipe is stable under any value of internal pressure. The same result is valid for the scheme shown in Fig. 1.11 c. It is pertinent here to make a comparison with the question of sta-

bility of a rod under all-sided external pressure (§ 5).

Now let us somewhat change the problem. Let the pipe be fastened by its end to rigid walls the distance between which does not change (Fig. 1.13b). Can it buckle under action of internal pressure p_i ? Because of radial expansion, the axial stretching force occurs $-P = -2\pi r_i N_x$, where N_x is the force on longitudinal band of unit width of the wall. We neglect the bending end effect of the wall near the end sections.

Using Hooke's law, we obtain

$$N_x = K(\varepsilon_x + \nu\varepsilon_\theta),$$

$$N_\theta = K(\varepsilon_\theta + \nu\varepsilon_x).$$

Because of absence of axial deformation ($\varepsilon_x = 0$), we have $N_x = K\nu\varepsilon_\theta = \nu N_\theta$, from the condition of ring equilibrium, $N_\theta = r_i p_i$. Therefore, $-P = -2\pi\nu r_i^2 p_i$ and, according to (6.6),

$$p_i \geq \frac{4\pi^2 E h r_i}{L^2(1-2\nu)}. \quad (6.8)$$

Thus, buckling is possible. With increase of Poisson's ratio of material, the critical internal pressure increases. The straight linear form of a pipe made out of incompressible material ($\nu = 1/2$) is stable with respect to constant internal pressure. It should be checked if the pressure determined by (6.8) does not lead to large end stresses and rupture of the pipe. The allowable pressure value corresponding to this criterion is defined by the

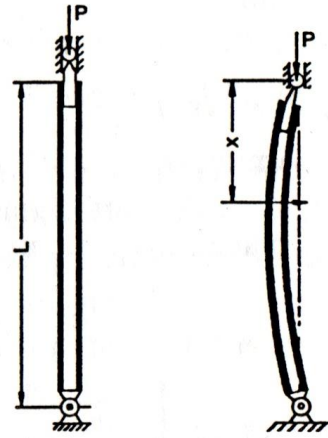


Fig. 1.12. Stability loss of the pipe in the absence of axial compression of its wall

formula $p_i = \sigma_b h / r_i$, where σ_b is the ultimate strength. Using (6.8), we find

$$\left(\frac{r_i}{L}\right)^2 = \frac{1 - 2\nu}{4\pi^2} \left(\frac{\sigma_b}{E}\right).$$

For steels $\sigma_b/E \sim 10^{-2} - 10^{-3}$, $\nu \approx 0.3$. Therefore, according to this formula $r_i/L \approx 0.003 - 0.01$. Thus, in the problem for pipes with small ratio of diameter to length, buckling of an elastic line takes place before its rupture.

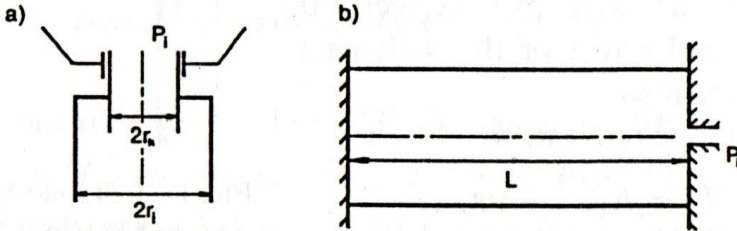


Fig. 1.13. a) End unit of a pipe with a step allowing for free slipping.
b) Pipe clamped by its ends in unmovable walls

Now consider stability of a pipe with liquid under its own weight ($P = p_i = 0$). The lower end of the pipe is clamped, the upper one free, $H_i = L$. From (6.3) we have

$$EJ \frac{d^4 w}{dx^4} + (F_0 \gamma_0 x + F_i \gamma_i x) \frac{d^2 w}{dx^2} + (F_0 \gamma_0 + F_i \gamma_i) \frac{dw}{dx} = 0.$$

As is seen, here lateral forces are produced not only by curvature but also by the angle of deflection of elastic line from the vertical. Similar to (4.1), the critical value of parameters can be presented in the form

$$F_0 \gamma_0 + F_i \gamma_i = 7.84 EJ / L^3. \quad (6.9)$$

In the case of circular pipe we shall have

$$\gamma_0 + \frac{r_i}{2h} \gamma_i = 3.92 \frac{Er_i^2}{L^2}.$$

§7. Stability of drilling and producing oil column tubes

A large number of investigations is devoted to studying stability of drilling and producing oil tubes, hydraulic columns, pipe pillars of sea-oil platforms and other structures [1–6, 10, 11, 16]. Different levels and densities of surrounding water and internal fluid (clay solution, oil etc.) are taken into account.

As was found in previous paragraphs, the external pressure improves stability of vertically standing tubes while internal pressure leads to decreasing critical values of parameters. Simultaneous consideration of these factors is recognized as important for such structures. Some solutions of such problems are presented below, following [1–6].

Unlike previous paragraphs, it is more convenient here to take the origin of the coordinate x at the lower tube foundation fastened at the bottom. The tension force $N(x)$ and lift P produced by supporting buoys, platform, ship, etc., are taken to be positive. The latter is applied to the upper end of the tube.

Thus, this problem belongs to the third type of initial state when the upper part of the tube is stretched while the lower one may be compressed (§1). Boundary of these zones is determined by formula like (1.4). But, as was shown in previous paragraph, the tube can buckle even if it is stretched along all its length.

Moreover, the upper end is joined to the hose feeding liquid in the tube. Assume the hose rigidity to be negligible as compared with the tube rigidity.

Levels H and H_i of the surrounding water and liquid in the tube, respectively, may be higher than the upper end of the tube (Fig. 1.10). Therefore, the pressure in the surrounding water at the level of the upper end of the tube is equal to $\gamma(H - L)$ while in the inner liquid it is $\gamma_i(H_i - L)$. The liquid is assumed not to

exert pressure on the circular end face of the tube. Note that liquid motion in the tube may give some additional effects [12]. But here its velocity is considered to be small and is not taken into account. For drilling column, torque and tube rotation are also not taken into consideration.

Using the aforesaid, the equation of neutral equilibrium

$$EJ \frac{d^4 \omega}{dx^4} + \frac{d}{dx} \left\{ \left[-P - F_\gamma (H - L) + F_i \gamma_i (H_i - L) + F_0 \gamma_0 (L - x) - F_\gamma (L - x) + F_i \gamma_i (L - x) \right] \frac{d\omega}{dx} \right\} = 0 \quad (7.1)$$

may be derived in a way similar to equations (3.3) and (6.3)

Let us introduce the following notations

$$\xi = x/H, \quad \beta = (F_0 \gamma_0 - F_\gamma + F_i \gamma_i) L^3 / (EJ),$$

$$\tau = (N(0) + F_\gamma H - F_i \gamma_i H_i) L^3 / (EJ), \quad N(0) = P - F_0 \gamma_0 L,$$

where $N(0)$ is the real force of the tube tension at the foundation ($x = 0$), β and τ are the nondimensional effective weight of unit length and the tension force at the foundation, respectively. The equation (7.1) takes the form

$$\frac{d^4 \omega}{d\xi^4} - \frac{d}{d\xi} \left[(\tau + \beta \xi) \frac{d\omega}{d\xi} \right] = 0. \quad (7.2)$$

For both ends hinged its solution must satisfy

$$\omega = d^2 \omega / d\xi^2 = 0 \quad (x = 0, L). \quad (7.3)$$

In order to cover the values of β , τ of practical interest, two methods were used in [1–6] for solving the stated problem. These are the power series method employed in §5 and the solution in the closed form.

In the latter case, we have

$$w(\xi) = \beta^{-1/3} [C_1 W_1(z) + C_2 W_2(z) + C_3 W_3(z) + C_4], \quad (7.4)$$

where C_1, C_2, C_3, C_4 are the integration constants and

$$W_1(z) = \int^z Ai(\zeta) d\zeta, \quad W_2(z) = \int^z Bi(\zeta) d\zeta, \quad (7.5)$$

$$W_1(z) = \int^z Ai(\zeta) \int^\zeta Bi(\eta) d\eta d\zeta + \int^z Bi(\zeta) \int^\zeta Ai(\eta) d\eta d\zeta,$$

$$z = \beta^{1/3} \xi + \tau \beta^{-2/3}.$$

$Ai(z), Bi(z)$ being the Ary functions of the first and second kind, respectively.

Under satisfying the conditions (7.3), the solution (7.4), (7.5) allows one to find the critical value of dimensionless effective tension τ_* as a function of β . In these calculations we have to use the values of functions $Ai(z), Bi(z)$ for $\xi = 0, \xi = 1$ and $z_0 = \tau \beta^{-2/3}, z_1 = \beta^{1/3} + \tau \beta^{-2/3}$. But for large z_0 and z_1 , the function $Ai(z)$ rapidly decreases while $Bi(z)$ increases, namely

$$Ai(z) \underset{z \rightarrow \infty}{\sim} \frac{1}{2} \pi^{-1/2} z^{-1/4} \exp\left(-\frac{2}{3} z^{3/2}\right),$$

$$Bi(z) \underset{z \rightarrow \infty}{\sim} \frac{1}{2} \pi^{-1/2} z^{-1/4} \exp\left(\frac{2}{3} z^{3/2}\right).$$

That was why the solution of equation (7.2) was also found in terms of series (5.2). Four constants are determined from condi-

ons (7.3). This solution allows one to make evaluations for large argument values. Hence, all values of parameters τ and β are covered by calculations.

Critical value τ_* as a function of β is given in Fig. 1.14. The curve is marked by (T) . Buckling may occur if $\tau \geq \tau_*$. Knowing τ_* , one can find the effective tension force at the lower foun-

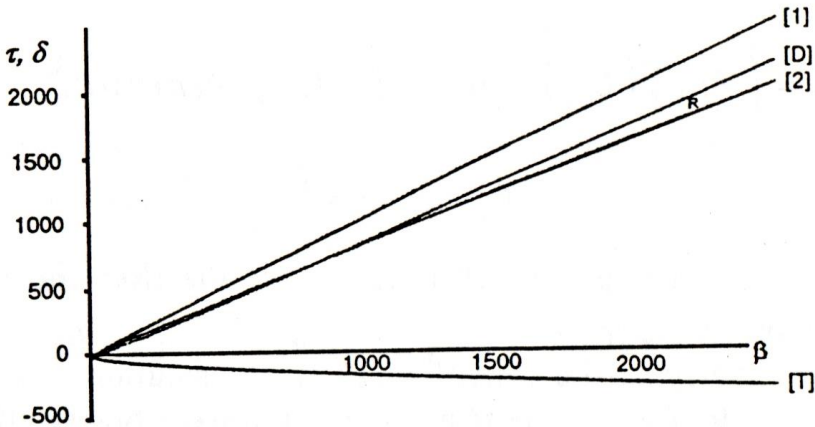


Fig. 1.14. Critical parameters versus nondimensional effective weight of unit tube length

dation. But the lift which should be applied to the upper end of the tube (P) is more useful for practice. It should be large enough to prevent tube buckling. In the dimensionless form, this force is

$$\delta = PL^3/(EJ) = \tau + \beta. \quad (7.6)$$

Critical values δ_* , when buckling may occur, are also shown in Fig. 1.14 (curve (D)). For stability, it is necessary that $\delta \geq \delta_*$.

Two approaches are usually used for evaluating these dependencies. The first one is that the force applied to the upper end should

be equal to the sum of weights of the whole column and drilling solution inside the tube minus the weight of surrounding water displaced by the column. If there are supporting buoys, their lift is also subtracted. In the dimensionless form, the first approach means

$$\delta \geq \beta. \quad (7.7)$$

In the plane $\delta - \beta$, this forms a domain where stability takes place (curve (1)). But this criterion may lead to high lift values.

The second approach is based on the notion that the tube should be in tension along all its length. The criterion leads to an inequality

$$\delta \geq \eta\beta, \quad \eta = \frac{(F_0\gamma_0 - F_i\gamma_i)}{F_0\gamma_0 + F_i\gamma_i - F\gamma}. \quad (7.8)$$

The curve (2) is given in Fig. 1.14 for $\eta = 0.8$. In plane $\delta - \beta$, the second approach may form domains of stability as well as instability. Its application is related to necessity of introducing some security coefficient. The thin area R between curves (D) and (2) shows parameters for which the tube with tension along all its length may be buckled under the action of hydrostatic pressure of internal liquid.

Fig. 1.15 shows the necessary lift at the upper end of the tube as a function of its length. Plots are presented for all three criteria mentioned above.

In doing so, the following values have been used [4]:

$$D_i = 2r_i = 0.476 \text{ m}, \quad h = 0.016 \text{ m}, \quad \gamma_0 = 7.85 \text{ g kg}/(\text{m}^2\text{s}^2),$$

$$E = 2.07 \cdot 10^{11} \text{ N/m}^2, \quad \gamma_i = 1.5\gamma.$$

From (7.8), we obtain $\eta = 0.663$. Moreover, the buoyancy of buoys was taken to be 0.3 times the weight of the water displaced by the tube.

As is seen in the figure, the first approach leads to high values of necessary lift applied to the upper end of the tube. The second approach allows buckling of stretched tube. It is possible when the length $L \geq 260$ m.

In closing, we present in the Fig. 1.16 the results corresponding to the first six forms of stability loss in the case of both ends

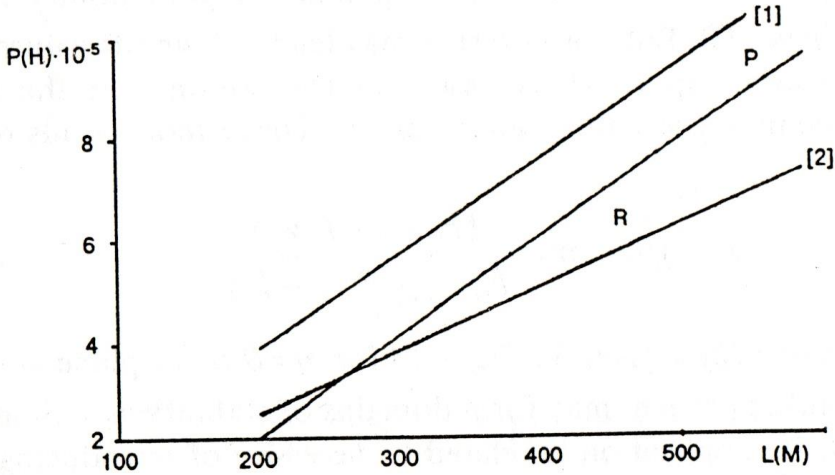


Fig. 1.15. The necessary stretching lift at the upper end of the tube as a function of its length. Exceeding shown values ensures stability of the tube. Tube ends are hinged

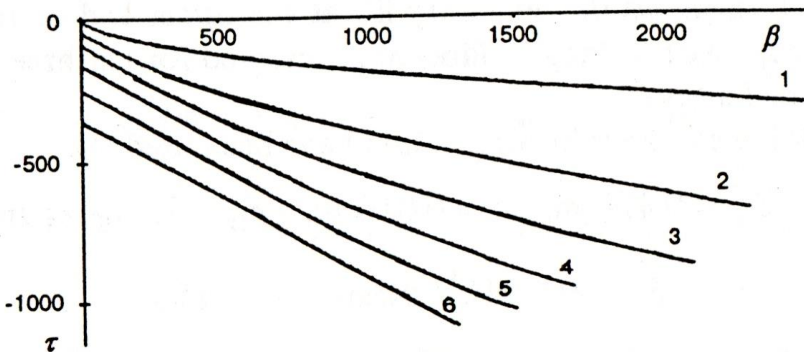


Fig. 1.16. Dimensionless effective tension force at the tube foundation as a function of effective weight of unit length. Critical values are presented for the first six buckling forms. Ends of the tube are hinged motionlessly

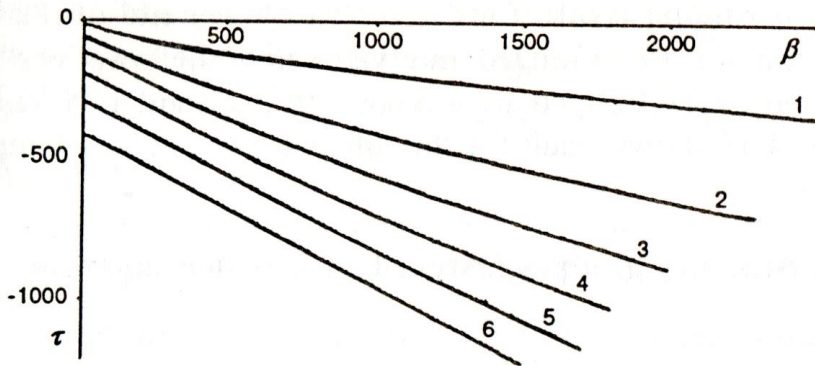


Fig. 1.17. Same as in Fig.1.16 but for the case of the lower end clamped and the upper one hinged

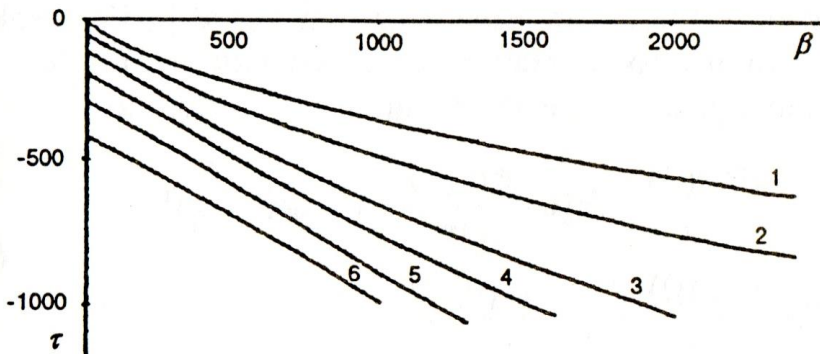


Fig. 1.18. Same as in Fig.1.16 but for the case of the lower end hinged and the upper one clamped

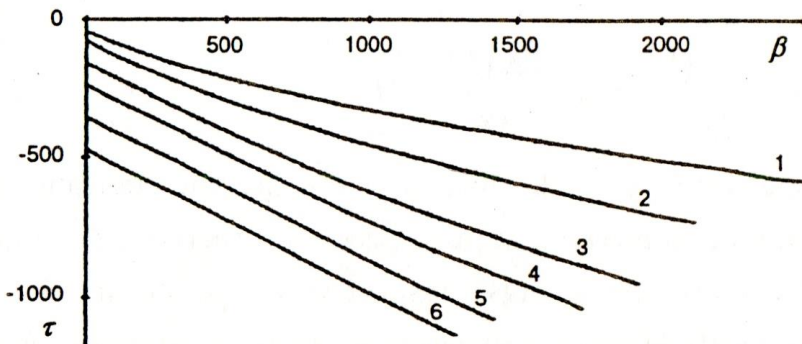


Fig. 1.19. Same as in Fig. 1.16, but for the case of both ends clamped

hinged [1,3]. Similar results for the cases of lower end of the tube clamped, the upper one hinged and, vice versa, the lower end hinged, the upper one clamped are given in Fig. 1.17 and 1.18, respectively. Fig. 1.19 shows result for the tube with both ends clamped.

§8. Stability of pipes fastened on movable supports

In actual conditions, in the problem considered in the previous paragraph, more complex fastening of the ends of vertical tube takes place. For simulating horizontal mobility of floating means to which the upper end of the tube is fastened the cases of movable hinge and movable clamp have been considered [2,5]. Displacements are assumed to be small as compared with the tube length.

In the more general case, the boundary conditions are

$$\begin{aligned}
 EJ \frac{d^3 w(0)}{dx^3} - N(0) \frac{dw(0)}{dx} + C_B w(0) &= 0, \\
 EJ \frac{d^2 w(0)}{dx^2} + r_B \frac{dw(0)}{dx} &= 0
 \end{aligned}
 \tag{8.1}$$

for the lower end ($x = 0$) and

$$\begin{aligned}
 EJ \frac{d^3 w(L)}{dx^3} - N(L) \frac{dw(L)}{dx} + C_T w(L) &= 0, \\
 EJ \frac{d^2 w(L)}{dx^2} + r_T \frac{dw(L)}{dx} &= 0
 \end{aligned}
 \tag{8.2}$$

for the upper one ($x = L$). Here C_B , C_T are the coefficients of elastic resistance to movement in horizontal direction of the lower and upper ends (linear strings), respectively, r_B , r_T are the corresponding coefficients of resistance to section rotation, N the actual axial force in the tube.

Conditions of unmovable clamp are derived from (8.1), (8.2) by putting $C_B = C_T = \infty$. Clamped end corresponds to $r_B = r_T = \infty$ while the absence of moments to $r_B = r_T = 0$. The upper end is freely displacing if $C_T = 0$, $r_T = 0$.

For solving the problem, both methods of previous paragraph are used. Thus, the wide range of dimensionless parameters τ , β is covered.

In the Fig. 1.20, the critical values of nondimensional force at the lower foundation of the tube τ_* are given as functions of

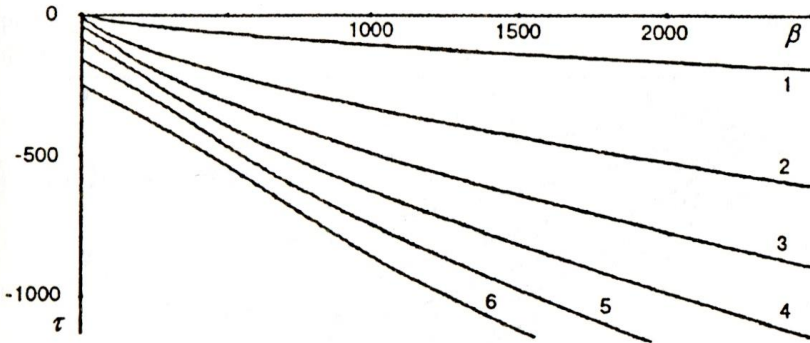


Fig. 1.20. Same as in Fig.1.16 but for the case of the lower end motionlessly hinged, the upper one movable (in horizontal direction)

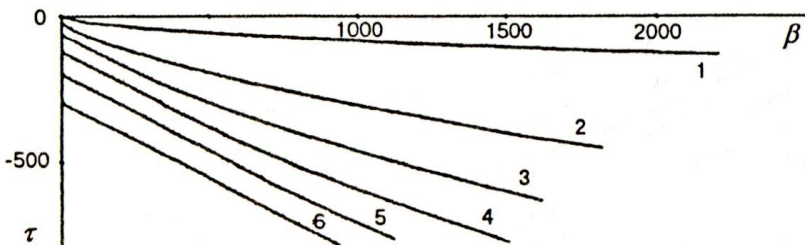


Fig. 1.21. Same as in Fig.1.16 but for the case of the lower end motionlessly hinged, the upper one clamped and movable (in the horizontal direction)

nondimensional effective weight β . The tube foundation is hinged to prevent motion while the hinge at the upper end may move in horizontal direction ($C_B = \infty$, $r_B = 0$, $C_T = 0$, $r_T = 0$). Numbers 1–6 mark data of the corresponding first six eigenforms of stability loss. The necessity of having values of $\tau_*(\beta)$ for the higher eigenforms is due to the fact that the small initial deflections of the tube several hundred meter long may lead to developing elastic line deflections from the vertical not only with respect to the first form.

Fig. 1.21 shows the function $\tau_*(\beta)$ for the first six buckling forms in the case of motionlessly hinged foundation and movable

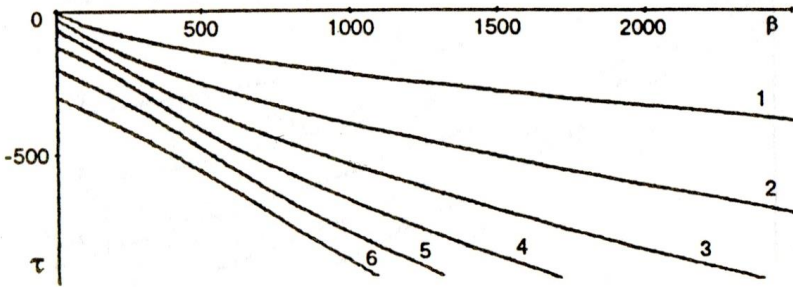


Fig. 1.22. Same as in Fig. 1.16 but for the case of the lower end motionlessly clamped, the upper one hinged and movable (in the horizontal direction)

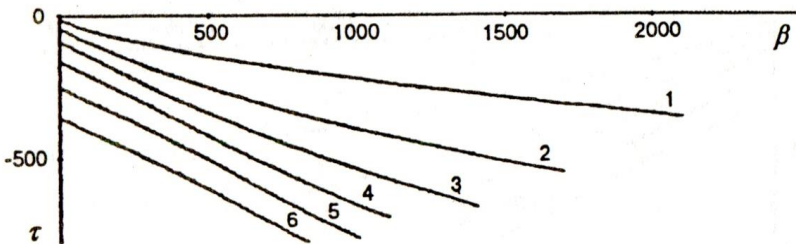


Fig. 1.23. Same as in Fig.1.16 but for the case of the lower end motionlessly clamped, the upper one clamped and movable (in the horizontal direction)

clamped upper end. Motion is allowed along the horizontal. In conditions (8.1), (8.2), $C_B = \infty$, $C_T = 0$, $r_B = 0$, $r_T = \infty$.

Fig. 1.22 shows the similar dependences for the case of a completely clamped foundation and movable hinged upper end.

Finally, Fig. 1.23 illustrates the buckling domains for the case of completely clamped foundation and movable clamped upper end.

For long heavy tubes, fastening conditions at the foundation where there is either compression or, along the length, tension, are of more importance. For the large β , the stability domains are slightly affected by the conditions at the upper end. For the hinged foundation, the asymptotic behavior of critical value has the form

$$\tau_* = -1.02\beta^{2/3},$$

while for the clamped foundation

$$\tau_* = -2.34\beta^{2/3}.$$

CHAPTER II

EQUILIBRIUM OF A MEMBRANE CONTACTING A LIQUID

§1. Linear theory of equilibrium of a membrane under liquid weight

Consider the planar problem of the equilibrium of a membrane which is the bottom of some container with vertical rigid walls and of width $2L$ (Fig. 2.1 *a*). The depth of the fluid in the container with an undeformed bottom is $H_0 = S/2L$ where S is the planar area of the liquid. Consequently, according to (0.1), the pressure acting on the bottom is equal to γH_0 where γ is the specific weight of liquid (pressure on the upper liquid surface is assumed to be zero).

When there is no deflection from the horizontal plane, the membrane is stretched over the walls of the container ($x = \pm L$) by a prescribed force T_0 . The force is related to membrane elongation 2Δ by the linear function $T_0 = Eh \Delta/L$, where E , h are the Young's modulus and the thickness of the membrane, respectively. The deflection of the membrane $w(x)$ due to the weight of the liquid and the membrane itself is assumed to be small as compared with its length. Evidently, this deflection will be symmetric about the vertical middle line of the plane $x = 0$ of the area S . Let the pressure on the membrane and its deflection from the horizontal position be positive in the downward direction.

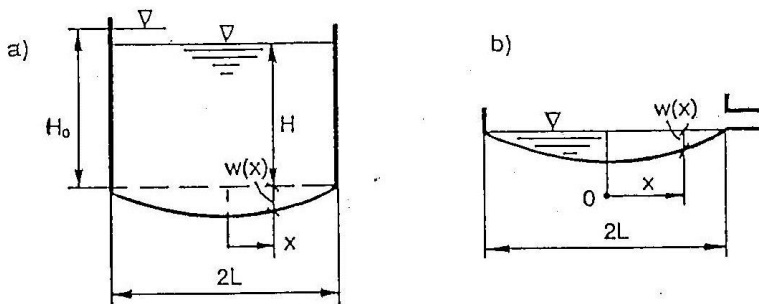


Fig. 2.1. *a*) The case of given fluid volume in container with the deformed bottom (the height H is known, H is found from the solution of the problem). *b*) The case of known height $H=0$ (problem degeneration)

The differential equation of equilibrium of the membrane for small deflections w is

$$T_0 \frac{d^2 w}{dx^2} + p_* = 0, \quad (1.1)$$

where the pressure on the deformed membrane is

$$p_* = \gamma[H + w(x)] + \gamma_0 h. \quad (1.2)$$

Here H is the height of the fluid level from the membrane edges (Fig. 2.1), and γ_0 is the specific weight of the membrane material. We shall consider only the case $H \geq 0$, which means that the free fluid surface may not be lower than the level of the membrane fastening to the walls.

It follows from the incompressibility condition (0.3) that

$$2LH_0 = 2LH + \int_{-L}^L w dx. \quad (1.3)$$

The equations (1.1), (1.2) may be written in the form

$$\frac{d^2 w}{dx^2} + \alpha^2 w = -\alpha^2 H - \alpha_0^2 h, \quad \alpha^2 = \frac{\gamma}{T_0}, \quad \alpha_0^2 = \frac{\gamma_0}{T_0}. \quad (1.4)$$

Now H and H_0 are independent of x . Therefore, the general solution of the equation (1.4) is

$$w = A \sin \alpha x + B \cos \alpha x - H - (\alpha_0/\alpha)^2 h.$$

Boundary conditions for the membrane are

$$w = 0 \quad (x = \pm L). \quad (1.5)$$

Satisfying the conditions (1.5), we obtain

$$w = \left(H + \frac{\alpha_0^2}{\alpha^2} h \right) \left(\frac{\cos \alpha x}{\cos \alpha L} - 1 \right). \quad (1.6)$$

This solution is valid if $\cos \alpha L > 0$. For αL small as compared with unity, we have

$$w = \frac{L^2}{2} (H\alpha^2 + h\alpha_0^2) \left(1 - \frac{x^2}{L^2} \right) = \frac{L^2}{2T_0} (H\gamma + h\gamma_0) \left(1 - \frac{x^2}{L^2} \right). \quad (1.7)$$

Consider two cases with respect to values of H_0 and H [4].

1. For a given H_0 (for example, $H_0 = S/2L$, as was mentioned at the beginning of the chapter), H is unknown. Then the latter is found from the equation (1.3) so that

$$H = H_0 \frac{\alpha L \cos \alpha L}{\sin \alpha L} - h \frac{\alpha_0^2}{\alpha^2} \left(1 - \frac{\alpha L \cos \alpha L}{\sin \alpha L} \right). \quad (1.8)$$

The membrane deflection is determined by substituting H from (1.8) into (1.6) to give

$$w = \left(H_0 + h \frac{\alpha_0^2}{\alpha^2} \right) \frac{\alpha L}{\sin \alpha L} (\cos \alpha x - \cos \alpha L). \quad (1.9)$$

For αL small as compared with unity, we have

$$H = H_0 - \frac{2}{3} \frac{h\gamma_0}{T_0} L^2, \quad w = \frac{L^2}{2T_0} (H_0\gamma + h\gamma_0) \left(1 - \frac{x^2}{L^2} \right). \quad (1.10)$$

Since $H \geq 0$ the value of αL should be limited. For example, when the specific weight of membrane $\gamma_0 h$ may be neglected as compared with the weight of fluid column γH_0 , the value of αL should be bounded by $0 < \alpha L \leq \pi/2$ or $0 < \gamma \leq (\pi/2L)^2 T_0$ because $\cos \alpha L \geq 0$ should be in (1.6), (1.8).

Under the above mentioned assumption of specific weights, the case $H = 0$ (Fig. 2.1b) corresponds to the value $\alpha L = \pi/2$ since only $H_0 > 0$ makes physical sense. Then the membrane deflection from undisturbed state is

$$w = \frac{\pi}{2} H_0 \cos \frac{\pi x}{2L}.$$

Though H_0 is given, its value corresponding to $H = 0$ cannot be found in this case. Consequently, the value of the amplitude of the deflection w is also unknown.

As was shown in Introduction, this is caused by the fact that for $H = 0$, $h = 0$ the system (1.4), (1.5) degenerates into an eigenvalue problem, $w_{xx} + \alpha^2 w = 0$, $w = 0$ ($x = \pm L$). The lowest eigenvalue is $\alpha L = \pi/2$, and the corresponding eigenfunction is $\cos(\pi x/2L)$.

But if the weight of membrane is not neglected, it follows from (1.8) that for $H = 0$

$$H_0 = h \left(\frac{\alpha_0}{\alpha} \right)^2 \left(\frac{\sin \alpha L}{\alpha L \cos \alpha L} - 1 \right).$$

Since the height of liquid column H_0 is positive and finite, then $\operatorname{tg} \alpha L > \alpha L$, i.e. $\alpha L < \pi/2$. Now from (1.9) we have

$$w = h \left(\frac{\alpha_0}{\alpha} \right)^2 \left(\frac{\cos \alpha x}{\cos \alpha L} - 1 \right).$$

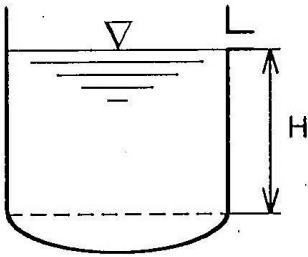


Fig. 2.2. The height of the fluid level H is given (H_0 is found from solution of the problem)

This function is quite determined.

2. Here the depth H_0 is to be determined for a known H . The depth H may be given, for example, when there is an orifice in the lateral wall of the container (Fig. 2.2) or if the container of Fig. 2.1 *a* is always full up to its edge. In the latter case H is equal to the height of lateral walls of the container. The deflection of membrane is here determined by expression (1.6), and the

volume of fluid in the container by the formula

$$H_0 = H \frac{\sin \alpha L}{\alpha L \cos \alpha L} + h \frac{\alpha_0^2}{\alpha^2} \left(\frac{\sin \alpha L}{\alpha L \cos \alpha L} - 1 \right), \quad (1.11)$$

$$S = 2LH_0.$$

Note also the singularity of the solution (1.6), (1.11) when the weight of the membrane itself is not taken into account ($h\gamma_0 \rightarrow 0$). Such a problem has been considered in [7]. Putting $H = 0$ in (1.6), we obtain $w = 0$ for all αL except for $\alpha L = (1 + k)\pi/2$ ($k = 0, 2, 4, \dots$). As was mentioned above, the last αL are eigenvalues of the homogeneous problem. Since $w > 0$, $H_0 > 0$ only the value for $k = 0$ makes physical sense. When w and H_0 are determined by (1.6), (1.11), an indeterminate form of the 0/0-type arises.

It was pointed out in [7] that this drawback of solution is due to the linearity of equations. The solution of the nonlinear problem was also given in [7]. In the next paragraph we shall consider this problem without taking into account the weight of the membrane [4].

§2. Nonlinear theory of the equilibrium of a membrane under a liquid layer

Instead of (1.1), we use now the following system of geometrically nonlinear equations of the membrane equilibrium which also take into account the deflection u along x -axis

$$Eh \frac{d}{dx} \left[\left(\frac{du}{dx} + \frac{1}{2} \left(\frac{d\omega}{dx} \right)^2 \right) \frac{d\omega}{dx} \right] + p_* = 0, \quad (2.1)$$

$$Eh \frac{d}{dx} \left(\frac{du}{dx} + \frac{1}{2} \left(\frac{d\omega}{dx} \right)^2 \right) = 0.$$

Expression for p_* follows from (1.2) by putting $h\gamma_0 = 0$.

Boundary conditions are

$$\begin{aligned} \omega &= 0 \quad \text{for } x = \pm L, \\ u &= -\Delta \quad \text{for } x = -L, \quad u = \Delta \quad \text{for } x = L, \end{aligned} \quad (2.2)$$

where, as in §1, 2Δ is the elongation of the membrane resulting from the tension force T_0 ($\Delta = T_0 L/Eh$).

Introduction of the second equation of (2.1) gives

$$\frac{du}{dx} + \frac{1}{2} \left(\frac{d\omega}{dx} \right)^2 = \frac{T_*}{Eh}, \quad (2.3)$$

where the constant T_* is the total tension of membrane $T_* = T_0 + T$, T is the force which appears in deflecting the membrane from the horizontal (as a result of fluid pressure).

Using (2.3), the first equation of (2.1) may be written in the form of (1.4) as

$$d^2\omega/dx^2 + \alpha_*^2 \omega = -\alpha_*^2 H, \quad \alpha_*^2 = \gamma/T. \quad (2.4)$$

Therefore, its solution may be presented in the form of (1.6) from the linear theory (utilizing the condition (2.2) for ω) so that

$$w = H \left(\frac{\cos \alpha_* x}{\cos \alpha_* L} - 1 \right), \quad \alpha_* = \sqrt{\frac{\gamma}{T_0 + T}} \quad (2.5)$$

but here the parameter α_* and the additional force T are unknown.

Integrate (2.3) between 0 and x to obtain (note that for the symmetrical problem $u(0) = 0$)

$$u(x) = \frac{T_* x}{Eh} - \frac{1}{2} \int_0^x \left(\frac{dw}{dx} \right)^2 dx. \quad (2.6)$$

Using condition (2.2) for u , we find from (2.6)

$$\Delta = \frac{T_* L}{Eh} - \frac{1}{2} \int_0^L \left(\frac{dw}{dx} \right)^2 dx.$$

Substitution of function (2.5) into this expression and integration give the relation between H and α_*

$$H = \sqrt{\frac{2\gamma L}{Eh\alpha_*^2} \left(1 - \Delta \frac{Eh\alpha_*^2}{\gamma L} \right)} \frac{2 \cos \alpha_* L}{\sqrt{2\alpha_* L - \sin 2\alpha_* L}}. \quad (2.7)$$

According to the assumption $H \geq 0$ the positive sign has been chosen in (2.7) for the root.

Expression (2.5), (2.6), (2.7) are the solution to the nonlinear problem (2.1), (2.2). Given γ , E , L , h , Δ , H , we can find $\alpha_* L$ from (2.7) and the components of the membrane deflection from (2.5) and (2.6) [4]. When H_0 is given, then formula (1.8) should also be used to determine

$$H \operatorname{tg} \alpha_* L = H_0 \alpha_* L.$$

Consider the case of small fluid height H . Since for $H = 0$ (2.7) gives $\cos \alpha_* L = 0$, $\alpha_* L = \pi/2$ (the other roots $\alpha_* L$ do not make physical sense), for small value of H we take $\alpha_* L =$

$= \pi/2 - \varepsilon$, where $\varepsilon^2 \ll 1$. Then, making use of $\cos(\pi/2 - \varepsilon) \approx \varepsilon$, $\sin(\pi - 2\varepsilon) \approx 2\varepsilon$, we find from (2.7) that for small H in the first approximation

$$\varepsilon \approx \frac{\pi^2 H}{4L} \left[\gamma_* \left(1 - \frac{\pi^2 \Delta}{\gamma_* L} \right) \right]^{-1/2}, \quad \gamma_* = \frac{4L^2 \gamma}{Eh}. \quad (2.8)$$

Now from (2.5) and (2.7), the following expression can be obtained approximately

$$\begin{aligned} \frac{w}{2L} = \frac{2}{\pi^2} \sqrt{\frac{\pi \gamma_*}{\pi - 10\varepsilon} \left[1 - \frac{\pi^2 \Delta}{\gamma_* L} \left(1 - \frac{4\varepsilon}{\pi} \right) \right]} \times \\ \times \left[\cos \frac{\pi x}{2L} - \varepsilon \left(1 - \frac{x}{L} \sin \frac{\pi x}{2L} \right) \right]. \end{aligned} \quad (2.9)$$

The deflection of membrane is determined from (2.9) and (2.8). Thus it depends on the liquid height nonlinearly (in ε). The additional tension of membrane is

$$T = \frac{4L^2 \gamma}{\pi^2 (1 - 4\varepsilon/\pi)} - T_0. \quad (2.10)$$

When $H = 0$ ($\varepsilon = 0$), (2.9) leads to the finite expression

$$\frac{w}{2L} = \frac{2}{\pi^2} \sqrt{\gamma_* \left(1 - \frac{\pi^2 \Delta}{\gamma_* L} \right)} \cos \frac{\pi x}{2L} \quad (2.11)$$

which has been considered in detail in [7].

Since $\Delta \geq 0$ there is a bifurcation point for $\gamma_* = \pi^2 \Delta/L$. Use definitions of Δ and γ_* to obtain $\gamma = (\pi/2L)^2 T_0$. This corresponds to the first eigenvalue found in previous paragraph from linear solution. Indeed, for small values of deflection, i.e. when $\pi^2 \Delta/(\gamma_* L) \rightarrow 1$, the linear solution is valid.

Note that according to (2.11), in the absence of initial tension ($\Delta = 0, T_0 = 0$) the nonzero solution (the deflection of the membrane) exists for any $\gamma_* > 0$. But if the initial tension is present ($\Delta > 0$), the nonzero solution exists only for $\gamma_* > \pi^2 \Delta/L$.

§3. The circular membrane under hydrostatic load

Consider a circular cylindrical vessel, the bottom of which is a membrane (Fig. 2.1). Now we have a radial coordinate r instead of x and $2R$ instead of $2L$. The other notations are unchanged. Corresponding linear problem has been considered in [1,2] under the assumption that H is known. Here we shall take into account that H depends on volume Q_0 ($H_0 = Q_0/(\pi R^2)$). Clearly, the problem is axisymmetric.

In place of (1.3), (1.4) we now write

$$\frac{d^2 w}{dr^2} + \frac{1}{r} w + \alpha^2 w = -\alpha^2 H - \alpha^2 h, \quad (3.1)$$

$$H = H_0 - \frac{2}{R^2} \int_0^R w r dr, \quad \alpha^2 = \frac{\gamma}{T_0}, \quad \alpha_0^2 = \frac{\gamma_0}{T_0}.$$

Conditions of fastening to the wall are $w = 0$ ($r = R$).

General solution of nonhomogeneous equation (3.1) has the form

$$w = AJ_0(\alpha r) + BN_0(\alpha r) - H - (\alpha_0/\alpha)^2 h,$$

where J_0, N_0 are, respectively, the Bessel's and Neumann's functions of zero order.

Requiring the solution at $r = 0$ ($B = 0$) to be finite and im-

sing the boundary condition of zero displacement at $r = R$, we find

$$w = \left(H + \frac{\alpha_0^2}{\alpha^2} h \right) \left(\frac{J_0(\alpha r)}{J_0(\alpha R)} - 1 \right). \quad (3.2)$$

Compare (3.2) to (1.6).

This solution depends on H , H_0 in the same way as in §1. The following relation between H , H_0 is derived from (3.1), (3.2)

$$H_0 = H - \left(H + \frac{\alpha_0^2}{\alpha^2} h \right) \left(1 - \frac{2}{\alpha R} \frac{J_1(\alpha R)}{J_0(\alpha R)} \right), \quad (3.3)$$

where J_1 is the Bessel's function of the first order.

For small αR , putting

$$J_0(\alpha R) \approx 1 - \frac{1}{4}(\alpha R)^2, \quad J_1(\alpha R) \approx \frac{1}{2}\alpha R - \frac{1}{16}(\alpha R)^3,$$

we obtain

$$H_0 = H + \frac{(\alpha R)^2}{8} \left(H + \frac{\alpha_0^2}{\alpha^2} h \right).$$

The solution (3.2) is valid for $\alpha R < 2.4$. As in §1, the linear solution for $\alpha R = 2.405$ degenerates, being the first root of the equation $J_0(\alpha R) = 0$. As it is seen from §2, the nonlinear terms in the equations of membrane equilibrium should be taken into consideration to obtain a finite solution for large αR .

Thus, given values of the specific weight of the liquid and the initial tension of membrane, the solution (3.2) is valid only for $R < 2.4\sqrt{T_0/\gamma}$.

Now consider the buckling of the membrane enclosing the cylindrical vessel in which the pressure is due to the difference H of liquid levels in communicating ves-

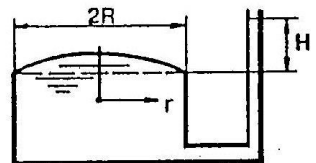


Fig. 2.3. The cover of reservoir in the form of circular membrane

sels (Fig. 2.3). In this case (positive w are directed upwards).

$$p_* = \gamma[H - w(x)] - \gamma_0 h, \quad (3.4)$$

therefore

$$\frac{d^2 w}{dx^2} + \frac{1}{r} w - \alpha^2 w = -\alpha^2 H + \alpha_0^2 h. \quad (3.5)$$

Its general solution is

$$w = AI_0(\alpha r) + BK_0(\alpha r) + H - (\alpha_0/\alpha)^2 h,$$

where I_0 , K_0 are the zero-order Bessel's functions of imaginary argument. Using boundary conditions to obtain A and $B = 0$, one has

$$w = \left(H - \frac{\alpha_0^2}{\alpha^2} h \right) \left(1 - \frac{I_0(\alpha r)}{I_0(\alpha R)} \right). \quad (3.6)$$

The function I_0 is positive and increases with increasing its argument. That is why here, in contrast to the previous problem, there is no degeneration for any value of the argument αR .

Let H_0 , Q_0 be respectively the height and volume of liquid which is added to the tube at state $w = 0$ and under equal levels of liquid in the reservoir and in the tube. Then

$$H_0 = \frac{Q_0}{s_0}, \quad H = H_0 - \frac{2\pi}{s_0} \int_0^R w r dr.$$

Here s_0 is the tube cross-section area.

Clearly, the presented results can also be used for analyzing cylindrical containers shown in Fig. 2.4. There are many air supporting and pneumatic engineering structures [7] for which estimations similar to those presented in the above paragraphs are also necessary.

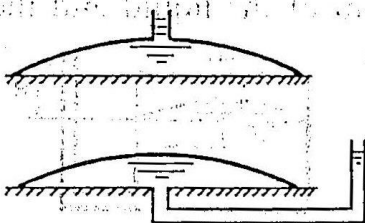


Fig. 2.4. Examples of containers of fluids

§4. Interaction of membrane with liquid in closed vessel

In previous paragraphs of this chapter we have considered such cases of interaction in which there is a free fluid surface in the vessel. The problem statement somewhat changes if the liquid fills the closed vessel completely [3, 6].

Assume the weightless membrane covers the liquid in a volume and is subjected to load from its upper side by pressure p_e (Fig. 2.5a) of some prescribed value. Membrane is tensed by force T_0 and fastened to the walls at $x = \pm L$. A small deflection will be considered under the action of a symmetric load $p_e = P_e \cos(\pi x/2L)$. Thus, the linear problem is to be solved in a planar formulation. Pressure and deflection are taken as positive in the downward direction.

The total pressure on the membrane is

$$p_* = p_e - (p_0 + \gamma w), \quad (4.1)$$

where p_0 is the constant part of hydrostatic pressure in the liquid

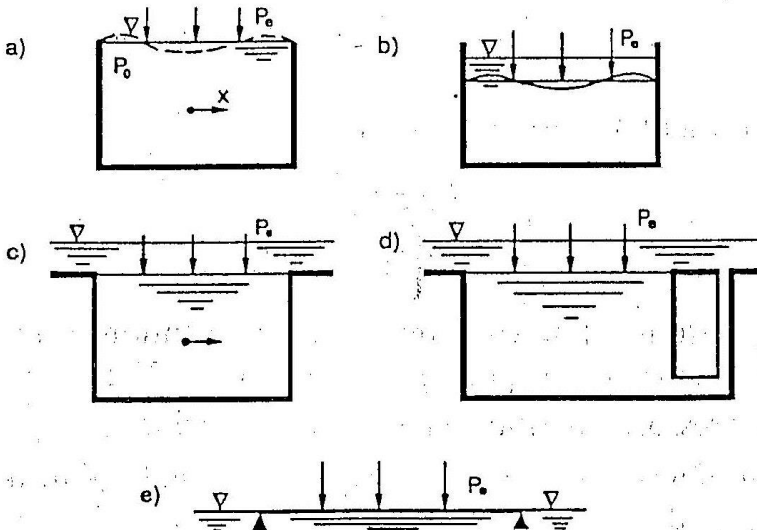


Fig. 2.5. Examples of dosed container with liquid

which in the previous paragraphs has been taken to be zero. Now it is to be determined along with the membrane deflection w . It follows from (1.1) and (4.1) that

$$\frac{d^2 w}{dx^2} - \alpha^2 w = -\frac{p_e - p_0}{T_0}, \quad \alpha^2 = \frac{\gamma}{T_0}. \quad (4.2)$$

The solution of this equation, using the pressure distribution p_e given above, has the form

$$w = A \operatorname{sh} \alpha x + B \operatorname{ch} \alpha x - \frac{p_0}{T_0 \alpha^2} + \frac{P_e}{T_0 (\alpha^2 + \pi^2/4L^2)} \cos \frac{\pi x}{2L}. \quad (4.3)$$

Imposing conditions $w = 0$ at $x = \pm L$, we have

$$w = \frac{p_0}{T_0 \alpha^2} \left(\frac{\operatorname{ch} \alpha x}{\operatorname{ch} \alpha L} - 1 \right) + \frac{P_e}{T_0 (\alpha^2 + \pi^2/4L^2)} \cos \frac{\pi x}{2L}. \quad (4.4)$$

The pressure p_0 is found from the incompressibility condition

$$\int_{-L}^L w \, dx = 0. \quad (4.5)$$

Substituting (4.4) into (4.5), we find

$$p_0 = \frac{2P_e (\alpha L)^3}{\pi (\alpha L - \operatorname{th} \alpha L) \left[(\alpha L)^2 + (\pi/2)^2 \right]}. \quad (4.6)$$

The expressions (4.4), (4.6) represent the solution of the linear problem stated in the beginning of the section. For an arbitrary symmetric pressure distribution p_e the solution may be presented in the form of a cosine series. The expressions (4.4), (4.6) will then also be changed.

Eliminating p_0 in (4.4), we obtain

$$\omega = \frac{P_e L^2}{T_0 [(\alpha L)^2 + (\pi/2)^2]} \left[\frac{2\alpha L}{\pi(\alpha L - \text{th } \alpha L)} \left(\frac{\text{ch } \alpha x}{\text{ch } \alpha L} - 1 \right) + \cos \frac{\pi x}{2L} \right].$$

As is seen, the relative deflection (ω/L) depends on the nondimensional parameters $P_e L/T_0$ and $\alpha L = L\sqrt{\gamma/T_0}$.

It is of interest to make comparison of the pressure (4.6) constant over liquid volume with its value when the membrane is changed for the rigid piston slipping without friction along the walls of the container (under the same external action). Clearly, it is

$$p_0 = \frac{P_e}{2L} \int_{-L}^L \cos \frac{\pi x}{2L} dx = \frac{2}{\pi} P_e. \quad (4.7)$$

The value $\alpha L \ll 1$ corresponds to the large tension T_0 of membrane when its width L is small. Therefore, it follows from (4.6) that $(\pi/2P_e)p_0 = 12/\pi^2 = 1.216$, which is somewhat higher than by (4.7). Thus, under equal loading of rigid piston and membrane the pressure in liquid beneath them differ by more than 21%. When $\alpha L \ll 1$ the nondimensional deflection is

$$\frac{\pi^2 T_0}{4P_e L^2} \omega = \cos \frac{\pi x}{2L} - \frac{3}{\pi} \left(1 - \frac{x^2}{L^2} \right). \quad (4.8)$$

The downward deflection by the value $(1 - 3/\pi)$ takes place in the center while the maximum deflection upwards is at the points $x/L = \pm 0.74$. With increasing αL , the function $(\pi/2P_e)p_0$ smoothly decreases up to 1.210 for $\alpha L = 1.0$ and then also smoothly increases. For example, $(\pi/2P_e)p_0 = 1.379$ for $\alpha L = 1.4$, i.e. the pressure increase beneath the membrane amounts to $\sim 40\%$ (as compared with the case of a rigid piston). When $\alpha L \gg 1$ we obtain from (4.6) that the value of p_0 coincides with that by (4.7).

Now let us consider the same problem except there is a liquid layer from the upper side of the membrane (Fig. 2.5*b*). And the specific weight of the liquid in the space under the membrane. Then the expression for total pressure (4.1) will not have the term $-\gamma w$ since in this case the membrane is subjected to the pressure $\gamma(H + w)$ of the upper liquid layer. Here H is the height of the upper liquid layer measured from the membrane edges (the pressure on the free surface is assumed to be zero). According to (1.3), $H = H_0$ due to the incompressibility condition for the lower liquid. Thus, the total pressure on the membrane is $p_* = p_e + \gamma H - p_0$.

Thus, instead of (4.2), (4.4) and (4.6), we shall have

$$\frac{d^2 w}{dx^2} = \frac{p_e + \gamma H - p_0}{T_0},$$

$$w = \frac{(p_0 - \gamma H)L^2}{2T_0} \left(1 - \frac{x^2}{L^2}\right) + \frac{4P_e L^2}{\pi^2 T_0} \cos \frac{\pi x}{2L}, \quad (4.9)$$

$$p_0 = \frac{2A}{\pi^3} P_e + \gamma H.$$

Expression for w will coincide with (4.9) if p_0 is eliminated in (4.9). But p_0 itself is here also dependent on γH . The solution (4.9) remains valid also for the case when the upper layer is extended without limit (Fig. 2.5*c*). It is due to the fact that there will be no term $-\gamma w$ in the equation of the membrane while the incompressibility condition will hold in the same form (4.5).

If the space under the membrane is connected to the upper layer of liquid (Fig. 2.5*d*), the condition (4.5) is not used. The space under membrane is not closed. In this case the integral in (4.5) allows one to determine the volume of liquid displaced from

the lower space. The constant part of the hydrostatic pressure is $p_0 = \gamma H$. Therefore, in the case under consideration

$$\frac{d^2 w}{dx^2} = -\frac{p_e}{T_0}. \quad (4.10)$$

Taking in (4.10) the previous distribution $p_e(x)$ and satisfying conditions of $w = 0$ at $x = \pm L$, we find

$$w = \frac{4P_e L^2}{\pi^2 T_0} \cos \frac{\pi x}{2L}. \quad (4.11)$$

Thus here the distribution of deflection w along the membrane mimics the shape of the given external load.

Consider for comparison the linear problem of deflection of a membrane stretched over the supports and contacting with the surface of unlimited liquid (Fig. 2,5e). Assume the external pressure to be same as above. Then the pressure on the membrane is $p_* = p_e - \gamma w$, while $p_0 = 0$. Since the liquid is unlimited, the condition (4.5) is not valid. Here equations (4.2) and (4.4) are valid for $p_0 = 0$. As is seen from (4.4), in this case the membrane deflection is also dependent on the liquid density ($\alpha^2 = \gamma/T_0$).

§5. Stability of membrane between liquids of different density

As it follows from (4.9), for $P_e = 0$ the constant part of the pressure under the membrane is $p_0 = \gamma H$, its deflection w is absent. Consider this problem in more detail, assuming that specific liquid weights are different in the lower (γ_1) and upper (γ_2) spaces. Moreover, there is no external pressure ($p_e = 0$)

and the lower space is closed (Fig. 2.6a). We restrict our consideration to the linear problem.

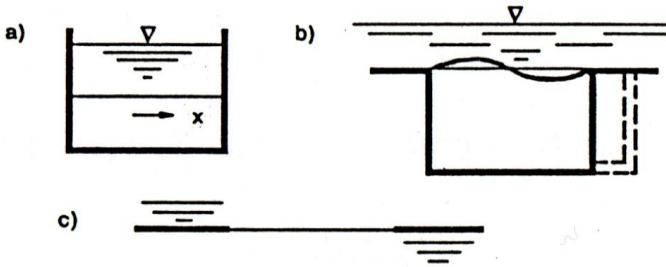


Fig. 2.6. Examples of stability problems of the membrane between liquids of different specific weights

The pressure on the membrane deflected by $w(x)$ is

$$p_* = -(p_0 + \gamma_1 w) + \gamma_2 (H + w). \quad (5.1)$$

Since in this case $P_e = 0$ and, according to (4.9), $p_0 = \gamma H = \gamma_2 H$, it follows from (5.1) that we obtain $p_* = (\gamma_2 - \gamma_1)w$. Here instead of (4.2), we have

$$\frac{d^2 w}{dx^2} + \alpha^2 w = 0, \quad \alpha^2 = \frac{\gamma_2 - \gamma_1}{T_0}. \quad (5.2)$$

Consider the case when the heavier liquid is in the upper layer ($\gamma_2 > \gamma_1$, $\alpha^2 > 0$). Using condition (4.5) for closed containers with incompressible liquid, we obtain from the solution of equation (5.2)

$$w = A \sin \alpha x + B \cos \alpha x \quad (5.3)$$

that

$$B \sin \alpha L = 0. \quad (5.4)$$

Boundary conditions $w = 0$ ($x = \pm L$) give

$$A \sin \alpha L + B \cos \alpha L = 0,$$

$$A \sin \alpha L - B \cos \alpha L = 0$$

or

$$B \cos \alpha L = 0, \quad A \sin \alpha L = 0. \quad (5.5)$$

The first equation of (5.5) and the equation (5.4) are valid simultaneously only if $B = 0$. Then, putting $A \neq 0$, it follows from the second equation of (5.5) that $\sin \alpha L = 0$ whence $\alpha L = 0, \pi, 2\pi, \dots$. Consider the first nonzero root $\alpha L = \pi$. The solution (5.3) takes the form

$$w = A \sin(\pi x/L).$$

Hence, on reaching the value

$$\gamma_2 - \gamma_1 = \pi^2 T_0 / L^2, \quad (5.6)$$

the membrane may deflect from the planar nontensed state of equilibrium creating two halfwaves along the width (with node at $x = 0$).

If the lower liquid is heavier ($\gamma_1 > \gamma_2$) the solution of equation (5.2) has the form

$$w = A e^{\alpha x} + B e^{-\alpha x}, \quad \alpha^2 = (\gamma_1 - \gamma_2) / T_0.$$

It follows from the condition (4.5) that

$$(A + B)(e^{\alpha L} - e^{-\alpha L}) = 0.$$

Since $\alpha = 0$ ($\gamma_1 = \gamma_2$) is not considered, we have $A = -B$. Taking this into account, the fastening conditions give

$$A(e^{\alpha L} - e^{-\alpha L}) = 0$$

or $A = -B = 0$. Hence, for $\gamma_1 > \gamma_2$ there are no deflections of the membrane from its plane equilibrium state. Since the solution (4.7) valid for $\gamma_1 = \gamma_2$ gives $w = 0$ for $P_e = 0$ one can also write $\gamma_1 \geq \gamma_2$.

These results are also valid for the case when the lower space is closed while the upper liquid layer is extended without limit (Fig. 2.6*b*).

In Fig. 2.6*c* the liquids of specific weights γ_1 and γ_2 are extended without limit from both sides of horizontal rigid screen a part of which is a tensed membrane of width $2L$. Because the liquid areas are not limited, the condition (4.5) is not imposed. Small membrane deflections are described by the equation (5.2). The conditions for the membrane edges ($w = 0$ at $x = \pm L$) give the equations (5.5).

Unlike the problems described in Fig. 2.6*a* and Fig. 2.6*b*, equations (5.5) may here lead to two possibilities:

1) $A \neq 0$, $B = 0$ and hence $\sin \alpha L = 0$, whence $\alpha L = 0, \pi, 2\pi, \dots$. For the root $\alpha L = \pi$ we have

$$w = A \sin \frac{\pi x}{L}, \quad \gamma_2 - \gamma_1 = \frac{\pi^2 T_0}{L^2}, \quad (5.7)$$

which coincides with the solution obtained above.

2) $A = 0$, $B \neq 0$ and hence $\cos \alpha L = 0$ whence $\alpha L = 0, \pi, 2\pi, \dots$. For the first root we have

$$w = B \cos \frac{\pi x}{L}, \quad \gamma_2 - \gamma_1 = \frac{\pi^2 T_0}{4L^2}. \quad (5.8)$$

In the first case the membrane deflection from the tensed planar state can occur with two halfwaves. In the second case a deflection may occur with one halfwave if the difference $\gamma_2 - \gamma_1$ becomes equal to $(\pi/2L)^2 T_0$. It is less than that in the first case by a factor of 4. So, when $\gamma_2 - \gamma_1$ is gradually increasing we come to the latter variant of the membrane behaviour.

§6. Determination of membrane deflection in stability problem

In the previous paragraph the critical parameters (5.6), (5.7), (5.8) and corresponding forms of membrane deflections from the planar state were found. But the amplitudes of these deflections remained unknown. To determine them, it is necessary to use the nonlinear relations. Let us turn to the set of the nonlinear equations (2.1).

In order to somewhat diversify the problem statement, assume the absence of the initial tension of the membrane. Since $T_0 = 0$, then according to (5.6), the plane form of the membrane is unstable for any positive difference between specific weights of the upper (γ_2) and lower (γ_1) liquids. Now we present the results of [3].

For $\Delta = 0$, $T_0 = 0$ and $T_* = T$, the equation (2.3) takes the form

$$\frac{T}{Eh} = \frac{du}{dx} + \frac{1}{2} \left(\frac{dw}{dx} \right)^2. \quad (6.1)$$

Such a statement implies that the membrane can be in tension only due to its deflection from the planar form.

The first equation of (2.1) or the equation (2.4), according to (5.1), will be written as

$$\frac{d^2w}{dx^2} + \alpha_*^2 w = 0, \quad \alpha_*^2 = \frac{\gamma_2 - \gamma_1}{T}. \quad (6.2)$$

Equations (6.1) and (6.2) have the solution

$$w = A \sin \alpha_* x + B \cos \alpha_* x,$$

$$u = \beta_* x + C - \frac{\alpha_*^2}{2} \int (A \cos \alpha_* x - B \sin \alpha_* x)^2 dx, \quad (6.3)$$

$$\beta_* = T/(Eh).$$

The incompressibility condition for the liquid in lower closed space (4.5) gives

$$B \sin \alpha_* L = 0. \quad (6.4)$$

Boundary conditions $u = w = 0$ ($x = \pm L$) lead to

$$\begin{aligned} B \cos \alpha_* L &= 0, \\ A \sin \alpha_* L &= 0, \end{aligned} \quad (6.5)$$

$$4C - AB\alpha_* \cos \alpha_* L = 0,$$

$$8\beta_* L - 2\alpha_*^2 L (A^2 + B^2) + \alpha_* (A^2 - B^2) \sin 2\alpha_* L = 0.$$

Equations (6.4) and the first equation of (6.5) may be satisfied together only if $B = 0$. Then, putting $A \neq 0$, we find from the second equation in (6.5) that $\sin \alpha_* L = 0$ whence $\alpha_* L = n\pi$ ($n = 0, 1, 2, \dots$). Hence, the membrane tension force is

$$T_n = \left(\frac{L}{n\pi} \right)^2 (\gamma_2 - \gamma_1) \quad (n = 1, 2, \dots). \quad (6.6)$$

It follows from the third equation in (6.5) that $C = 0$ while the last equation gives

$$A^2 = \frac{4T^2}{Eh(\gamma_2 - \gamma_1)}. \quad (6.7)$$

Using (6.6), (6.7), the expression for the normal deflection may be presented in the form

$$w_n = \pm \frac{2L^2}{n^2 \pi^2} \sqrt{\frac{\gamma_2 - \gamma_1}{Eh}} \sin \frac{n\pi x}{L} \quad (n = 1, 2, \dots). \quad (6.8)$$

Here the signs \pm indicate an equal possibility of deviation according to an asymmetrical form of the right or left halves of the membrane.

The planar shape of the membrane and the interface of the liquids is always unstable for $\gamma_1 < \gamma_2$ and stable for $\gamma_1 \geq \gamma_2$. This

is valid in the absence of initial tension of the membrane ($T_0 = 0$). For vanishingly thin membrane these results are obvious. It is pointed out in [5] that a thin layer of mercury flows down from the water surface by fine jets. A Rayleigh–Taylor's instability occurs.

It follows from (6.8) that the planar shape of the membrane is unstable for any number of halfwaves n . Moreover, the deflection amplitudes and the tension force (6.6) rapidly decreases as n increases. Analysing the system energy, one can conclude that the larger n the more severe the instability of the system.

But there is an upper limit for the number n . For large values, no matter how small the thickness h may be, the bending rigidity begins to exert its effect. To estimate the upper limit of n , one can take approximately

$$D d^4 w/dx^4 + (\gamma_2 - \gamma_1)w = 0.$$

Substitute here the solution in the form $w = W \sin(n\pi x/L)$ to obtain the upper value of halfwave number

$$n_+ \approx \frac{2L}{\pi} \left(\frac{\gamma_2 - \gamma_1}{D} \right)^{1/4}. \quad (6.9)$$

If $\gamma_2 - \gamma_1 = 0.6 \cdot 10^{-4} \text{ kgf/cm}^3$, $h = 0.01 \text{ cm}$, $L = 5 \text{ cm}$, $E = 90 \text{ kgf/cm}^3$, the upper limit for n , according to (6.9), is $n_+ \approx 5$.

An experiment was made for a square oblong glass vessel [3]. The liquid under the membrane was water ($\gamma_1 = 10^{-3} \text{ kgf/cm}^3$), on the surface of which a thin rubber of thickness $h = 0.01 \text{ cm}$ was slightly stretched and fastened to the edges of vessel. Then a silicate glue of specific weight $\gamma_2 \approx 1.4 \cdot 10^{-3} \text{ kgf/cm}^3$, was poured along the wall by a fine jet. A deflection in the form of two half-

waves occurred. The state was stable. After being somewhat deflected and then released, the membrane oscillated and took its shape of two halfwaves. For a large forced deflection, a sinusoid in antiphase may occur, which means that the deflection with the opposite sign in (6.8) is realized. In the given experiment, stable deflected states in the form of many waves were not observed. When water ($\gamma_2 = \gamma_1$) was poured instead of glue, the plane shape of the membrane was stable.

All results presented in this paragraph were related to the scheme shown in Fig. 2.6*a*. Moreover, we used the incompressibility condition (4.5) for the liquid in the lower closed space. If this space is filled with a gas, the condition (4.5) is not used.

Let the gas pressure under the membrane in the planar state be $p_0 = \gamma_2 H$. The pressure is assumed to be kept constant in the course of deflecting the membrane from its plane state. Fig. 2.6*c* also leads to the same problem.

So, now the equation (6.4) is not valid. Putting $B = 0$, $A \neq 0$, $\sin \alpha_* L = 0$ in (6.5), we come to the solution (6.6), (6.8) considered above. If we put $A = 0$, $B \neq 0$, $\cos \alpha_* L = 0$ we obtain $\alpha_* L = n\pi/2$, where $n = 1, 3, \dots$. From the last two equations in (6.5), we find $C = 0$, $B^2 = 4\beta_*/\alpha_*$. Using definitions of β_* and α_* , we come to the following expressions for the membrane tension force

$$T_n = \left(\frac{2L}{n\pi}\right)^2 (\gamma_2 - \gamma_1) \quad (n = 1, 3, \dots) \quad (6.10)$$

and for the membrane deflection

$$w_n = \pm \frac{4L^2}{n^2\pi^2} \sqrt{\frac{\gamma_2 - \gamma_1}{Eh}} \sin \frac{n\pi x}{2L} \quad (n = 1, 3, \dots). \quad (6.11)$$

A comparison of (6.10), (6.11) to (6.6), (6.8) shows that the deflection and tension force according to the first symmetric form are respectively two and four times as much as those according to the first asymmetric form.

§7. Nonlinear deflection of membrane under concentrated action

So far the equilibrium of the tensile membrane has been considered in this chapter. But many materials have large rigidity in tension. In studying their behaviour under action of predominant transverse force, their tensility may be neglected.

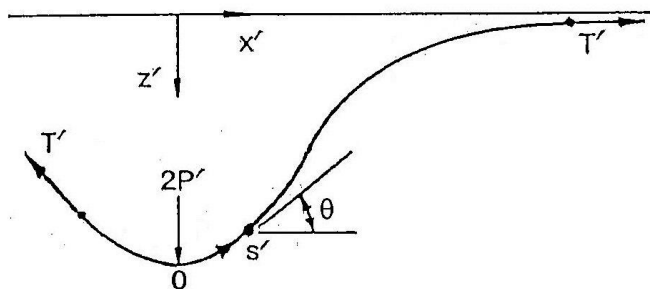


Fig. 2.7. The nontensile weightless plate infinite in size under action of forces $2P$ and T

Such problems will be considered in detail in chapters V and VI.

In this paragraph we present the solution of the equilibrium problem of a nontensile membrane (film) infinite in size, resting on the liquid surface, which is under action of forces distributed along line $x' = 0$ (Fig. 2.7). Their intensity is $2P'$. The film is assumed to be tensed along the axis x' at infinity by the uniform force T' . The weight of the film is neglected.

In §2 of this Chapter, for solving the equilibrium problem of the tensile membrane the system of nonlinear equations has been

used. Unlike that solution we shall now consider the arbitrary large deflection of the nontensile infinitely long film. In the chapter IV the same problem will be stated for the flexible plate. That is why the bending equation will be derived here, taking into account the bending rigidity. Since the interaction problem is two-dimensional we consider the beam/band under the concentrated force $2P'$. In doing so, we follow [9].

The local curvature is assumed to be proportional to the local bending moment $M = D d\theta/ds'$ where θ is the angle of the element rotation, s' the Lagrange coordinate ($s' = 0$ under the force $2P'$), D , M the bending rigidity and bending moment, respectively. The origin of Cartesian coordinates x' , z' lies on the undeformed surface of the plate.

The pressure from the liquid side is $p = \gamma z'$. Moreover, we have

$$\frac{dx'}{ds'} = \cos \theta, \quad \frac{dz'}{ds'} = -\sin \theta, \quad (7.1)$$

$$x'(0) = 0, \quad z'(0) = w'_0, \quad z'(\infty) = 0.$$

Equating the sum of moments to zero, we obtain

$$D \frac{d^2\theta}{ds'^2} = \left(\gamma \int_0^{s'} z' \cos \theta ds' - P' \right) \cos \theta + \left[T' - \frac{\gamma}{2} (z')^2 \right] \sin \theta. \quad (7.2)$$

In what follows in this paragraph, we use $D = 0$. Dividing the linear dimensions by $(T'/\gamma)^{1/2}$, we obtain from (7.1), (7.2)

$$(u - \alpha) \cos \theta + \left(1 - \frac{1}{2} z^2 \right) \sin \theta = 0, \quad \alpha = P'/T', \quad (7.3)$$

$$\frac{du}{ds} = z \cos \theta, \quad \frac{dx}{ds} = \cos \theta, \quad \frac{dz}{ds} = -\sin \theta. \quad (7.4)$$

Here an additional function u is introduced.

Boundary conditions have the form

$$\begin{aligned} u(0) = x(0) = 0, \quad z(0) = w_0, \\ u(\infty) = \alpha, \quad \theta(\infty) = z(\infty) = 0. \end{aligned} \quad (7.5)$$

The nonlinear problem (7.3)–(7.5) is interesting in that its exact analytical solution can be found. Given α , one may determine θ , u , x , z , w .

Differentiation of (7.3) with respect to s gives

$$(u - \alpha) \frac{d\theta}{ds} = z \sin \theta. \quad (7.6)$$

Using the expression

$$\frac{d\theta}{ds} = \frac{d\theta}{du} \frac{du}{ds} = \frac{d\theta}{du} z \cos \theta,$$

integrate (7.6) to find $u = \alpha + C \sin \theta$ where C is the integration constant. Then it follows from (7.3) that

$$\frac{1}{2} z^2 = 1 + C \cos \theta.$$

Conditions at infinity give $C = -1$. Hence

$$\frac{d\theta}{ds} = -z = -\sqrt{2 - 2 \cos \theta} = -2 \sin \frac{\theta}{2}. \quad (7.7)$$

The subsequent integration leads to the equation

$$s = -\ln \frac{\operatorname{tg}(\theta/4)}{\operatorname{tg}(\theta_0/4)}, \quad (7.8)$$

where θ_0 is the value of θ for $s = 0$. From the equation $u = -\alpha - \sin \theta$ we have $\theta_0 = \arcsin \alpha$.

The parametric form of the membrane deflection is found by integrating the equations (7.4), (7.7), (7.8) to obtain

$$x = -\ln \frac{\operatorname{tg}(\theta/4)}{\operatorname{tg}(\theta_0/4)} - 2 \cos \frac{\theta}{2} + 2 \cos \frac{\theta_0}{2}, \quad z = 2 \sin \frac{\theta}{2}. \quad (7.9)$$

Fig. 2.8 shows the variation of the deflection along the x -coordinate for three values of parameter α .

The relationship between the load parameter α and the membrane deflection under the concentrated force has the form

$$w_0 = 2 \sin(\theta_0/2) = \sqrt{2 - 2\sqrt{1 - \alpha^2}}. \quad (7.10)$$

As is seen, α can not be greater than unity. Hence, we should have $P' \leq T'$.

The maximum value of the membrane deflection under the load $2P'$ is attained for $\alpha = 1$. Then $w_0 = \sqrt{2}$ while the dimen-

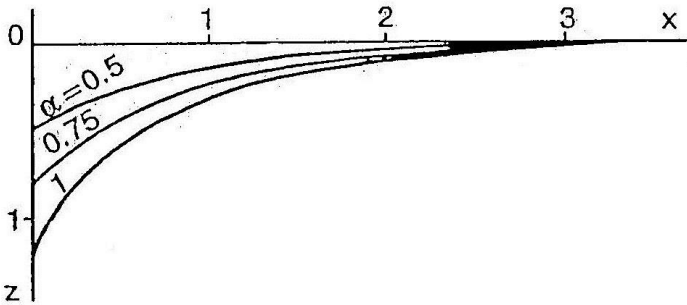


Fig. 2.8. Forms of large deflections of the nontensile film, infinite in size, on the liquid surface

sional value is $w'_0 = w_0 \sqrt{T'/\gamma} = w_0 \sqrt{P'/\gamma}$ or $w'_0 = \sqrt{2P'/\gamma}$.

The film and the load of weight $2P'$ "sink" if $\alpha > 1$ ($P' > T'$).

The membrane deflection in the horizontal direction at a large distance from the coordinate origin is

$$s - (x)_{s \rightarrow \infty} = 2 - 2 \cos \frac{\theta_0}{2} = 2 - \sqrt{2 + 2\sqrt{1 - \alpha^2}}.$$

CHAPTER III

EQUILIBRIUM OF A PLATE CONTACTING A LIQUID

§1. Bending of a beam resting on a water surface

A beam with specific weight γ_0 rests on a liquid with infinite extent. The liquid specific weight is γ . Evidently $\gamma_0 < \gamma$. The depth of submersion H of the lower surface of the beam with dimensions L , b , h is found from the equilibrium condition of buoyancy force and body weight to be

$$H = h\gamma_0/\gamma. \quad (1.1)$$

There is no bending in this state.

If some force P acts in the center of the beam (Fig. 3.1), then bending occurs. We are to find the maximum value of P under which liquid does not reach the upper beam surface, as well as the corresponding stresses and elastic deflections arising in the state. The latter are measured from the equilibrium state with submersion depth H . The deflection w is positive in the downward direction. We present a solution of the problem, following [2].

The equation of beam bending is

$$EJ d^4w/dx^4 = q$$

and the distributed load q consists only of the buoyancy force of the liquid ($-\gamma bw$) since the beam weight has already been taken

into account in determining the submersion depth (1.1). The equation may be written in the form

$$\frac{d^4 w}{dx^4} + 4\beta^4 w = 0, \quad 4\beta^4 = \frac{\gamma b}{EJ}. \quad (1.2)$$

Krylov's functions may be used for the solution. The table of these functions and their derivatives is given below [2]

n	$Y_n(\beta x)$	$Y'_n(\beta x)$	$Y''_n(\beta x)$	$Y'''_n(\beta x)$	$Y''''_n(\beta x)$
1	$\text{ch } \beta x \cos \beta x$	$-4\beta Y_4$	$-4\beta^2 Y_3$	$-4\beta^3 Y_2$	$-4\beta^4 Y_1$
2	$\frac{1}{2}(\text{ch } \beta x \sin \beta x + \text{sh } \beta x \cos \beta x)$	βY_1	$-4\beta^2 Y_4$	$-4\beta^3 Y_3$	$-4\beta^4 Y_2$
3	$\frac{1}{2} \text{sh } \beta x \sin \beta x$	βY_2	$\beta^2 Y_1$	$-4\beta^3 Y_4$	$-4\beta^4 Y_3$
4	$\frac{1}{4}(\text{ch } \beta x \sin \beta x - \text{sh } \beta x \cos \beta x)$	βY_3	$\beta^2 Y_3$	$\beta^3 Y_1$	$-4\beta^4 Y_4$

With w_0 , w'_0 , M_0 , Q_0 denoting the deflection, bending angle, bending moment and transverse force at $x = 0$, respectively, the solution of (1.2) by the method of initial parameters may be presented in the form

$$w = w_0 Y_1(\beta x) + \frac{w'_0}{\beta} Y_2(\beta x) + \frac{M_0}{EJ\beta^2} Y_3(\beta x) + \frac{Q_0}{EJ\beta^3} Y_4(\beta x). \quad (1.3)$$

In Fig. 3.1 the origin of coordinates is taken at the left end of the beam. Here $M_0 = 0$, $Q_0 = 0$. Values of w_0 and w'_0 are determined from the symmetry conditions

$$w'_0 = 0, \quad Q = P/2 \quad (x = L/2). \quad (1.4)$$

According to (1.3) and the table given above, we can write

$$w' = -4\omega_0\beta Y_4(\beta x) + \omega'_0 Y_1(\beta x),$$

$$w''' = -4\omega_0\beta^3 Y_2(\beta x) - 4\omega'_0\beta^2 Y_3(\beta x).$$

Satisfying the conditions (1.4), we find the deflections involved in (1.3) and the bending angle at point $x = 0$, i.e.

$$\omega_0 = \frac{P}{8EJ\beta^3 Y} Y_1\left(\frac{\beta L}{2}\right), \quad \omega'_0 = \frac{P}{2EJ\beta^2 Y} Y_4\left(\frac{\beta L}{2}\right),$$

$$Y = Y_2\left(\frac{\beta L}{2}\right) Y_1\left(\frac{\beta L}{2}\right) + 4Y_3\left(\frac{\beta L}{2}\right) Y_4\left(\frac{\beta L}{2}\right).$$

Substituting these values into (1.3), we determine the expression for deflection from the equilibrium state under the action of force P as

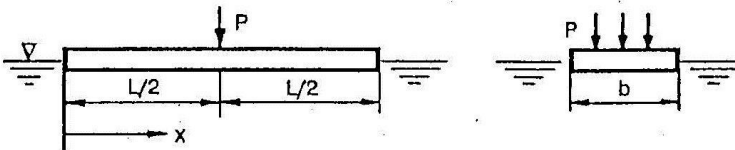


Fig. 3.1 Beam on the liquid surface under the action of force P

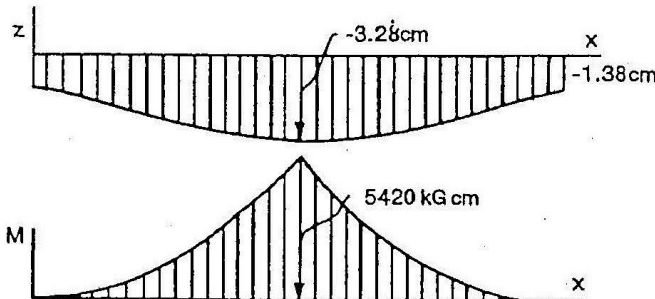


Fig. 3.2. Diagrams of deflection and bending moment arising under action of the force P

$$\omega = \frac{P}{8EJ\beta^3Y} \left[Y_1\left(\frac{\beta L}{2}\right) Y_1(\beta x) + Y_4\left(\frac{\beta L}{2}\right) Y_2(\beta x) \right]. \quad (1.5)$$

This solution is valid in so far as the upper beam surface is not in water, i.e. when $H + \omega < h$. From (1.5) the bending moment and stresses are found in the usual fashion.

In [2] the following data are taken: $\gamma_0 = 0.6 \text{ gf/cm}^3$, $\gamma = 1 \text{ gf/cm}^3$, $E = 10^5 \text{ kgf/cm}^2$, $L = 10^3 \text{ cm}$, $b = 20 \text{ cm}$, $h = 10 \text{ cm}$, $P = 50 \text{ kgf}$.

The depth of the uniform submersion without bending is $H = 6 \text{ cm}$. The coefficient $\beta = 2.34 \cdot 10^{-1} \text{ cm}^{-1}$, $\beta L/2 = 1.17$. Using the table of functions Y_n given above, we find

$$\begin{aligned} Y_1(1.17) &= 0.69, & Y_2(1.17) &= 1.10, \\ Y_3(1.17) &= 0.67, & Y_4(1.17) &= 0.26. \end{aligned}$$

Fig.3.2 shows the distribution of deflection ω along the beam. It may be seen that its total deflection is 1.38 cm (in addition to the submersion of $H = 6 \text{ cm}$ due to its own weight). Moreover the force P causes bending with a maximum deflection in the center. Its value is $(3.28 - 1.38) \text{ cm} = 1.9 \text{ cm}$. The diagram of the bending moment is also presented in this figure.

§2. Bending of a circular plate under liquid weight

The problem to be solved here is similar to one from §3 of the previous chapter (Fig. 2.1). The only difference is that the circular bottom of thickness h , of elasticity modulus E and Poisson's ratio ν is taken as a plate instead of a membrane.

Its own weight is neglected as compared with the liquid loading. Liquid level H in the deformed state of the plate is assumed

to be known. Under such an assumption the problem was considered in [1]:

The equation of axisymmetric bending of plate has the form

$$D \left(\frac{d^4 w}{dr^4} + \frac{2}{r} \frac{d^3 w}{dr^3} - \frac{1}{r^2} \frac{d^2 w}{dr^2} + \frac{1}{r^3} \frac{dw}{dr} \right) = \gamma (w + H). \quad (2.1)$$

Introducing the following notation for the ratio of specific liquid weight to stiffness of the plate

$$\beta^4 = \frac{\gamma}{D}, \quad D = \frac{Eh^3}{12(1-\nu^2)} \quad (2.2)$$

and finding the solution to the (2.1) in the class of cylindrical functions, we have

$$w = C_1 J_0(\beta r) + C_2 I_0(\beta r) + C_3 N_0(\beta r) + C_4 K_0(\beta r) - H. \quad (2.3)$$

Here $J_0(z)$, $N_0(z)$, $I_0(z)$, $K_0(z)$ are the conventional notations for zero-order Bessel's functions of real and imaginary argument.

For a continuous plate (without a hole in the center), the constants $C_3 = C_4 = 0$. Consider two types of conditions for fastening the plate to the walls. The edges are clamped, so that the deflection and slope are zero

$$w = dw/dr = 0 \quad (r = R) \quad (2.4)$$

or they are freely supported (deflection and bending moment are zero)

$$w = 0, \quad \frac{d^2 w}{dr^2} + \frac{\nu}{r} \frac{dw}{dr} = 0 \quad (r = R). \quad (2.5)$$

Requiring the solution (2.3) to satisfy conditions (2.4), we find

$$w = \frac{H}{\Delta(\beta R)} [I_1(\beta R) J_0(\beta r) - J_1(\beta R) I_0(\beta r) - \Delta(\beta R)], \quad (2.6)$$

$$\Delta(\beta R) = J_0(\beta R) I_1(\beta R) - J_1(\beta R) I_0(\beta R),$$

where J_1, I_1 are the Bessel's functions of the first order.

Given w , we may determine values of all plate stresses by common formulae. The derivations are valid only if the determinant $\Delta > 0$. As is known from §1,2 of Chapter II, this restriction is due to the assumption of model. "Critical" value $\beta R = 3.19$ is obtained from the equation $\Delta(\beta R) = 0$. Utilizing notation (2.2), we also find the value of the radius

$$R = 3.19/\beta = 3.19(D/\gamma)^{1/4}$$

up to which the solution (2.6) is valid.

For a metal plate with $E = 2 \cdot 10^6$ kgf/cm², $\nu = 0.3$, $h = 2$ cm the bending stiffness is $D = 1.46 \cdot 10^6$ kgf·cm. Specific weight of water is $\gamma = 10^{-3}$ kgf/cm³. Therefore $\beta^{-1} = 195.6$ cm, while the "critical" radius is equal to 624 cm. Let the plate radius be $R = 195.6$ cm. Then, from (2.6) we obtain

$$\frac{w}{H} = 0.5711J_0\left(\frac{r}{R}\right) + 0.4447I_0\left(\frac{r}{R}\right) - 1.$$

By this formula, the deflection $w = 0$ for $r = R$ and $w = 0.0158H$ in the plate center ($r = 0$).

If we drop γw in the right side of (2.1), i.e. we neglect additional load depending on deflection, it follows that

$$\frac{w}{H} = \frac{\gamma R^4}{64D} \left(1 - \frac{r^2}{R^2}\right)^2. \quad (2.7)$$

The deflection in the center calculated from (2.7) utilizing the numerical data presented above is $w(r=0) = 0.0156H$.

The slight difference between exact and approximate values in this example is due to the high plate stiffness and relatively small radius. The difference in bending moments and stresses is larger.

In the case of a freely supported edge from (2.3) and (2.5) we have the following constants

$$\begin{aligned} C_1 &= \frac{H(1-\nu)}{\beta R \Delta} I_0(\beta R) + \frac{H}{\Delta} I_0(\beta R), \\ C_2 &= -\frac{H(1-\nu)}{\beta R \Delta} J_0(\beta R) + \frac{H}{\Delta} J_0(\beta R), \end{aligned} \quad (2.8)$$

$$\Delta = \frac{1-\nu}{\beta R} [J_0(\beta R) I_1(\beta R) - I_0(\beta R) J_1(\beta R)] + 2J_0(\beta R) I_0(\beta R).$$

Substituting these into (2.3), we find the deflection value. It follows from conditions $\Delta(\beta R) = 0$ that $\beta R = 1.57$. This value is one half of that in the case of the clamped edge.

Using numerical data presented above, we obtain $R = 307$ cm. The expression for deflection is

$$\frac{w}{H} = 0.6993 J_0\left(\frac{r}{R}\right) + 0.3672 I_0\left(\frac{r}{R}\right) - 1.$$

According to this formula, the deflection in the center is $w = 0.0612H$.

Neglecting the additional load $g\omega$ we find, instead of (2.7), the following approximate value

$$\frac{w}{H} = \frac{\gamma R^4}{64D} \left(1 - \frac{r^2}{R^2}\right) \left(\frac{5+\nu}{1+\nu} - \frac{r^2}{R^2}\right). \quad (2.9)$$

From (2.9) the deflection of the plate center is $w = 0.0637H$.

§3. Bending of a circular plate covering cavity with liquid

Consider the equilibrium problem of an elastic cover of a cylindrical vessel filled with liquid (Fig. 2.3). This problem is similar to one in §3 of Chapter II except now the cover is a circular plate [1] rather than a membrane.

In the right side of equation (2.1) the loading term is $\gamma(H - w)$. Here w is supposed to be positive in the upward direction. The solution of this equation for a continuous plate has the form

$$w = \bar{C}_1 J_0(\beta r \sqrt{i}) + \bar{C}_2 J_0(\beta r \sqrt{-i}) + H. \quad (3.1)$$

Cylindrical function of complex argument may be presented as follows

$$J_n(z\sqrt{\pm i}) = u_n(z) \pm i v_n(z).$$

The functions $\text{ber}_n(z)$ and $\text{bei}_n(z)$ are also used in place of $u_n(z)$, $v_n(z)$. In what follows, we shall use these both denotations.

Derivatives of functions u_n and v_n are

$$u'_0(z) = -\frac{1}{\sqrt{2}}(u_1 - v_1), \quad v'_0(z) = -\frac{1}{\sqrt{2}}(u_1 + v_1),$$

$$u''_0(z) = v_0 + \frac{1}{\sqrt{2}z}(u_1 - v_1), \dots$$

Then (3.1) may be written as

$$w = C_1 u_0(\beta r) + C_2 v_0(\beta r) + H, \quad (3.2)$$

where C_1 , C_2 are new constants.

Satisfying the conditions (2.4) for the clamped edge, we obtain

$$C_1 \Delta = -H [u_1(\beta R) + v_1(\beta R)],$$

$$C_2 \Delta = -H [u_1(\beta R) - v_1(\beta R)], \quad (3.3)$$

$$\Delta = u_0(\beta R) [u_1(\beta R) - v_1(\beta R)] - v_0(\beta R) [u_1(\beta R) + v_1(\beta R)].$$

Thus, equations (3.2) and (3.3) represent solution of the problem stated. It is of interest that unlike the previous paragraph the equation $\Delta(\beta R) = 0$ does not have real roots. Therefore the obtained solution is valid for arbitrary values of parameter βR . Particularly, the critical plate radius does not exist.

For numerical data from previous paragraph the expression for the deflection (to be more precise, for the lift since $w > 0$ in upward direction) may be written as

$$\frac{w}{H} = 1 - 0.9846 u_0 \left(\frac{r}{R} \right) + 0.1235 v_0 \left(\frac{r}{R} \right).$$

In the plate center $w = 0.0154H$.

In the case of freely supported edges we find from (2.5) and (3.1) that

$$\begin{aligned} C_1 \Delta &= H \left\{ u_0(\beta R) - \frac{1-\nu}{\beta R \sqrt{2}} [u_1(\beta R) + v_1(\beta R)] \right\}, \\ C_2 \Delta &= H \left\{ v_0(\beta R) + \frac{1-\nu}{\beta R \sqrt{2}} [u_1(\beta R) - v_1(\beta R)] \right\}, \end{aligned} \quad (3.4)$$

$$\begin{aligned} \Delta &= -[u_0(\beta R)]^2 - [v_0(\beta R)]^2 + \left\{ \frac{1-\nu}{\beta R \sqrt{2}} u_0(\beta R) \times \right. \\ &\quad \left. \times [u_1(\beta R) + v_1(\beta R)] - v_0(\beta R) [u_1(\beta R) - v_1(\beta R)] \right\}. \end{aligned}$$

And here the equation $\Delta(\beta R) = 0$ also does not have real roots. Consequently, the solution (3.2), (3.4) is valid for any value of βR .

For the numerical data of §2 it follows from (3.2) and (3.4) that the deflection is

$$\frac{w}{H} = 1 - 0.9388 u_0 \left(\frac{r}{R} \right) + 0.3038 v_0 \left(\frac{r}{R} \right).$$

In the plate center $w = 0.0612H$.

§4. Hertz's problem of a floating plate

In one of the papers of German Physicist Hertz [3] the equilibrium of a circular plate is considered with load P in its center. The plate floats on a liquid surface. In Dinnik's work [1] this prob-

lem is solved, using cylindrical functions, which made it possible to simplify all manipulations. Consider this solution, following [1].

We shall use the equation (2.1) in which it is necessary to take distributed load $\gamma_0 h$ rather than γH . Here γ_0 , h are the specific weight and plate thickness, respectively. Moreover, the load $P\delta(r_0 - r)$ is acted over the area of small radius r_0 in the center of the plate, where $\delta = 1$ for $r < r_0$ and $\delta = 0$ for $r > r_0$. So, the equation of axially symmetric bending of circular plate has the form

$$D \left(\frac{d^4 w}{dr^4} + \frac{2}{r} \frac{d^3 w}{dr^3} - \frac{1}{r^2} \frac{d^2 w}{dr^2} + \frac{1}{r^3} \frac{dw}{dr} \right) = \gamma_0 h - \gamma w + P\delta(r_0 - r). \quad (4.1)$$

The deflection w is positive in the downward direction.

The solution of the homogeneous equation (3.1) may be written in the form

$$w = C_1 u_0(\beta r) + C_2 v_0(\beta r) + C_3 f_0(\beta r) + C_4 g_0(\beta r), \quad (4.2)$$

$$\beta = (\gamma/D)^{1/4},$$

where u_0 , v_0 are functions introduced in the previous paragraph.

Functions f_0 , g_0 are introduced in the same way

$$H_n(z\sqrt{\pm i}) = f_n(z) \pm i g_n(z), \quad n = 0, 1, \dots,$$

where H_n are Hankel's functions which vanish as $z \rightarrow \infty$. Values of the functions u_0 , v_0 , f_0 , g_0 are given in reference books on mathematics.

Consider first the solution of the problem with neglecting plate's own weight $\gamma_0 h$. It may be shown [1] that under a force P concentrated in the center, the constants in (4.2) are

$$C_3 = P/(4\beta^2 D), \quad C_4 = 0, \quad (4.3)$$

the constants C_1, C_2 are determined from conditions on the outer contour $r = R$.

In the case of an infinitely large radius R we shall have $C_1 = 0, C_2 = 0$ since the functions u_0, v_0 do not vanish for $r \rightarrow \infty$. Therefore, according to (4.2), (4.3), the deflection of plate will be

$$w = \frac{P}{4\beta^2 D} f_0(\beta r). \quad (4.4)$$

Tables in reference books may be used for deflection calculations. Asymptotic formulae are available for large values of the arguments ($\beta r > 6$). With increasing argument the function $f_0(\beta r)$ is a decaying oscillation. Its first few roots are 3.92; 8.33, etc. The subsequent roots may be presented in the approximate form as

$$(\beta r)_n = \pi \sqrt{2} (n - 1/8), \quad n = 0, 1, \dots$$

Waves have the form of concentric circles around the point of load application. For $n \gg 1/8$ the distance between neighboring waves is $\pi \sqrt{2} / \beta = \pi (4D/\gamma)^{1/4}$. The amplitude decreases quite rapidly. At the loading point ($r = 0$), the maximum deflection downward takes place and $f_0(0) = 1/2, w(0) = P/(8\beta^2 D)$. In moving away from the center along the radius of the plate, the deflection decreases. When $\beta r = 3.92$ the deflection vanishes. Then the plate surface becomes higher than the mean level of the liquid. After that the plate deflects downwards again and when $\beta r = 8.33$ the deflection becomes $w = 0$, etc.

For an ice cover, if $E = 27600 \text{ kgf/cm}^2, \nu = 1/4, h = 1 \text{ cm}, \gamma = 10^{-3} \text{ kgf/cm}^3$ the deflection under load point is $w(0) = 0.08P \text{ cm/kgf}$. For $h = 10 \text{ cm}, w(0) = 0.0025P \text{ cm/kgf}$.

In the case of a plate of finite radius R , floating on a liquid surface, it is necessary to impose the edge conditions. Suppose that the edge is free, i.e. the bending moment and transverse force are equal to zero

$$\frac{d^2w}{dr^2} + \frac{\nu}{r} \frac{dw}{dr} = 0, \quad \frac{d}{dr} \left(\frac{d^2w}{dr^2} + \frac{1}{r} \frac{dw}{dr} \right) = 0 \quad (r = R). \quad (4.5)$$

When the plate weight is not taken into account the constants C_3, C_4 in (4.2) are, as before, determined by (4.3). Constants C_1, C_2 are found from (4.5) to be

$$C_1 \Delta = \frac{P}{4\beta D} \left[\frac{(1-\nu)\sqrt{2}}{\beta R} (\hat{h}_1 u_1 + g_1 v_1) + g_0 (u_1 - v_1) - u_0 (\hat{h}_1 + g_1) \right],$$

$$C_2 \Delta = -\frac{P}{4\beta D} \left[\frac{(1-\nu)\sqrt{2}}{\beta R} (u_1 g_1 - v_1 \hat{h}_1) + \right. \\ \left. + v_0 (\hat{h}_1 + g_1) - g_0 (u_1 + v_1) \right], \quad (4.6)$$

$$\Delta = -\frac{(1-\nu)\sqrt{2}}{\beta R} (u_1^2 + v_1^2) + u_0 (u_1 + v_1) - v_0 (u_1 - v_1).$$

All the functions $u_0, v_0, g_0, u_1, v_1, \hat{h}_1, g_1$ here are for the argument $\beta r = \beta R$.

When the radius R is small (in comparison with the half wave length of the deflection) the deflection w on the contour is positive. Since we have taken the positive values of w in the downward direction, it follows that in this case the edge goes down lower than the liquid level.

Let us introduce the following criterion: if the edge is lower than liquid level the plate cannot be floating and to ensure the buoyancy of the plate, the deflection w has to be negative for

$r = R$. This condition together with (4.2), (4.3), (4.6) gives the following equation

$$\begin{aligned} \frac{(1-\nu)\sqrt{2}}{\beta R} \left[\dot{f}_0(u_1^2 + v_1^2) - u_0(\dot{f}_1 u_1 + g_1 v_1) - v_0(\dot{f}_1 v_1 - g_1 u_1) \right] + \\ + (\dot{f}_1 + g_1)(u_0^2 + v_0^2) + (u_1 + v_1)(\dot{f}_0 u_0 + g_0 v_0) - \\ - (u_1 - v_1)(\dot{f}_0 v_0 - g_0 u_0) = 0. \end{aligned} \quad (4.7)$$

Here again all the functions u_n , v_n , \dot{f}_n , g_n have the argument βR . It was found [1] that the first root of this equation is $\beta R = 2.64$ (note that in the case of the infinite plate the first root of equation $\dot{f}_0(\beta R) = 0$ from (4.4) is equal to 3.92). The second root is $\beta R = 7.12$. The following roots are determined by

$$(\beta R)_n = \pi \sqrt{2} (n - 3/8), \quad n = 3, 4, \dots$$

Consequently, if the plate radius is less than $2.64/\beta = 2.64(D/\gamma)^{1/4}$ the plate together with load P does not have an equilibrium state on the liquid surface. The equilibrium is attained when $R \geq 2.64/\beta$.

The analysis becomes more complicated if the first term in the right side of (4.1) is taken into consideration. Allowing for the corresponding partial solution, we have

$$w = C_1 u_0(\beta r) + C_2 v_0(\beta r) + \frac{P}{4\beta^2 D} \dot{f}_0(\beta r) + \frac{\gamma_0 h}{\gamma}. \quad (4.8)$$

When determining the constants C_1 , C_2 by (4.5) the influence of the last term in (4.8) is absent since it is independent of r . Therefore the expressions (4.6) are valid in this case as well. A total plate immersion of $\gamma_0 h/\gamma$ takes place as compared with the case of weightless plate.

Equating (4.8) to zero, we obtain an equation similar to (4.7) for the case of a weightless plate. According to (4.7), the least value of βR for which the plate equilibrium on the water surface is possible was independent of load P . Now it depends on both P and $\gamma_0 h$.

Consider an example in which $E = 2 \cdot 10^6$ kgf/cm², $\nu = 0.3$, $h = 0.1$ cm, $\gamma = 10^{-3}$ kgf/cm³, $\gamma_0 = 7.8 \cdot 10^{-3}$ kgf/cm³. If the plate weight $\gamma_0 h$ is neglected, the least radius of a floating plate is independent of P and equal to 54.3 cm.

When the plate weight $\gamma_0 h$ is taken into account the solution depends also on P . For example, if $P = 100$ kgf this radius is $R = 272$ cm. For $P = 10$ kgf the equation does not have real positive roots. Consequently, the plate with load $P = 10$ kgf cannot be floating. The same is valid for smaller P .

Thus, a circular plate of a certain radius with a load in the center floats while without a load or with a load not large enough it goes down. This is due to the larger immersion of the central part of the plate as compared with its periphery and to the corresponding displacement of the liquid from under it.

§5. Bending of a circular plate under concentrated load

A thin circular plate covers a container with liquid. There is also a liquid layer over the plate. Axisymmetrical bending of the plate takes place under the action of concentrated force P applied in the center of the plate. The case of pressure by rod (Fig. 3.3) will also be considered. The force of this action will be denoted by $q(r)$.

As is shown in chapter II, in the presence of liquid layers from the upper and lower sides of a membrane (or a plate), the term

γw is not involved in the expression of pressure on the membrane. The expression will include it if there is some difference in densities of layers above and under the membrane. Assume that a circular plate is clamped along both external ($r = a$) and internal ($r = b$) contours.

Let positive deflection and pressure be directed downwards. The equation of axisymmetrical bending of the plate is

$$D \left(\frac{d^2}{dr^2} + \frac{1}{r} \frac{d}{dr} \right)^2 w = q(r) - p_0. \quad (5.1)$$

As in chapter II, to determine the pressure p_0 , we use the incompressibility condition for the closed space

$$\int_0^a \omega r dr = 0. \quad (5.2)$$

When the radius b is small as compared with the external radius a , the action of the force $q(r)$ may be reduced to the concentrated load P . Such a problem was considered in [7].

In this case the general solution of equation (5.1) has the form

$$\omega = C_1 + C_2 \ln \frac{r}{a} + C_3 \left(\frac{r}{a} \right)^2 + C_4 \left(\frac{r}{a} \right)^2 \ln \frac{r}{a} - \frac{p_0 r^4}{64D}. \quad (5.3)$$

According to clamped boundary conditions and to condition (5.2), we obtain from (5.3) that

$$\omega = \frac{Pa^4}{64\pi D} \left[1 + 2 \left(\frac{r}{a} \right)^2 - 3 \left(\frac{r}{a} \right)^4 + 8 \left(\frac{r}{a} \right)^2 \ln \frac{r}{a} \right]. \quad (5.4)$$

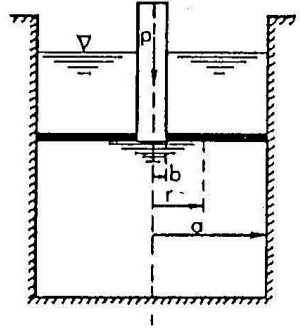


Fig. 3.3. A plate covering a container with liquid under action of central force

Without assuming the lower space to be closed and if $p_0 = 0$ the conditions (5.2) is not necessary. Then the solution of the equation (5.1) will have the form

$$w = \frac{Pa^4}{64pD} \left[4 - 4 \left(\frac{r}{a} \right)^2 + 8 \left(\frac{r}{a} \right)^2 \ln \frac{r}{a} \right] \quad (5.5)$$

rather than (5.4). This result is also valid for the case of no liquid.

Fig. 3.4a shows the results obtained from (5.4) (solid line) and from (5.5) (dashed line). These behave differently along the radius

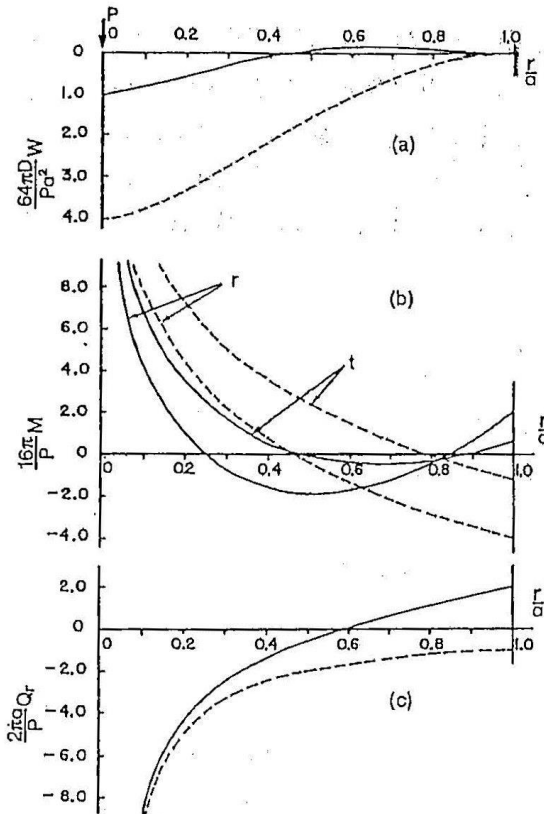


Fig. 3.4. Distributions of deflection (a), bending moments (b) and transverse force (c) along radius of circular plate (r , t are the radial and tangential moments, respectively, solid lines correspond to the case of closed space, dashed lines to nonclosed space)

as well as being different in the deflection values. The deflection in the center of the plate covering the nonclosed space is greater than that obtained from the condition (5.2) by a factor of 4.

The bending moments and transverse force, according to (5.4), are

$$M_r = -\frac{P}{16\pi} \left[(7 + 3\nu) - 3(3 + \nu) \left(\frac{r}{a}\right)^2 + 4(1 + \nu) \ln \frac{r}{a} \right],$$

$$M_\theta = -\frac{P}{16\pi} \left[(3 + 7\nu) - 3(1 + 3\nu) \left(\frac{r}{a}\right)^2 + 4(1 + \nu) \ln \frac{r}{a} \right], \quad (5.6)$$

$$Q_r = \frac{P}{2\pi a} \left[3 \frac{r}{a} - \frac{a}{r} \right].$$

Solid lines in Fig. 3.4*b* and Fig. 3.4*c* correspond to the Poisson's ratio $\nu = 0.3$ and were obtained from (5.6). Similar results for (5.5) are shown by dashed lines.

The value of pressure p_0 in closed space is

$$p_0 = 3P/(\pi a^2), \quad (5.7)$$

which is 3 times as much as that in the case of the action of the force P on the same plate but freely slipping along the container wall (this result has been presented in the Introduction).

Now consider the problem for the finite radius b of the rod (Fig. 3.3). In this case, the boundary conditions have the form

$$\frac{d\omega}{dr} = 0, \quad D \frac{d}{dr} \left(\frac{d^2\omega}{dr^2} + \frac{1}{r} \frac{d\omega}{dr} \right) = -\frac{bp_0}{2} + \frac{P}{2\pi b} \quad (r = b) \quad (5.8)$$

while $q = 0$ is taken in the equation (5.1).

Condition (5.2) transforms to

$$2 \int_b^a \omega r \, dr + b^2 \omega(b) = 0. \quad (5.9)$$

Fig. 3.5 shows the distribution of the bending moments M_r and M_θ as well as the transverse force for $b/a = 0.1$ and $\nu = 0.3$ (solid lines). Dashed lines show results for the case without liquid.

The pressure of the liquid in the space is

$$p_0 = \frac{3P}{\pi a^2} \frac{1 - \left(\frac{b}{a}\right)^4 + 4\left(\frac{b}{a}\right)^2 \ln \frac{b}{a}}{\left[1 - \left(\frac{b}{a}\right)^2\right]^3}. \quad (5.10)$$

For $b/a \rightarrow 0$ from (5.10) we obtain the expression (5.7).

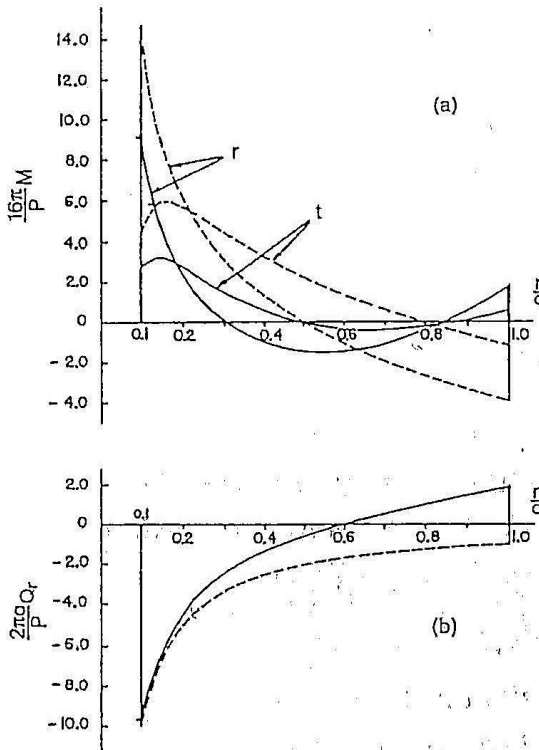


Fig. 3.5. Distribution of bending moments (a) and transverse force (b) along the radius of circular plate (r , t are the radial and tangential bending moments, respectively); solid lines correspond to the case of closed space, dashed lines to nonclosed space)

§6. Circular plate under the action of a noncentral concentrated load

If in the problem considered in the previous paragraph the concentrated load P is applied at a distance ρ from the center of the plate (Fig. 3.6), then the following incompressibility condition for the liquid in the closed space is used instead of (5.2)

$$\int_0^{2\pi a} \int_0^0 \omega r dr d\theta = 0. \quad (6.1)$$

The solution of the corresponding bending equation, after satisfying (6.1) and the clamped conditions for the edge, will have the form [6,8]

$$\begin{aligned} \omega = & \frac{Pa^2}{16\pi D} \left\{ \left(\frac{\rho}{a} \right)^2 \left[1 + \left(\frac{r}{\rho} \right)^2 - 2 \left(\frac{r}{\rho} \right) \cos \theta \right] \times \right. \\ & \left. \left(\frac{\rho}{a} \right) \left[1 + \left(\frac{r}{\rho} \right)^2 - 2 \left(\frac{r}{\rho} \right) \cos \theta \right]^{1/2} \right. \\ & \times \ln \frac{\left[1 + \left(\frac{r}{\rho} \right) \left(\frac{\rho}{a} \right)^2 - 2 \left(\frac{r}{\rho} \right) \left(\frac{\rho}{a} \right) \cos \theta \right]^{1/2} +}{\left[1 + \left(\frac{r}{\rho} \right) \left(\frac{\rho}{a} \right)^2 - 2 \left(\frac{r}{\rho} \right) \left(\frac{\rho}{a} \right) \cos \theta \right]^{1/2}} + \\ & \left. + \left[1 - \left(\frac{\rho}{a} \right)^2 \right] \left[1 - \left(\frac{r}{a} \right)^2 \right] - \frac{3}{4} \left[1 - \left(\frac{\rho}{a} \right)^2 \right]^2 \left[1 - \left(\frac{r}{a} \right)^2 \right]^2 \right\}. \end{aligned} \quad (6.2)$$

Pressure p_0 in the closed space produced by the action of the force P on the plate is [8]

$$p_0 = \frac{3P}{\pi a^2} \left[1 - \left(\frac{\rho}{a} \right)^2 \right]^2. \quad (6.3)$$

When the force is applied in the center ($\rho = 0$) the solutions (6.2) and (6.3) are reduced to expressions (5.4) and (5.7), respectively. In Fig. 3.7 line 1 shows the deflection along the diameter

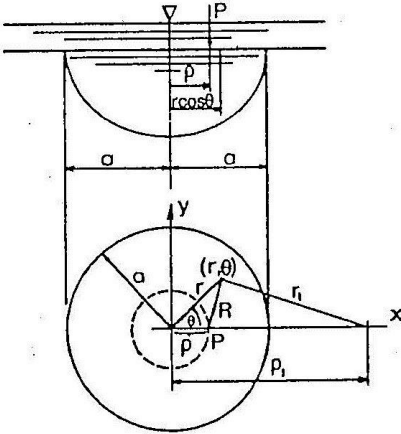


Fig. 3.6. Bending of a circular plate, covering the space with liquid under action of noncentrally applied force

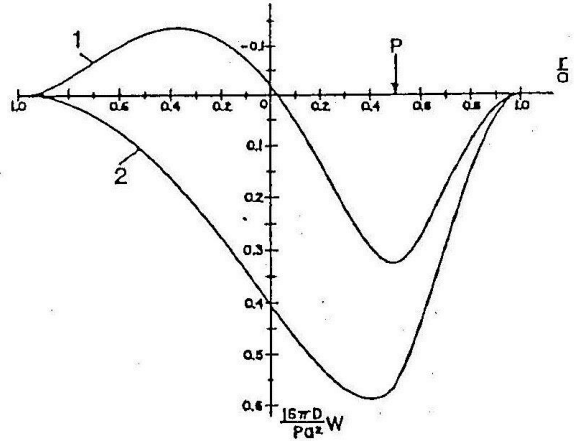


Fig. 3.7. Deflection diagram of circular plate under action of noncentrally applied force (1—in the case of closed space, 2—in the case of nonclosed space)

$\theta = 0$, $\theta = \pi$ for $\rho/a = 1/2$, line 2 presents the deflection distribution for the case when the space under the plate is not closed. This has been considered in more detail in the previous paragraph.

In the absence of the upper liquid layer the term γw occurs in the equation of the plate bending, as was discussed in Chapter II in detail. In this case the solution may be written [8] as

$$w = \frac{P}{2\pi\beta^2 D} \left\{ \text{kei}(\beta R) + E + \left[\Phi_0(r) + 2 \sum_{n=1}^{\infty} \Phi_n(r) \cos(n\theta) \right] \right\}, \quad (6.4)$$

where the following notations have been used

$$\begin{aligned}\Phi_0 &= A_0 \operatorname{ber}(\beta r) + B_0 \operatorname{bei}(\beta r), \\ \Phi_n &= A_n \operatorname{ber}_n(\beta r) + B_n \operatorname{bei}_n(\beta r), \\ E &= 2\pi p_0 / (\beta^2 P), \\ R &= (r^2 + \rho^2 - 2r\rho \cos \theta)^{1/2}.\end{aligned}\tag{6.5}$$

The cylindrical functions kei , ber , bei , ber_n , bei_n involved in (6.5) are given in mathematical reference books.

Satisfying the clamped conditions for the plate edge and using equation (6.1), we obtain the following values of the constants

$$\begin{aligned}A_0 &= \frac{1}{\Delta_0} \begin{vmatrix} \lambda_0 & \operatorname{bei}(\beta a) & 1 \\ \gamma_0 & \operatorname{bei}'(\beta a) & 0 \\ \kappa_0 & -\operatorname{ber}'(\beta a) & \beta a/2 \end{vmatrix}, \\ B_0 &= \frac{1}{\Delta_0} \begin{vmatrix} \operatorname{ber}(\beta a) & \lambda_0 & 1 \\ \operatorname{ber}'(\beta a) & \gamma_0 & 0 \\ \operatorname{bei}'(\beta a) & \kappa_0 & \beta a/2 \end{vmatrix}, \\ A_n &= \frac{\lambda_n \operatorname{bei}'_n(\beta r) - \gamma_n \operatorname{bei}_n(\beta r)}{\operatorname{ber}_n(\beta r) \operatorname{bei}'_n(\beta r) - \operatorname{ber}'_n(\beta r) \operatorname{bei}_n(\beta r)}, \\ B_n &= \frac{\gamma_n \operatorname{ber}_n(\beta r) - \lambda_n \operatorname{ber}'_n(\beta r)}{\operatorname{ber}_n(\beta r) \operatorname{bei}'_n(\beta r) - \operatorname{ber}'_n(\beta r) \operatorname{bei}_n(\beta r)}.\end{aligned}$$

The prime here denotes the derivative with respect to r . Moreover, the following notations have been used

$$\Delta_0 = \begin{vmatrix} \operatorname{ber}(\beta a) & \operatorname{bei}(\beta a) & 1 \\ \operatorname{ber}'(\beta a) & \operatorname{bei}'(\beta a) & 0 \\ \operatorname{bei}'(\beta a) & -\operatorname{ber}'(\beta a) & \beta a/2 \end{vmatrix},$$

$$\lambda_n = -[\operatorname{kei}_n(\beta a) \operatorname{ber}_n(\beta \rho) + \operatorname{ker}_n(\beta a) \operatorname{kei}_n(\beta a)],$$

$$\gamma_n = -[\text{kei}'_n(\beta a) \text{ber}_n(\beta \rho) + \text{ker}'_n(\beta a) \text{bei}_n(\beta a)],$$

$$n = 0, 1, 2, \dots,$$

$$\kappa_0 = \frac{1}{\beta a} - [\text{kei}'(\beta a) \text{bei}(\beta \rho) - \text{ker}'(\beta a) \text{ber}(\beta \rho)].$$

The condition (6.1) influences only the constants A_0 and B_0 whereas the constants A_n, B_n remain unchanged even in the case

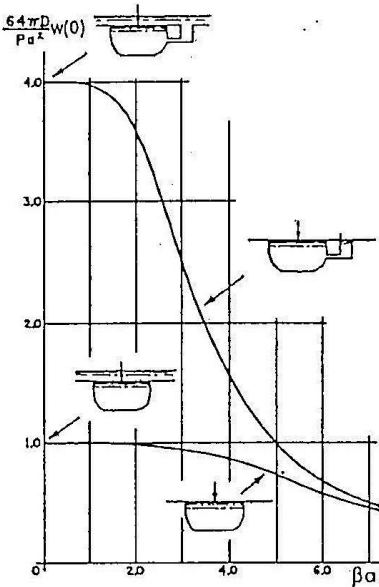


Fig. 3.8. The deflection in the center of the circular plate as a function of specific liquid weight

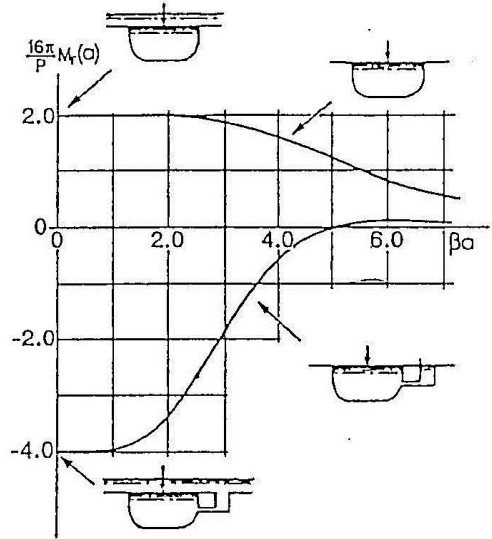


Fig. 3.9. Variation of radial bending moment at the clamped edge of the circular plate

of nonclosed space. The expression of the pressure p_0 in the space has the form [8]

$$p_0 = \begin{vmatrix} \text{ber}(\beta a) & \text{bei}(\beta a) & \lambda_0 \\ \text{ber}'(\beta a) & \text{bei}'(\beta a) & \gamma_0 \\ \text{bei}'(\beta a) & -\text{ber}'(\beta a) & \kappa_0 \end{vmatrix}. \quad (6.6)$$

Nondimensional deflection in the center of the circular membrane as a function of the parameter βa for $\rho = 0$ is shown in Fig. 3.8. The numerical values of D and a are unchanged, only the value of γ varies. The results for both closed and nonclosed spaces are given. The presence of the upper liquid layer corresponds to the deflection values for $\beta a = 0$.

It may be concluded from the plot, that the effect of the lift in the bending equation is insignificant within $0 \leq \beta a \leq 2.0$ in the case of closed space and within $0 \leq \beta a \leq 1.0$ in the case of a nonclosed space. Within these limits the effect of the lift may be neglected. With increasing liquid density the deflections decrease and more rapidly in the case of a nonclosed space. For $\beta a > 0$ the curves approach each other. Thus, for the heavy liquid the condition of its incompressibility does not exert appreciable effect on the solution. As is seen from Fig. 3.9, the same estimations are valid for the bending moment M_r at $r = a$.

§7. Cylindrical bending of a vertical plate contacting a liquid of limited volume

Consider the linear problem of bending for a vertical plate or beam-wall subjected to a hydrostatic pressure (Fig. 3.10). Assume that in undeformed state the plate is planar and the liquid height H_0 is equal to plate length L . The plate edges are hinged. In the bent state of the plate the liquid height is H . Consequently, the liquid load on the plate varies, depending on its deflection value. Suppose that the liquid surface is sub-

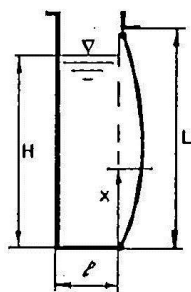


Fig. 3.10. Cylindrical bending of vertical plate under hydrostatic pressure

jected to the pressure p_0 equal to the pressure on the external side of the plate, the pressure acting on the plate is determined only by the height of the liquid column.

So, the incompressibility condition has the form

$$\int_0^H w \, dx = (L - H)l, \quad (7.1)$$

where l is the width of the container filled with liquid for the undeformed plate.

The equation of plate bending is

$$D \frac{d^4 w}{dx^4} = \gamma(H - x), \quad D = \frac{Eh^3}{12(1 - \nu^2)}, \quad (7.2)$$

where the right side corresponds to $x < H$. It vanishes if $x \geq H$.

Boundary conditions are

$$w = d^2 w / dx^2 = 0 \quad (x = 0, L). \quad (7.3)$$

An approximate solution is found in the form satisfying the condition (7.3)

$$w = W_1 \sin \frac{\pi x}{L} + W_2 \sin \frac{2\pi x}{L}. \quad (7.4)$$

Substituting (7.4) into (7.1), we have

$$\left(1 - \cos \frac{\pi H}{L}\right) W_1 + \frac{1}{2} \left(1 - \cos \frac{2\pi H}{L}\right) W_2 = \pi l \left(1 - \frac{H}{L}\right),$$

H is to be found from this expression using deflection amplitudes W_1, W_2 .

Consider the case when H is insignificantly different from L , i.e. the liquid level does not come down strongly. Hence, the value

$$\tilde{h} = 1 - H/L \quad (7.5)$$

is small as compared with unity.

Using formulae of the form $\cos \pi(1 - \tilde{h}) = -\cos \pi\tilde{h}$ and expanding the trigonometric functions into a power series, we have

$$2\left(1 - \frac{\pi^2 \tilde{h}^2}{4}\right) W_1 + \pi^2 \tilde{h}^2 W_2 = \pi \tilde{h} l.$$

The first approximation is $\pi \tilde{h} l = 2W_1$. Substituting it into non-linear terms, we obtain a refined relationship

$$\pi \tilde{h} = \frac{2}{l} \left(1 - \frac{1}{l^2} W_1^2\right) W_1 + \frac{4}{l^3} W_1^2 W_2.$$

It shows that the first approximation $\pi \tilde{h} l = 2W_1$ suffices for the linear problem if $(W_1/l)^2 \ll 1$.

Taking into account (7.5), we have an approximate value for the height of the liquid column

$$H = L(1 - 2W_1/\pi l). \quad (7.6)$$

Note that this expression does not have the amplitude of the second harmonic of (7.4). It is seen from (7.6) that with increasing container width, the liquid level tends to its initial value ($H \rightarrow L$).

Integration of equation (7.2) is made by Bubnov-Galerkin's method, using (7.4). In doing so, the left side of equation (7.2) is integrated between 0 and L while the right one between 0 and H . The value of the upper limit is given by expression (7.6). We have

$$D \int_0^L \frac{d^4 w}{dx^4} \begin{pmatrix} \sin \frac{\pi x}{L} \\ \sin \frac{2\pi x}{L} \end{pmatrix} dx = \gamma \int_0^H (H - x) \begin{pmatrix} \sin \frac{\pi x}{L} \\ \sin \frac{2\pi x}{L} \end{pmatrix} dx.$$

For these two equations in W_1 , W_2 we make the same expansion of the trigonometric functions into power series in terms of $\pi \tilde{h}$. And it turns out that in terms of the amplitudes W_1 , W_2 , the

upper limit H does not affect the solution (the corresponding effect is of order $(\pi\tilde{h})^2$). Lowering the level influences the solution through the expression under the integral.

Introducing the dimensionless parameter

$$\gamma_* = \frac{2\gamma}{\pi D} \left(\frac{L}{\pi}\right)^4 \approx 0.07 \frac{\gamma L}{E} \left(\frac{L}{\pi}\right)^3, \quad (7.7)$$

we obtain the following amplitude values

$$W_1 = \frac{\pi l L \gamma_*}{\pi l + 4L\gamma_*}, \quad W_2 = \frac{\gamma_* L}{32}.$$

According to (7.4), the deflection of the plate referred to its length is

$$\frac{w}{L} = \frac{\pi l \gamma_*}{\pi l + 4L\gamma_*} \sin \frac{\pi x}{L} + \frac{\gamma_*}{32} \sin \frac{2\pi x}{L}. \quad (7.8)$$

The bending of the plate takes place mainly as one half wave of the sinusoid. The presence of the term with γ_* in the denominator violates the direct proportionality between the parameters of deflection and hydrostatic pressure. It is due to the fact that when the liquid level falls, the pressure acting on the plate decreases. And the greater the ratio L/l (i.e. the narrower the cavity occupied by the liquid) the more significant this effect. For the same parameter γ_* , the deflection of the plate is greater for a wider cavity since H in this case is slightly different from L . This may be seen from (7.6)

$$\frac{H}{L} = 1 - \frac{2L\gamma_*}{\pi l + 4L\gamma_*}. \quad (7.9)$$

Note that when $4L\gamma_*/(\pi l) \gg 1$, it follows from (7.8), (7.9) that $W_1/L \rightarrow \pi l/(4L)$, $H/L \rightarrow 1/2$. But the linear approximation here does not correspond to a realistic case.

§8. Stability of a vertical plate in a liquid

In a vessel with an open upper cover, the thin partition-plate is subjected to compression by a force referred to the unity of the edge width. The notations are given in Fig. 3.11. Consider the problem of the stability of a compressed plate in planar formulation [10].

As a result of partition buckling, the difference between liquid levels $H_2 - H_1$ and lateral pressure occur. They are related by

$$q = \gamma (H_2 - H_1) = \frac{1}{m} \int_{-L/2}^{L/2} w \, dx, \quad m = \frac{l_1 l_2}{\gamma (l_1 + l_2)}. \quad (8.1)$$

Here the condition of liquid incompressibility has been used. The true limits of integration (liquid levels) have been substituted for mean value $L/2$. The corresponding difference, as was shown in previous paragraph, is of order $(\pi \tilde{h})^2$, where $\tilde{h} = 1 - H/L$ and in the linear problem it is small as compared with unity. The pressure q (8.1), acting on the plate is directed into the side of the liquid with the higher level. That is why it plays a stabilizing role when the plate is buckled symmetrically.

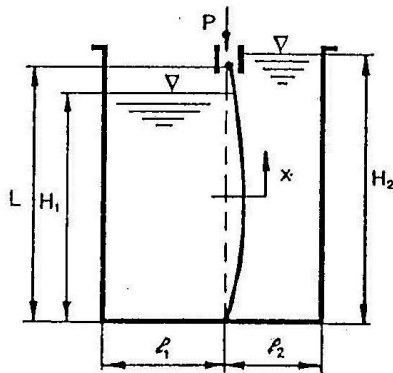


Fig. 3.11. Buckling of vertical partition contacting liquid

The differential equation for buckling of the partition has the form

$$D \frac{d^4 w}{dx^4} + P \frac{d^2 w}{dx^2} = q. \quad (8.2)$$

According to (8.1), the right side of equation (8.2) is independent of x . Therefore, its solution may be written as follows

$$w = C_1 \sin \alpha x + C_2 \cos \alpha x + C_3 \alpha x + C_4 + qx^4/(2P), \quad (8.3)$$

$$\alpha^2 = P/D.$$

Let both partition edges be hinged, i.e. $w = d^2w/dx^2 = 0$ ($x = -L/2, L/2$). In considering the asymmetric buckling about the middle ($x = 0$), it is necessary to take $C_2 = C_4 = 0$ in (8.3). In this case the levels from two sides of the partition do not change. Therefore, $q = 0$ and the problem reduces to a classical buckling problem. Two half waves occur. The minimum critical force is known in this case to be

$$P = 4\pi^2 D/L^2 \quad (\alpha L = 2\pi). \quad (8.4)$$

Now consider the symmetric form of buckling about the middle of the plate. Substitute the value of deflection for symmetric form

$$w = C_2 \cos \alpha x + C_4 + qx^2/(2P) \quad (8.5)$$

into (8.1) and satisfy the plate fastening conditions. Putting the determinant equal to zero, we derive the equation in αL

$$\operatorname{tg} \frac{\alpha L}{2} = \frac{\alpha L}{2} + \frac{\alpha^3 L^3}{24} - \frac{m\alpha^3 P}{2}. \quad (8.6)$$

For unlimited width of vessel, $m \rightarrow \infty$, it follows from (8.6) that $\alpha L = \pi$. Therefore

$$P = \pi^2 D/L^2. \quad (8.7)$$

This is a critical value of compressive force for a simply supported plate (buckling with one-half wave formation). Thus the liquid here does not affect the critical force value.

Turn back to the case of a vessel of limited dimensions. Rewriting (8.6) in the form

$$\frac{mD}{L^5} = -\frac{1}{(\alpha L)^5} \operatorname{tg} \frac{\alpha L}{2} + \frac{1}{2(\alpha L)^4} + \frac{1}{24(\alpha L)^2}$$

and varying αL , we obtain the function presented in Fig. 3.12. It shows that when $mD/L^5 > 1.4 \cdot 10^{-3}$ the loss of stability of the partition is accompanied by a one half-wave deformation (the buckling form is symmetrical about the middle $x = 0$) and in the case of $mD/L^5 < 1.4 \cdot 10^{-3}$ it is accompanied by a two half-waves deformation (asymmetric form). The critical force is found from (8.4).

The latter occurs for narrow vessels, thin partitions and a dense liquid. In fact, the thin plate, bent in the form of one half-wave, is not "able" to hold the large difference of heavy liquid levels and the related lateral pressure and therefore "prefers" to take the form of two half-waves where the mentioned difference and pressure disappear.

As follows from Fig. 3.12, for a vessel of large width and a plate of large bending stiffness ($mD/L^5 \rightarrow \infty$), the root $\alpha L \rightarrow \pi$. Critical force is determined by expression (8.7). One half-wave appears.

If the vessel is closed and completely full with liquid, the problem is known to change essentially. Here the difference of liquid levels from two sides of the partition cannot appear ($H_1 = H_2 = 0$). The buckling has to satisfy the condition

$$\int_{-L/2}^{L/2} w dx = 0. \quad (8.8)$$

The necessity of taking into account the pressure p_0 arises. Since it is constant in the whole volume and consequently along the length of the plate, the general solution (8.3) is also valid in this case. The lateral pressure $q = p_0$, as well as the constants C_i cannot be found in the linear stability problem.

So, for a symmetric buckling, we have

$$w = C_2 \cos \alpha x + C_4 + C_5 x^2, \quad C_5 = q/(2P).$$

Making use of the conditions of hinged fastening and (8.8) and setting the corresponding determinant equal to zero, we find

$$\operatorname{tg} \frac{\alpha L}{2} = \frac{\alpha L}{2} + \frac{(\alpha L)^3}{24}. \quad (8.9)$$

The lowest nonzero root of (8.9) is $\alpha L = 9.374$. Therefore the critical force

$$P = \frac{(\alpha L)^2 D}{L^2} = \frac{87.87 D}{L^2}$$

is greater than that for the symmetric form (8.4). The loss of stability for the symmetric form takes also place in the case of a closed vessel completely filled with liquid.

Note in conclusion that in the case of partition buckling with respect to the symmetric form, the compressive force and relevant half-wave number depend on the parameters of liquid and vessel whereas in the asymmetric case there is no such an explicit depen-

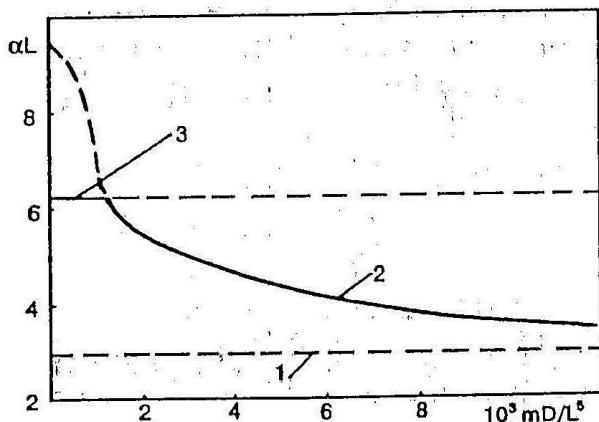


Fig. 3.12. Critical values of parameter aL as functions of parameter mD/L^5 : 1 – for the plate not contacting liquid (buckling with one half wave deformation); 2 – for the plate contacting liquid (buckling with one half wave deformation); 3 – for the plate contacting liquid (buckling with two half waves deformation, asymmetric form)

dence. The latter case is as if there were no influence of the environment at all. But this conclusion is not valid. Without a liquid, the loss of stability with two half-waves deformation does not arise.

Turn now to the stability problem of horizontal plate which is between layers of liquid with different specific weights (Fig. 2.6). Its formulation has been given in § 5 of chapter II for the case of a membrane. The critical difference of specific weights is [5]

$$\frac{\gamma_2 - \gamma_1}{D} = \left(\frac{5\pi}{4L} \right)^4.$$

Here γ_1 and γ_2 correspond to the upper and lower layers, respectively, $2L$ is the plate width.

§9. Influence of medium compressibility on plate bending

To understand the influence of compressibility, let us consider, as an example, the bending of a long plane plate germetically covering the cavity with rigid walls, being under action of forces distributed along the line $x = 0$. The coordinate origin is in the middle of the span of length $2L$. Positive values of deflection w are directed downwards.

The fluid compression in the cavity of unit length under plate bending is assumed to be adiabatic, i.e. the law (0.8) from Introduction governs. In changing the initial volume of the cavity V_0 by value v due to plate bending, the initial mass M_0 of the medium enclosed in the cavity remains the same. Therefore $\rho_0 = M_0/V_0$,

$$\rho = M_0/(V_0 - v). \text{ Because } v = \int_{-L}^L w dx, \text{ then according to (0.8)}$$

we can write

$$p = p_0 \left[1 - \frac{1}{V_0} \int_{-L}^L w dx \right]^{-\kappa}. \quad (9.1)$$

Here p_0 is the pressure in the cavity before deformation, w the deflection, κ the ratio of the specific heats (for air $\kappa = 1.4$, water $\kappa = 7$, ethyl alcohol $\kappa \approx 1.15$, incompressible fluid $\kappa = \infty$).

The pressure will change adiabatically if the plate is loaded quite rapidly. We assume that the loading rate cannot be such that the dynamic effects in the system should be taken into account. Such an investigation was made in [4].

The linear equation of band bending under the action of the pressure (9.1) and concentrated load P applied to the middle of the span has the form

$$D \frac{d^4 w}{dx^4} = P \delta(x - 0) - \frac{\kappa p_0}{V_0} \int_{-L}^L w dx, \quad (9.2)$$

where $\delta = 1$ for $x = 0$ and $\delta = 0$ for $x \neq 0$. The external uniform pressure is taken to be p_0 .

Using hinge fastening, taking w in the form

$$w = \sum_{n=1,3,\dots}^N W_n \cos \frac{n\pi x}{2L} \quad (9.3)$$

and solving the equation (9.2) by Bubnov-Galerkin's method, we obtain

$$W_1 = \frac{P}{A} \left(1 + \frac{B}{A} \right)^{-1}, \quad W_3 = \frac{1}{3^4} \frac{P}{A} \left(1 + \frac{4}{3} \frac{B}{A} \right) \left(1 + \frac{B}{A} \right)^{-1}, \quad (9.4)$$

$$A = DL \left(\frac{\pi}{2L} \right)^4, \quad B = \frac{4\kappa p_0}{V_0} \left(\frac{2L}{\pi} \right)^2.$$

In (9.4) the terms of order 3^{-6} as compared to unity have been dropped (taking $A \sim B$).

The influence of fluid on the plate bending depends on the ratio (putting $\nu = 0.3$, $V_0 = 2LH$)

$$\frac{B}{A} = 0.091\kappa \frac{p_0}{E} \frac{2L}{H} \left(\frac{2L}{h}\right)^3, \quad (9.5)$$

i.e. it depends on the elastic features and geometrical dimensions of the plate and medium (in the cavity). With increasing relative depth $H/2L$ this dependence decreases.

If $p_0/E = 10^{-6}$, $\kappa = 1.4$, $2L/H = 2$, $h/2L = 10^{-2}$, we shall have $B/A = 0.255$ and $W_1 = 0.797 P/A$, $W_3 = 1.067 \cdot 3^{-4} P/A$ versus $W_1 = P/A$ and $W_3 = 3^{-4} P/A$ for the case when the cavity is not taken into account ($B/A = 0$). For $\kappa = 7$ and other data same as above, B/A amounts to 1.27, that means that the equation (9.2) and subsequent formulae cannot be used since they are valid only for small values of B/A . In such cases more terms in the binomial expansion of expression (9.1) should be retained. Note that the necessity of including nonlinear terms in the right side of (9.2) may arise earlier than that for the nonlinear term due to the membrane force in the plate.

Using this simplest problem as an example, consider the step-by-step method with the scheme

$$D \frac{d^4 \omega^{(i)}}{dx^4} = P \delta(x-0) - \frac{\kappa p_0}{V_0} \int_{-L}^L \omega^{(i-1)} dx \quad (i = 1, 2, \dots), \quad (9.6)$$

where $\omega^{(0)} = 0$ is assumed. After the first step we obtain $W_1^{(1)} = P/A$ as a first approximation to W_1 in the expansion (9.3). The

second and third approximations are

$$W_1^{(2)} = \frac{P}{A} \left(1 - \frac{B}{A} \right), \quad W_1^{(3)} = \frac{P}{A} \left(1 - \frac{B}{A} + \frac{B^2}{A^2} - \dots \right). \quad (9.7)$$

Thus, the approximations (9.7) converge to the exact value $W_1 = (P/A)(1 + B/A)^{-1}$ under condition $B/A < 1$. For small values of B/A two or three approximations may be quite enough. For data considered above $W_1^{(2)} = 0.745 P/A$; $W_1^{(3)} = 0.810 P/A$. The exact value is $W_1 = 0.797 P/A$.

This method turns to be also useful in solving more complex problems. They include, for example, the case of a plate when the lengths of its sides are of the same order.

The solution (9.4) cannot be used in the case of incompressible fluid. Corresponding plate bending has been examined in previous paragraphs. Now let us consider the solution of the problem by the method used here and compare the results obtained with (9.4).

The back pressure on the plate, instead of (9.1), is

$$p = \frac{P}{2L} + \frac{R}{L}, \quad R = -D \left. \frac{d^3 w}{dx^3} \right|_{x=L}. \quad (9.8)$$

It is found from the condition of the whole plate equilibrium. In (9.8) R is the reaction at the support. Substituting (9.3) into incompressibility condition, we obtain

$$W_N = -N \sum_{n=1,3,\dots}^{N-2} \frac{1}{n} W_n (-1)^{(n-N)/2}. \quad (9.9)$$

This condition reduces the approximation (9.3) with $(N + 1)/2$ variational parameters to approximation with $(N - 1)/2$ variational parameters

$$w = \sum_{n=1,3,\dots}^{N-2} W_n \left[\cos \frac{n\pi x}{2L} - \frac{N}{n} (-1)^{(n-N)/2} \cos \frac{n\pi x}{2L} \right]. \quad (9.10)$$

The pressure (9.8) does not do work on deflections (9.10). On integrating the bending equation

$$D(d^4w/dx^4) = P\delta(x-0) - p$$

by Bubnov-Galerkin's method the last term in it disappears. So, we shall have

$$\begin{aligned} W_n \left[1 + \left(\frac{N}{n} \right)^6 \right] + \frac{N^6}{n^5} \sum_{k=1,3,\dots}^{N-2} \frac{1}{k} W_r (-1)^{(n+k)/2-N} = \\ = \frac{P}{A} \left[1 - \frac{N}{n} (-1)^{(n-N)/2} \right]. \end{aligned} \quad (9.11)$$

In the sum over k the member corresponding to $k = n$ is dropped.

Consider an example with three members in expansion (9.3) ($N = 5$). Then, according to (9.10)

$$w = W_1 \left(\cos \frac{\pi x}{2L} - 5 \cos \frac{5\pi x}{2L} \right) + W_3 \left(\cos \frac{3\pi x}{2L} - \frac{5}{3} \cos \frac{5\pi x}{2L} \right).$$

We find W_1 and W_3 from (9.11) and W_5 from (9.9). Their values with error of 3^{-6} as compared with the unity are

$$W_1 = \frac{4P}{3^6 A} \left[1 - \left(\frac{3}{5} \right)^6 \right], \quad W_3 = \frac{4P}{3^5 A}, \quad W_5 = \frac{4P}{5^5 A}.$$

Unlike the case of incompressible fluid when the first member of the expansion (9.3) is the largest one (then the series converges with the rate n^{-4}), in the case of compressible fluid the second member of (9.3) is the largest, namely it exceeds the first member approximately by a factor of three.

Note that the bending of plate contacting an incompressible fluid is completely independent of physical properties of the fluid and cavity dimensions. As follows from (9.4), (9.5), it depends on the mentioned properties in the case of a compressible fluid.

§10. Influence of medium compressibility on plate stability

Consider the stability of a plate which is subjected to compression by force N . As in previous paragraph, a long plate hermetically closes a cavity with compressible fluid.

We assume again that pressures from two sides of the plate are equal to each other before its buckling. In the linear approximation we shall have

$$D \frac{d^4 w}{dx^4} + N \frac{d^2 w}{dx^2} = - \frac{\kappa p_0}{V_0} \int_{-L}^L w dx. \quad (10.1)$$

Taking into account two first members of (9.3), we integrate (10.1) by Bubnov-Galerkin's method to find that the loss of stability with respect to symmetric form with one half-wave takes place for the following value of compressive load [4]

$$N = D \left(\frac{\pi}{2L} \right)^2 \left(1 + \frac{B}{A} \right), \quad (10.2)$$

while with respect to two half-waves deformation,

$$N = D \left(\frac{\pi}{L} \right)^2. \quad (10.3)$$

The ratio B/A is given by formula (9.5). From (10.2) and (10.3) we conclude that the load value under which the plate buckles with respect to the symmetric form depends on properties and dimensions of the cavity, while for the asymmetric form of stability loss it does not depend on these factors and is equal to the corresponding load for the plate not contacting fluids.

The linear approximation shows an equal possibility of plate buckling to either side. This corresponds to the considered form. Moreover, the correction for nonlinearity (due to adiabatic law as well as to occurrence of membrane forces in the plate) in the

bending equation for the asymmetric form of buckling does not lead to changing the mentioned fact. Something different takes place in the case of symmetric form of buckling.

Retaining, according to (9.1), three members of the expansion in the right side of the equation (10.1), we have

$$-\frac{\kappa p_0}{V_0} \left[\int_{-L}^L w dx + \frac{\kappa+1}{2V_0} \left(\int_{-L}^L w dx \right)^2 + \frac{(\kappa+1)(\kappa+2)}{6V_0^2} \left(\int_{-L}^L w dx \right)^3 \right] \quad (10.4)$$

Moreover, we take into account the effect of membrane forces in the plate which is also described in the bending equation by the cubic member [4].

Integrating the mentioned equation by Bubnov-Galerkin's method with one-term approximation, we have for the symmetric form

$$N = D \left(\frac{\pi}{2L} \right)^2 \left[1 + \frac{B}{A} + \frac{B}{A} \frac{2L}{\pi V_0} (\kappa+1) W_1 + \frac{B}{A} \frac{2}{3} \left(\frac{2L}{\pi} \right)^2 \frac{1}{V_0^2} (\kappa+1)(\kappa+2) W_1^2 + \frac{1}{16h^2} W_1^2 \right]. \quad (10.5)$$

Here the last term corresponds to the "geometrical" nonlinearity of the plate in bending.

For the case of rectangular cavity ($V_0 = 2LH$), the formula (10.5) may be written in the form

$$N = D \left(\frac{\pi}{2L} \right)^2 \left[1 + \frac{B}{A} + \frac{(\kappa+1)B}{\pi A} \left(\frac{W_1}{H} \right) + \frac{2(\kappa+1)(\kappa+2)B}{3\pi^2 A} \left(\frac{W_1}{H} \right)^2 + \frac{1}{16} \left(\frac{W_1}{h} \right)^2 \right], \quad (10.6)$$

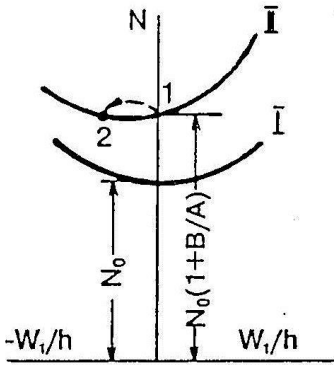


Fig. 3.13. Deflection of the plate with one of its sides contacting a compressible medium as a function of compressive force. The plate "prefers" buckling outwards

whence one can see that unlike the role of usual nonlinear term of the plate theory which depends on the ratio of the deflection to the wall thickness (W_1/h), the role of the nonlinear term taken into account here depends in particular on the ratio of the deflection to the depth of the rectangular cavity (W_1/H). Clearly, these terms also depend on the other parameters, namely on the relation between the elastic properties and dimensions of the plate and cavity.

Fig. 3.13 shows the compressive force N as a function of the relative deflection W_1/h in the middle of the plate. The curve I obtained from the equation (without fluid effect)

$$N = N_0 \left[1 + \frac{1}{16} \left(\frac{W_1}{h} \right)^2 \right]$$

intersects the axis of ordinates at the point $N_0 = D(\pi/2L)^2$ and is symmetric about this axis.

The curve II obtained from (10.6) intersects the axis N at $N_0(1+B/A)$ and is asymmetric. The value $N_0(1+B/A)$ is the critical value of the compressive force (10.2). It is seen that at this point the curve has a slope to the side of negative W_1 , i.e. the plate will be trying to buckle outward. The least value of N will be for

$$\frac{W_1}{h} \approx -\frac{8(\kappa+1)h}{\pi H} \frac{B}{A}. \quad (10.7)$$

For a not very shallow cavity, the effect of the last but one term of (10.6) is small as compared with the last one, and it is dropped in the formula (10.7).

When the compressive force reaches the value $N_0(1 + B/A)$ the plate rapidly buckles outward from the position 1 to position 2. The relative deflection becomes equal to

$$\frac{W_1}{h} \approx -\frac{16(\kappa + 1)h}{\pi H} \frac{B}{A}$$

or, using (9.5), to

$$\frac{W_1}{h} \approx -0.464\kappa(\kappa + 1) \frac{p_0}{E} \left(\frac{2L}{H}\right)^2 \left(\frac{2L}{h}\right)^2.$$

The deflection may be significant. For $p_0/E = 10^{-6}$, $\kappa = 7$, $2L/H = 3$, $2L/h = 10^2$ it is $W_1/h \approx -2.34$.

In the case of an incompressible fluid the critical value for the asymmetric form of instability coincides with (10.3). Buckling with one half-wave deformation is impossible. Buckling with a combination of three and one half-waves but with a corresponding compressive force greater than that according to (10.3), is possible.

CHAPTER IV

SOME EXAMPLES OF NONLINEAR PROBLEMS

§1. Flexible plate on liquid surface under load distributed along line

In this chapter the nonlinear behavior of plates, shells and panels contacting fluid is considered in a more systematic way. In previous chapters, nonlinear effects were considered in a more ad hoc manner. The fluid may be incompressible or compressible. Deflections and rotations of the thin-walled elastic element may be arbitrary. In considering buckling of a cylindrical shallow panel the maximum rotation angles are of order b/R while the maximum deflections are of order $b^2/(4R)$ where b is the half the chord, R the panel curvature radius, $b^2/(4R)$ being a measure of the distance from a plane to the point on the shell of maximum height from that plane.

The simplest problem allowing exact integration of the equations under arbitrary deflections is the one considered in §7 of Chapter II, i.e. the equilibrium of a long membrane under a load distributed along a line (see Fig. 2.7). The same problem is stated in this paragraph. The difference consists in that here instead of the membrane we consider an infinitely long flexible plate with a bending stiffness D [8]. The weight of the plate is not taken into

account. The notations of Fig. 2.7 also hold here.

So, the bending equations have the form (7.1) and (7.2) from Chapter II. If all linear dimensions are referred to $(D/\gamma)^{1/4}$ and all force factors to $(D/\gamma)^{1/2}$, these equations will have the following form

$$\frac{d^2\theta}{ds^2} = (u - P) \cos \theta + \left(T - \frac{1}{2} z^2 \right) \sin \theta, \quad (1.1)$$

$$\frac{du}{ds} = z \cos \theta, \quad \frac{dx}{ds} = \cos \theta, \quad \frac{dz}{ds} = -\sin \theta. \quad (1.2)$$

Boundary conditions are

$$\theta(0) = 0, \quad u(0) = 0, \quad x(0) = 0, \quad (1.3)$$

$$\theta(\infty) = 0, \quad u(\infty) = P, \quad z(\infty) = 0. \quad (1.4)$$

From (1.1)–(1.4) the relation of dimensionless element rotation angle $\theta(s)$, coordinates $x(s)$, $z(s)$, maximum deflection value $w_0 = z(0)$ (under loading) and function $u(s)$ to dimensionless force factors P and T can be found.

In the case of small values of P as compared with unity the required functions may be represented in the form of power series as follows

$$\theta = P\theta_0 + P^3\theta_1 + \dots, \quad u = Pu_0 + P^3u_1 + \dots,$$

$$x = x_0 + P^2x_1 + \dots, \quad z = Pz_0 + P^3z_1 + \dots$$

According to (1.5), the equations a and boundary conditions (1.1)–(1.4) give the following system of equations in θ_0 , u_0 , x_0 , z_0 :

$$\begin{aligned} \frac{d^2\theta_0}{ds^2} &= u_0 - 1 + T\theta_0, \\ \frac{du_0}{ds} &= z_0, \quad \frac{dx_0}{ds} = 1, \quad \frac{dz_0}{ds} = -\theta_0, \\ \theta_0(0) &= 0, \quad u_0(0) = 0, \quad x_0(0) = 0, \\ \theta_0(\infty) &= 0, \quad u_0(\infty) = 1, \quad z_0(\infty) = 0. \end{aligned} \quad (1.6)$$

In the usual way, we also obtain the equations and boundary conditions in θ_1, u_1, x_1, z_1 .

Consider the solution of problem (1.6). Differentiate the first equation of (1.6) with respect to s to find

$$\frac{d^4z_0}{ds^4} - T \frac{d^2z_0}{ds^2} + z_0 = 0. \quad (1.7)$$

When $T = 0$ then (1.7) is the well-known bending equation of a plate (beam) on an elastic foundation.

For $T > -2, T \neq 2$, the solution (1.7) has the form

$$\begin{aligned} z_0 &= \frac{1}{\sqrt{T^2 - 4}} (\mu e^{\lambda s} - \lambda e^{\mu s}), \\ u_0 &= \frac{1}{\sqrt{T^2 - 4}} \left(\frac{\mu}{\lambda} e^{\lambda s} - \frac{\lambda}{\mu} \lambda e^{\mu s} \right) + 1, \\ \theta_0 &= -\frac{1}{\sqrt{T^2 - 4}} (e^{\lambda s} - e^{\mu s}), \\ x_0 &= s, \end{aligned} \quad (1.8)$$

$$\lambda = -\sqrt{\frac{1}{2}T + \frac{1}{2}\sqrt{T^2 - 4}}, \quad \mu = -\sqrt{\frac{1}{2}T - \frac{1}{2}\sqrt{T^2 - 4}}.$$

For the deflection under the concentrated force $2P$, we have

$$w_0 = P/\sqrt{2+T} \quad (T > -2). \quad (1.9)$$

When $-2 < T < 2$ then the solution is a wave decaying with the distance from the concentrated force.

When $T \geq 2$ the solution decays monotonically. For $T = 2$ it has the form

$$z_0 = \frac{1}{2}(1+s)e^{-s}, \quad x_0 = s, \\ u_0 = 1 - \frac{1}{2}se^{-s} - e^{-s}, \quad \theta_0 = \frac{1}{2}se^{-s}.$$

The solution in z_1, x_1, u_1, θ_1 can also be found. But now we turn to obtaining the first integral of the initial nonlinear equation [8]. Multiply (1.1) by $d\theta/ds$ and integrate with respect to s to obtain

$$\begin{aligned} \frac{1}{2} \left(\frac{d\theta}{ds} \right)^2 &= \int (u - P) \cos \theta \frac{d\theta}{ds} ds + \\ &+ \int \left(T - \frac{1}{2}z^2 \right) \sin \theta \frac{d\theta}{ds} ds = (u - P) \sin \theta - \\ &- \int z \sin \theta \cos \theta ds - \left(T - \frac{1}{2}z^2 \right) \cos \theta - \\ &- \int z \frac{dz}{ds} \cos \theta ds = (u - P) \sin \theta - \\ &- \left(T - \frac{1}{2}z^2 \right) \cos \theta + C. \end{aligned} \quad (1.10)$$

It follows from conditions at infinity (1.4) and from (1.10) that $C = T$. For $s = 0$ from (1.3) and (1.10) we find

$$d\theta/ds = w_0. \quad (1.11)$$

Multiply equation (1.1) by z and integrate with respect to s to obtain

$$z \frac{d\theta}{ds} - \cos \theta = \frac{1}{2}u^2 - Pu - \frac{1}{2}Tz^2 + \frac{1}{8}z^4 + C_1. \quad (1.12)$$

It follows from the conditions at infinity (1.4) and from (1.12) that $C_1 = (P^2/2) - 1$. Using equations (1.11), (1.12) and conditions (1.3), we obtain a quadratic equation in ω_0^2 whence

$$\omega_0 = \left[2(2+T) \pm 2\sqrt{(2+T)^2 - P^2} \right]^{1/2}. \quad (1.13)$$

Here we take the minus sign since $\omega_0 = 0$ for $P = 0$.

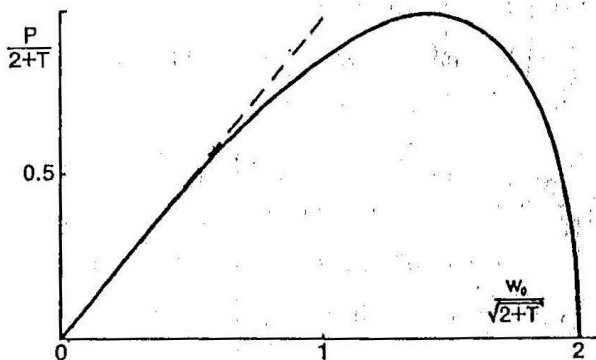


Fig. 4.1. Load versus plate submersion into fluid

Fig. 4.1 shows the plot drawn of (1.13). The linear function (1.9) is given by the dashed line. The nonlinear solution shows that the deflection $\omega_0 = \sqrt{4 + 2T}$ corresponds to a maximum value of $P = 2 + T$. The further increase of ω_0 (with decreasing P)

leads to an unstable solution. For a given axial tension T , the force P may grow up to $2 + T$. When $P > 2 + T$, the whole system submerges into the fluid without limit.

In dimensional units, the maximum load value which can be sustained by an infinitely long plate on a fluid surface is

$$2P' = 2T' + 4\sqrt{D\gamma}. \quad (1.14)$$

Note that the membrane force T' can be negative as well (compressive forces applied to the plate at infinity). In particular,

for $P' = 0$ according to (1.14) these forces are

$$T' = -2\sqrt{D\gamma} . \quad (1.15)$$

The value of T' by (1.15) may be thought of as critical one above which deflections of an infinitely long plate, resting on a fluid surface, occur.

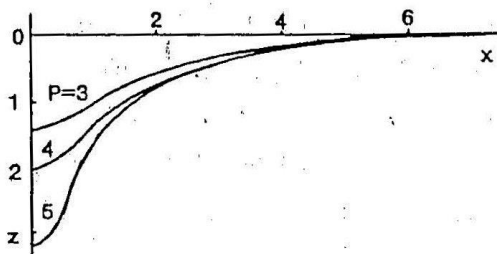


Fig. 4.2. Plate deflection diagram for a stretching force $T = 3$ and different values of load P

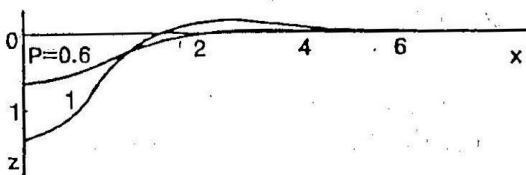


Fig. 4.3. Plate deflection diagram for compressive force $T = -1$. Maximum load is $P = 1$

The shape of deflection along all plate length was found by numerical integration of system (1.1)–(1.3) taking into account (1.13). Fig. 4.2 shows the deflection diagram for $T = 3$ and different values of P . It is similar to that in Fig. 2.8 for the membrane except for the load application zone ($s = 0$). In this case the maximum stable value of transverse force is $P = 5$ on exceeding which the system submerges into the fluid without limit.

Fig. 4.3 shows the case of a compressive load ($T = -1$). The solution here is oscillating, which is peculiar to $|T| < 2$.

§2. Cylindrical panel under the action of a load distributed along line

The convex side of an infinitely long panel with curvature radius R contacts the surface of a fluid extended without limit (Fig. 4.4). The panel weight is neglected. Uniformly distributed load of intensity $2P'$ is applied along the center line of the panel. Therefore, a plane problem symmetric about the arc middle is considered. The essential difference of this problem from that in the previous paragraph is that here the arc length of the panel is finite, part of which is not in contact with fluid. Thus, the interaction domain is variable here.

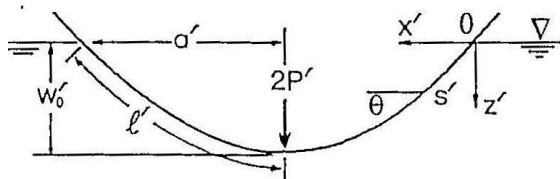


Fig. 4.4. Cylindrical panel under a concentrated load on the fluid surface

found. Radius R of unloaded panel is supposed to be a constant. Dividing all the lengths by $(D/\gamma)^{1/4}$, we have the equilibrium equation [9]

$$\frac{d^2\theta}{ds^2} + \left(\int_0^s z \cos \theta ds \right) \cos \theta + \frac{1}{2} z^2 \sin \theta = 0.$$

Introducing, as in the previous paragraph, the function u by the formula

$$\frac{du}{ds} = z \cos \theta, \quad (2.1)$$

we come to the set of equations

$$\frac{d^2\theta}{ds^2} + u \cos \theta + \frac{1}{2} z^2 \sin \theta = 0, \quad (2.2)$$

$$\frac{dz}{ds} = \sin \theta, \quad \frac{dx}{ds} = \cos \theta. \quad (2.3)$$

Boundary conditions have the form

$$\frac{d\theta}{ds}(0) = -\lambda, \quad (2.4)$$

$$u(0) = x(0) = z(0) = 0, \quad (2.5)$$

$$\theta(l) = 0, \quad \mu(l) = P'/(D\gamma)^{1/2} = P, \quad (2.6)$$

where λ , l are the dimensionless curvature of the unloaded panel and the half length of the contact of the unloaded panel with the fluid, respectively. Dimensionless half length of the arc a and maximal submergence in fluid w_0 are

$$a = x(l), \quad w_0 = z(l). \quad (2.7)$$

Consider the case of a planar plate ($\lambda = 0$) and values of P small as compared with unity. Then the solution in θ , u , x , z may be presented in the form of a series (1.5) and

$$l = l_0 + P^2 l_1 + \dots$$

The equations in functions θ_0 , u_0 , x_0 , z_0 , l_0 and corresponding boundary conditions have the form

$$\frac{d^2\theta_0}{ds^2} + u_0 = 0, \quad \frac{du_0}{ds} = z_0, \quad \frac{dz_0}{ds} = \theta_0, \quad \frac{dx_0}{ds} = 1, \quad (2.8)$$

$$\frac{d\theta_0}{ds}(0) = x_0(0) = z_0(0) = u_0(0) = 0, \quad (2.9)$$

$$u_0(l_0) = 1, \quad \theta_0(l_0) = 0. \quad (2.10)$$

The set of equations and boundary conditions in $\theta_1, u_1, x_1, z_1, l_1$ are determined in the usual way.

From (2.8) we obtain the resolvable equation in u_0

$$\frac{d^4 u_0}{ds^4} + u_0 = 0. \quad (2.11)$$

The solution of boundary value problem (2.8)–(2.11) has the form

$$\theta_0 = \frac{\operatorname{ch}(s/\sqrt{2}) \cos(s/\sqrt{2})}{\operatorname{sh}(\pi/2)}, \quad u_0 = \frac{\operatorname{sh}(s/\sqrt{2}) \sin(s/\sqrt{2})}{\operatorname{sh}(\pi/2)},$$

$$z_0 = \frac{\operatorname{ch}(s/\sqrt{2}) \sin(s/\sqrt{2}) + \operatorname{sh}(s/\sqrt{2}) \cos(s/\sqrt{2})}{\sqrt{2} \operatorname{sh}(\pi/2)}, \quad (2.12)$$

$$x_0 = s, \quad l_0 = \pi/\sqrt{2}.$$

From the expression of z_0 in (2.12) one can see the complicated character of deflection diagram. This linear result coincides with the solution of the problem in § 1 of Chapter III if in the latter case the weight of the beam is neglected. Moreover, no separation from the fluid was assumed there in any part of a beam. The solution was presented in Krylov's functions.

From expression of z_0 in (2.12) we obtain the maximum deflection (for $s = l_0 = \pi/\sqrt{2}$)

$$w_0 = \frac{1}{\sqrt{2}} P \operatorname{cth}\left(\frac{\pi}{2}\right). \quad (2.13)$$

Note that in the problem statement in the beginning of the paragraph the panel width has not been mentioned. It is valid if

its own weight is not taken into account. Clearly, the dimensional value should not be less than

$$2l' = 2l_0 (D/\gamma)^{1/4} = \sqrt{2}\pi (D/\gamma)^{1/4}. \quad (2.14)$$

Otherwise the weightless panel (in the given case a planar plate) on the fluid surface cannot bear any load.

Turn to the results of numerical solution of nonlinear system (2.1) – (2.6) [9]. Fig. 4.5 shows the load as a function of maximal penetration into fluid. The linear solution (2.13) for the planar

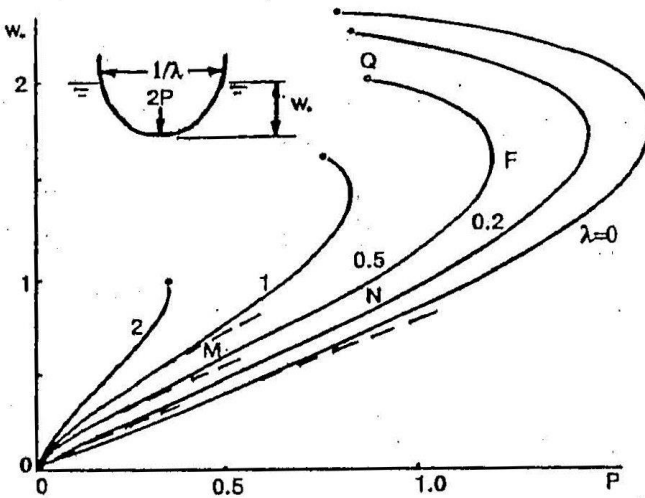


Fig. 4.5: Submersion into fluid as a function of load (P , w_0 are dimensionless values)

plate ($\lambda = 0$) is valid for small load P (dashed line). When $0 \leq P \leq 1$ it slightly differs from the nonlinear solution.

Let us consider in more detail, for example, the case of panel with dimensionless curvature $\lambda = 0.5$. With increasing P , w_0 grows in a nonlinear way. At point F in Fig. 4.5 the maximum possible load value is $2P = 2.42$. Larger values of P lead to submersion of the whole system into the fluid without limit. In the down-tending portion FQ the state is unstable for a given

value of P , but stable for a given deflection. The point Q corresponds to contact of the panel edges with each other (small circles at the ends of the presented curves for all λ correspond to closing of edges).

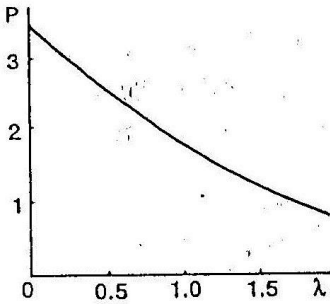


Fig. 4.6. Ultimate load versus initial panel curvature (P and λ are dimensionless values)

Fig. 4.6 shows the ultimate load which can be borne by a panel as a function of its curvature. The plane plate ($\lambda = 0$) can bear the maximum load $2P = 3.27$ or in dimensional form $2P' = 3.27 \sqrt{D\gamma}$. To accomplish this, the plate width should be large enough. Its approximate value is given by formula (2.14). With increasing curvature the ultimate load decreases and tends to zero as π/λ^2 .

Fig. 4.7 shows the load as a function of contact length of the panel with the fluid surface (P and λ are dimensional values). For ($\lambda \neq 0$) and small P the simple relation is valid

$$2P = \frac{l}{\lambda} - \frac{\sin(2l\lambda)}{2\lambda^2},$$

which is obtained by applying Archimede's law (0.2) from the Introduction to the undeformed panel contour. In the case of $\lambda = 0$ we obtain $l = \pi/\sqrt{2}$, which coincides with l_0 in (2.12).

The dimensional width of flat plate is restricted by

$$\sqrt{2}\pi(\gamma/D)^{1/4} < 2l' \leq 4.72(\gamma/D)^{1/4}.$$

Fig. 4.8 presents shapes of elastic panels with initial curvature $\lambda = 0.5$ under various loads. States M, N, F, Q correspond to

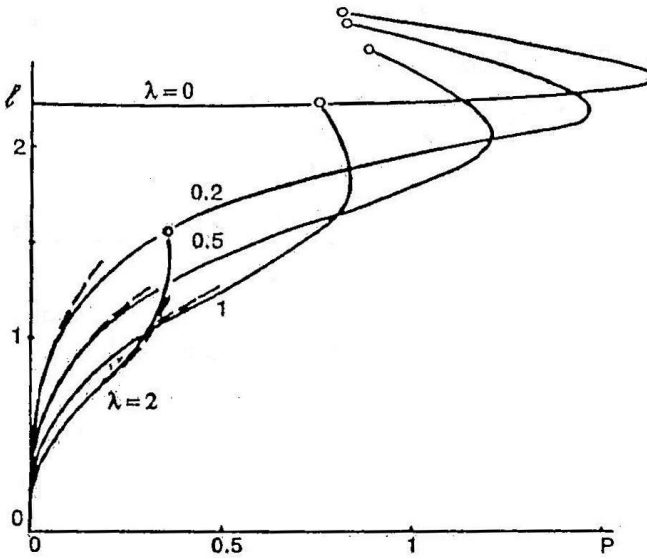


Fig. 4.7. Length of panel contact with fluid for various values of initial curvature as a function of load

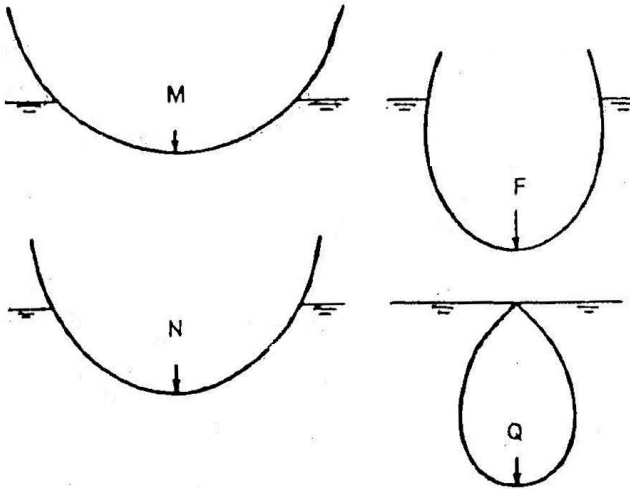


Fig. 4.8. Panel shape and its submersion depth under various loads (for $P=0.480$ the position M is realized, for $P=0.878$ the position N , for $P=1.214$ the position F , for $P=0.878$ the position Q)

the same points as in Fig. 4.5. States M , N are stable. In the state F the maximum bearing shape is reached. In the state Q the bearing capacity is the same as for N . But the state Q is unstable.

§3. Cylindrical shell in a liquid under load distributed along a line

Consider the equilibrium of a long horizontal thin-walled elastic cylindrical shell which is completely or partly submerged in a fluid. Uniformly distributed load of intensity $2P'$ is applied to the lower generator of the cylinder (Fig. 4.9). It balances the lift from the fluid side, which depends on the submersion depth and deformation of the shell. The weight of the latter is neglected. We can restrict ourselves to considering deformation of a ring generated by two cross-sections of the shell. Let us present the results of [1].

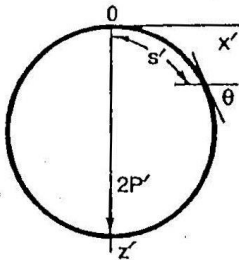


Fig. 4.9. Cylindrical shell in fluid under the distributed load $2P'$ per unit length

We shall use the following notations: x' , z' are the cartesian coordinates directed as shown in Fig. 4.9; s' the arc length measured from the point O ; θ the angle between the tangent and horizontal line; L the half ring perimeter; t' the force of ring compression in the tangential direction at point O ; p_0 the hydrostatic pressure at point O . The total hydrostatic pressure is $p = p_0 + \gamma z'$. Let us introduce nondimensional values as follows

$$s = \frac{s'}{L}, \quad x = \frac{x'}{L}, \quad z = \frac{z'}{L}, \quad \mu = \frac{p_0 L^3}{D},$$

$$\tau = \frac{\gamma L^4}{D}, \quad t = \frac{t' L^2}{D}, \quad P = \frac{P' L^2}{D}.$$

Since p_0 is the pressure in the fluid at the upper point O , the parameter μ defines the shell submersion depth. The parameter τ defines the pressure variation along the shell surface.

We consider separately the cases of complete and partial shell submersion in the fluid. In the first case equations of deformed shell equilibrium have the form [1]

$$\frac{d^2\theta}{ds^2} = \left(-t + \mu z + \frac{1}{2} \tau z^2\right) \sin \theta + (\mu x + \tau u) \cos \theta, \quad (3.1)$$

$$\frac{dx}{ds} = \cos \theta, \quad \frac{dz}{ds} = \sin \theta, \quad \frac{du}{ds} = z \cos \theta.$$

Boundary conditions are

$$\begin{aligned} \theta(0) = x(0) = z(0) = u(0) = 0, \\ x(1) = 0, \quad \theta(1) = \pi. \end{aligned} \quad (3.2)$$

In the case of partial shell submersion the length of the arc s^* ($0 \leq s^* \leq 1$) not contacting fluid is introduced. Correspondingly, $x^* = x(s^*)$, $z^* = z(s^*)$. The pressure on the shell is zero in its non-wetted portion and is linear with increasing depth $z - z^*$ in the wetted portion. We have the following equilibrium equations [1]

$$\frac{d^2\theta}{ds^2} = -t \sin \theta, \quad \frac{dx}{ds} = \cos \theta, \quad \frac{dz}{ds} = \sin \theta \quad (0 \leq s < s^*), \quad (3.3)$$

$$\begin{aligned} \frac{d^2\theta}{ds^2} = \left[-t + \frac{1}{2} \tau (z - z^*)^2\right] \sin \theta + \tau [u - z^*(x - x^*)] \cos \theta \\ (s^* \leq s \leq 1), \end{aligned} \quad (3.4)$$

$$\frac{dx}{ds} = \cos \theta, \quad \frac{dz}{ds} = \sin \theta, \quad \frac{du}{ds} = z \cos \theta,$$

as well as the interface conditions on the boundary $s = s^*$ and conditions (3.2). In (3.4), $u(s)$ is

$$u(s) = \int_{s^*}^s z(\xi) \cos \theta(\xi) d\xi.$$

From the equality condition of the vertical force $2P'$ and fluid buoyancy force for deformed shell, we have

$$P = -\tau u(1).$$

For $s^* = 0$, $\mu = 0$, the equations (3.3), (3.4) reduce to (3.1).

For small values of τ and in the interval $0 \leq \mu \leq \mu_2$, where $\mu_2 = 3\pi^3$, the solution of the problem may be presented in the form of a series,

$$\begin{aligned} \theta &= \theta_0 + \tau \theta_1 + \dots, & x &= x_0 + \tau x_1 + \dots, & z &= z_0 + \tau z_1 + \dots, \\ u &= u_0 + \tau u_1 + \dots, & t &= t_0 + \tau t_1 + \dots \end{aligned} \quad (3.5)$$

The solution for functions $\theta_0(s)$, $x_0(s)$, $z_0(s)$, $u_0(s)$, $t_0(s)$ is given in § 6 of this Chapter.

In [1] the solution for functions $\theta_1(s)$, $x_1(s)$, ... is found. In addition to the regular case $0 \leq \mu \leq \mu_2$ the solution for the singular case $\mu \sim \mu_2$ is also found. Omitting these solutions, we present the results of numerical analysis.

For each value of the nondimensional pressure gradient τ , we determine the maximum values achieved by P/τ as well as the values of μ under which points from the opposite sides of the ring are in contact. The arc length of the non-wetted portion s^* in the case of partial submersion is also found.

Fig. 4.10 presents the shell shapes for various values of τ and μ (or s^*). Because of the presence of the variable part of hydrostatic pressure, the lower part of the outlines is more compressed than their upper half.

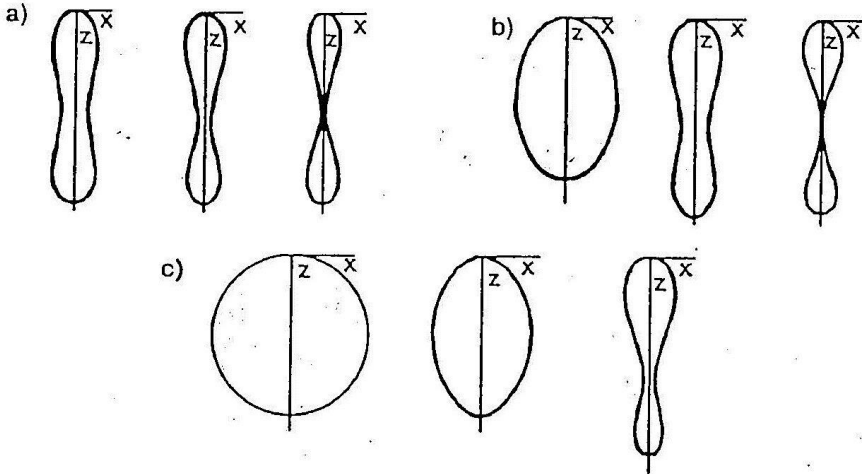


Fig. 4.10. Shell shape: a) for $\mu = 90, 100, 119$ and constant value $\tau = 100$, b) for $\tau = 100, 300, 385$ and constant value $\mu = 0$, c) for $s^* = 1, 0.6, 0.3$ and constant value $\tau = 700$

Fig. 4.11 shows $P/\tau = P'/(\gamma L^2)$ as a function of parameter μ (or s^*). Moving along the axis s^* (from 1 to 0) corresponds to the stable equilibrium of a partly submerged shell. The shell more and more submerges into the fluid and has a greater bearing capacity with increasing the load P . Those states which correspond to the curves going down with increasing the value of μ are

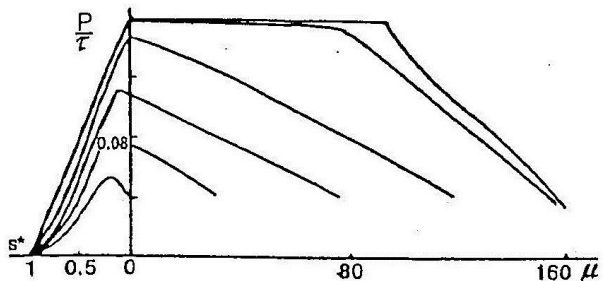


Fig. 4.11. Bearing capacity of the shell with varying depth of its submersion in a fluid

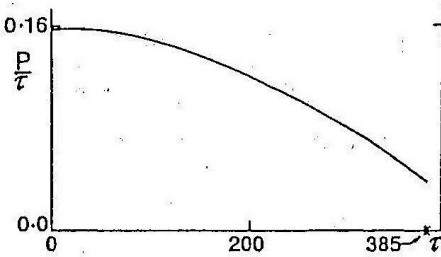


Fig. 4.12. Shell bearing capacity with varying the variable part of hydrostatic pressure τ and in the absence of its constant part ($\mu = 0$)

unstable under the constant load P . The shell sinks in the fluid until it is crushed completely. But these states are stable for the fixed shell positions along the vertical (i.e. when there are kinematic limiters). The end points of the curves with increasing μ correspond to the contact of the sides of the shell re-

sulting from the large shape changes.

Consider the regime of gradual loading of the shell by the force $2P'$. For small $2P'$ the shell is little submerged in fluid (in the

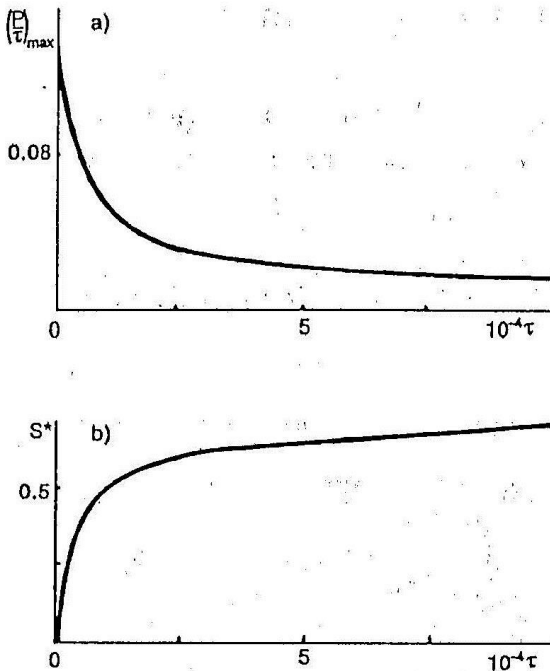


Fig. 4.13. The bearing capacity of the shell (a) and the submersion depth parameter (b) versus the variable part of the hydrostatic pressure τ

Fig. 4.11, s^* is close to unity). With increasing $2P'$, the shell goes down further until its complete submersion (s^* decreases to zero). After that the shell sinks, more and more flattening (if the value $2P'$ reached by the time of complete submersion is held).

The force P as a function of τ for $\mu = 0$ (i.e. the upper shell point O coincides with the fluid surface) is given in Fig. 4.12. The value of τ under which the lateral

shell surfaces come into contact is approximately equal to 385.

Fig. 4.13 shows the maximum values of P/τ as functions of τ within the limits $0 < \tau \leq 10^4$. It also presents the arc length of the non-wetted shell surface $s^*(\tau)$ corresponding to $(P/\tau)_{\max}$. Note that all the presented results are valid for the cases when the weight of the shell can be neglected.

§4. Stability of a shallow panel under a liquid layer

Stability of a long shallow cylindrical panel bearing liquid with a free surface is considered (Fig. 4.14). The structure is assumed to be able to have an upward acceleration with an overload coefficient n . All the walls are rigid. The mass forces of the shell itself are not taken into account. Let us present the results of [3].

The pressure on the shallow panel before its deformation is equal to $n\gamma \left[H_0 - \frac{b^2 - 2x^2}{4R} \right]$, where γ is the specific liquid weight. Notations are given in Fig. 4.14. With a panel bending of w , the free liquid surface descends by the value

$\sim (1/2l) \int_{-b}^b w dx$. Hence, the pressure on the deformed panel is

$$p = n\gamma \left(H_0 - \frac{b^2 - 2x^2}{4R} + w - \frac{1}{2l} \int_{-b}^b w dx \right). \quad (4.1)$$

If the free surface width $2l$ is much greater than the panel span $2b$ the last term in (4.1) may be omitted. On the other hand, when the free surface is at the level of thin section (Fig. 4.14) (and the layer thickness H_0 is significant, only the first and last terms in (4.1) are important.

The nonlinear bending equations of a long shallow cylindrical panel have the form [4-6, 10]

$$\frac{d^4 w}{dx^4} - \frac{N}{D} \left(\frac{1}{R} + \frac{d^2 w}{dx^2} \right) = \frac{p}{D}, \quad (4.2)$$

$$\frac{N}{K} = \frac{du}{dx} - \frac{w}{R} + \frac{1}{2} \left(\frac{dw}{dx} \right)^2 \quad \left(K = \frac{Eh}{1-\nu^2} \right), \quad (4.3)$$

where N is the membrane force constant along the arc. The pressures above the liquid surface and under the panel are equal to each other.

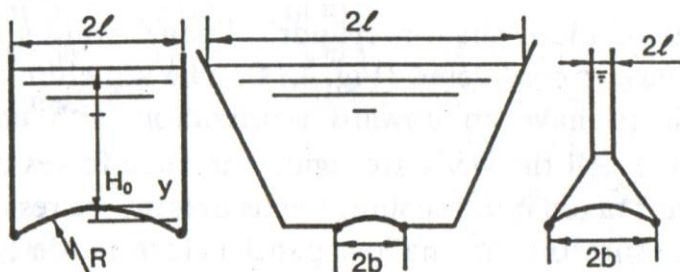


Fig. 4.14. Containers with different ratios of dimensions of elastic panel and fluid surface

Let us take the deflection function in the case when both panel ends are hinged ($w = d^2 w/dx^2 = u = 0$ for $x = \pm b$) in the following form

$$w = W_1 \cos \frac{\pi x}{2b} + W_3 \cos \frac{3\pi x}{2b} + W_2 \sin \frac{2\pi x}{2b}. \quad (4.4)$$

Integrating (4.3) one time, allowing for (4.4), and satisfying conditions $u = 0$ ($x = \pm b$), we find

$$\frac{2\pi}{k^2} \mu^2 = 3f_1 - f_3 - \frac{3\pi^3}{32} (f_1^2 + 9f_3^2 + 4f_2^2), \quad (4.5)$$

where the nondimensional parameters of the curvature, membrane force and relative deflection are introduced as

$$k = \frac{4b^2}{Rh}, \quad \mu^2 = -\frac{Nb^2}{D}, \quad \hat{f}_1 = \frac{RW_1}{b^2},$$

$$\hat{f}_2 = \frac{RW_2}{b^2}, \quad \hat{f}_3 = \frac{RW_3}{b^2}. \quad (4.6)$$

We integrate the equations (4.2) and (4.1) by Bubnov-Galerkin's method (setting $l = b$ (4.1)) to obtain

$$\left[\left(\frac{\pi}{2} \right)^4 - \left(\frac{\pi}{2} \right)^2 \mu^2 - g \left(1 - \frac{8}{\pi^2} \right) \right] \frac{\pi}{4} \hat{f}_1 - \frac{2g}{3\pi} \hat{f}_3 =$$

$$= q_0 + g \left(\frac{1}{4} - \frac{4}{\pi^2} \right) - \mu^2, \quad (4.7)$$

$$\frac{2g}{\pi} \hat{f}_1 - \left[\left(\frac{3\pi}{2} \right)^4 - \left(\frac{3\pi}{2} \right)^2 \mu^2 - g \left(1 - \frac{8}{9\pi^2} \right) \right] \frac{3\pi}{4} \hat{f}_3 =$$

$$= q_0 + g \left(\frac{1}{4} - \frac{4}{9\pi^2} \right) - \mu^2, \quad (4.8)$$

$$\left(\pi^4 - \pi^2 \mu^2 - g \right) \hat{f}_2 = 0, \quad (4.9)$$

where

$$g = \frac{n\gamma b^4}{D}, \quad q_0 = \frac{4n\gamma H_0 b^2}{khD}. \quad (4.10)$$

From equation (4.9) we have

$$1) \hat{f}_2 = 0, \quad \pi^4 - \pi^2 \mu^2 - g \neq 0, \quad (4.11)$$

$$2) \hat{f}_2 \neq 0, \quad \pi^4 - \pi^2 \mu^2 - g = 0. \quad (4.12)$$

The first case corresponds to the panel bending symmetric about its middle; \hat{f}_1 and \hat{f}_3 here are determined from (4.7) and (4.8), depending on q_0 , g and parameter μ .

The roots for μ are found from relation (4.5) in which $f_2 = 0$ while f_1 and f_3 are diminished, using the above mentioned expressions. In particular, when the influence of initial curvature and panel bending on the pressure (4.1) is neglected, then, putting $g = 0$ in (4.7) and (4.8), we come to the well-known problem of stability loss with respect to the symmetric form under the "dead" load [5,10] (the limit case for $g/q_0 = b^2/H_0 R \ll 1$).

Only quite shallow shells with a curvature parameter $k \leq 9.04$ (which corresponds to a rise nearly equal to the panel thickness) may lose stability with respect to the symmetric form. It will be shown further that in our problem this value may be even less. Therefore, in this case the effect of initial curvature and deflection on the pressure (4.1) is small. It may be significant only for large values of parameter g and small liquid layer thickness H_0 (or q_0). In connection with this, we consider only the stability loss asymmetric about the span middle to which the relation (4.12) is corresponding. The relation gives

$$\mu^2 = \pi^2 \left(1 - g/\pi^4\right). \quad (4.13)$$

Thus, unlike the known case of loading by pressure of constant intensity ($\mu^2 = \pi^2$) the loss of stability of panel bearing a liquid takes place under a smaller membrane force. Allowing for (4.13), from (4.7) and (4.8) we have

$$f_1 = \frac{1}{A} \left\{ \left[\left(\frac{3\pi}{2} \right)^4 + \left(\frac{9}{4} + \frac{8}{5\pi^2} \right) g \right] \left[\pi^2 - q_0 - \left(\frac{1}{4} - \frac{3}{\pi^2} \right) g \right] - \frac{8g}{5\pi^2} \left[\pi^2 - q_0 - \left(\frac{1}{4} + \frac{5}{9\pi^2} \right) g \right] \right\}, \quad (4.14)$$

$$f_3 = \frac{1}{A} \left\{ \left[\frac{9}{5} \left(\frac{\pi}{2} \right)^4 + \left(\frac{9}{20} - \frac{24}{5\pi^2} \right) g \right] \left[\pi^2 - q_0 - \left(\frac{1}{4} + \frac{5}{9\pi^2} \right) g \right] + \frac{24g}{5\pi^2} \left[\pi^2 - q_0 - \left(\frac{1}{4} - \frac{3}{\pi^2} \right) g \right] \right\}, \quad (4.15)$$

where

$$A = \frac{\pi}{4} \left[\left(\frac{3\pi}{2} \right)^4 + \left(\frac{9}{4} + \frac{8}{5\pi^2} \right) g \right] \left[3 \left(\frac{\pi}{2} \right)^4 + \left(\frac{3}{4} - \frac{8}{\pi^2} \right) g \right] + \frac{16g^2}{5\pi^3}.$$

Using known f_1 and f_3 as well as μ^2 , we find from (4.5) that

$$f_2 = \pm \left[-\frac{16}{3k^2} \left(1 - \frac{g}{\pi^4} \right) + \frac{8}{3\pi^3} (3f_1 - f_3) - \frac{1}{4} (f_1^2 + 9f_3^2) \right]^{1/2}. \quad (4.16)$$

Here the signs \pm indicate the equal possibility of up or down buckling with respect to the symmetric form.

To analyze expressions (4.14)–(4.16), we consider the panel stability loss under the invariable load $q_0 = 4gH_0/(kh)$, which is necessary for comparison of the results in the two different statements. Moreover, the deflection amplitude with respect to the asymmetric form are not determined in [4–6, 10].

Setting $g = 0$ in (4.14), (4.15), we find

$$f_1 = \frac{64}{3\pi^5} (\pi^2 - q_0), \quad f_3 = \frac{64}{135\pi^5} (\pi^2 - q_0), \quad \frac{f_3}{f_1} = \frac{1}{45}. \quad (4.17)$$

Because the ratio f_3/f_1 is small, we neglect f_3^2 in (4.16). Substitute (4.17) into (4.16) ($g = 0$) to obtain

$$f_2 = \pm 4 \left[-\frac{1}{3k^2} + \frac{32}{3\pi^8} \frac{134}{135} (\pi^2 - q_0) - \frac{64}{9\pi^{10}} (\pi^2 - q_0)^2 \right]^{1/2}. \quad (4.18)$$

If the term f_3 is not taken into account in (4.16), unity will appear in (4.18) instead of the ratio 134/135.

Equating the expression under the root in (4.18) to zero, we obtain the upper and lower critical pressure values

$$q_0^{(+,-)} = \pi^2 - \frac{134}{135} \frac{3\pi^2}{4} \left\{ 1 \mp \left[1 - \left(\frac{135}{134} \right)^2 \frac{\pi^6}{12k^2} \right]^{1/2} \right\}. \quad (4.19)$$

It follows that the stability loss with respect to the asymmetric form is possible if the curvature parameter is

$$k = \frac{134}{135} \cdot \frac{\pi^3}{\sqrt{12}} \approx 9.04.$$

The plot of function (4.18) is shown in Fig.4.15 (solid lines). It is seen that with increasing curvature parameter k the amplitudes of the asymmetric component of deflection also increase. The upper and lower values of the nondimensional critical pressure q_0 are in the ordinate axis.

In the case of $g = 0$, exact solutions of equations (4.1), (4.2) can be found [5]. The solution of (4.2) has the form

$$f = A \cos \mu \xi + B \sin \mu \xi + C \xi + D + \frac{1}{2} \left(\frac{q_0}{\mu^2} - 1 \right) \xi^2. \quad (4.20)$$

Here $f = \omega R/b^2$, $\xi = x/b$. The expression for q_0 is given in (4.10).

Letting (4.20) satisfy the conditions for panel with motionlessly hinged ends, we find

$$A = \frac{1}{\mu^2 \cos \mu} \left(\frac{q_0}{\mu^2} - 1 \right), \quad C = 0, \quad D = - \left(\frac{1}{2} + \frac{1}{\mu^2} \right) \left(\frac{q_0}{\mu^2} - 1 \right), \quad (4.21)$$

$$B \sin \mu = 0 \quad (4.22)$$

and, moreover, the equations for determining parameter μ .

Let us consider bending with respect to the asymmetric form. Putting $B \neq 0$, $\sin \mu = 0$, in (4.22), we find that the least non-zero value of the membrane force parameter is $\mu = \pi$, which coincides with the value (4.13) ($g = 0$) determined by Bubnov-Galerkin's method. From the boundary condition we find

$$B = \pm \frac{4}{\pi^2} \left[-\frac{\pi^4}{3k^2} + \frac{1}{4\pi^2} \left(1 + \frac{\pi^2}{3} \right) (\pi^2 - q_0) - \frac{1}{16\pi^4} \left(5 + \frac{2\pi^2}{3} \right) (\pi^2 - q_0)^2 \right]^{1/2}. \quad (4.23)$$

According to (4.20), (4.21), (4.23), we have

$$f = \left(1 - \frac{q_0}{\pi^2} \right) \left(\frac{1}{\pi^2} \cos \pi \xi - \frac{1}{2} \xi^2 + \frac{1}{\pi^2} + \frac{1}{2} \right) + B \sin \pi \xi. \quad (4.24)$$

Here the first term corresponds to the total panel deformation with respect to the symmetric form and the second one to the asymmetric component. Since the root for μ , independently of the parameters of load q_0 and curvature k , is equal to π then the symmetric component of deflection (4.24) is a linear function of q_0 .

Equating the expression under the root in (4.23) to zero, we obtain the following upper and lower values of the critical load

$$q_0 = \frac{9\pi^2}{15 + 2\pi^2} \pm \pi^2 \sqrt{\left(\frac{6 + 2\pi^2}{15 + 2\pi^2} \right)^2 - \frac{16\pi^4}{(15 + 2\pi^2)k}}.$$

For

$$k > \frac{2\pi^2 (15 + 2\pi^2)^{1/2}}{3 + \pi^2} \approx 9.04$$

the values of q_0 are real.

Results obtained from (4.24), (4.23) are given in Fig. 4.15 by the dashed lines (f_2 , B are the amplitude of the asymmetric form in the solution found by Bubnov-Galerkin's method and from the

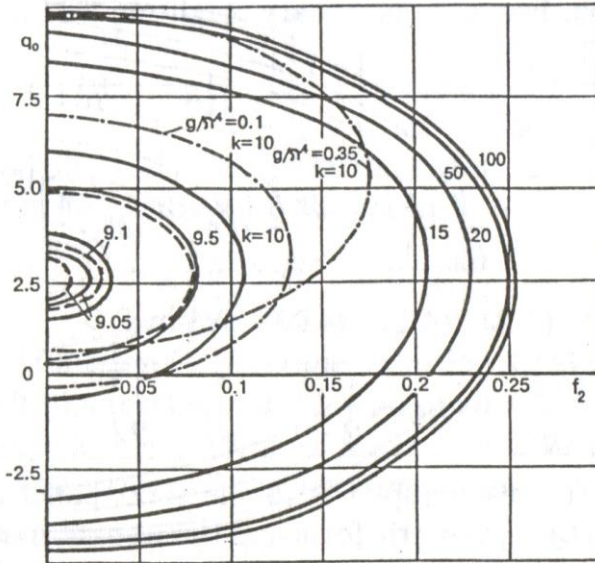


Fig. 4.15. Load versus deflection of cylindrical panel with respect to the asymmetric form

exact solution, respectively). The appreciable difference between the curves is observed only for small k . Even for $k = 10$ they are very close to each other.

Fig. 4.16 shows the relation between the pressure parameter q and deflection parameter $f = f_1 + f_3$ of the panel top ($\xi = 0$) plotted according to formulae (4.17). Under gradual loading the image point moves along the curve OA_0 of the symmetric deflection shape. After attaining the point A_0 it moves along the straight line A_0B_0 plotted according to (4.17) and then upward along the curve of symmetric deflection. The relation between q_0

and the parameter $f = 0.707(f_1 - f_3) + f_2$ is also given in the figure for $k = 1$ at quarter points ($\xi = \pm 1/2$). At first the movement is along the curve OA and then the point $\xi = +1/2$ moves along the ellipse-like curve to the right and the point $\xi = -1/2$ to the left (as arrows show). After arriving at the point B the displacements of both points are the same.

In the upper right corner of Fig. 4.16 functions q_0 and $f = 0.707(f_1 - f_3) + f_2$ are presented for $k = 10$ and $k = 50$. For large values of curvature parameter one of the points ($\xi = \pm 1/2$) has negative displacement at the beginning of stability loss.

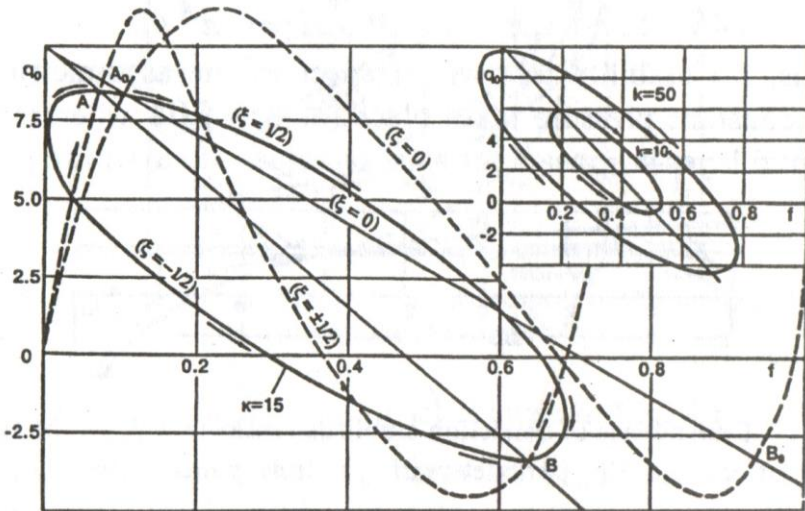


Fig. 4.16. Load-deflection relation at midpoint ($\xi = 0$) and quarter-points ($\xi = \pm 1/2$) of cylindrical panel span for different curvatures

Let us turn back to the case $g \neq 0$. The ratio $\psi = f_3/f_1$ for $g/\pi^4 = 0; 0.1; 0.352$ is presented in Fig. 4.17. Before $q_0 = 6$ it is not significantly different from $1/45$ ($g = 0$).

Since the term f_3 in (4.16) is small as compared with f_1 , then, replacing it by $f_3 = f_1/45$, we obtain

$$f_2 = \pm \left[-\frac{16}{3k^2} \left(1 - \frac{g}{\pi^4} \right) + \frac{1072}{135\pi^3} f_1 - \frac{1}{4} f_1^2 \right]^{1/2}. \quad (4.25)$$

The amplitudes f_2 and f_1 are real if

$$\left(\frac{536}{135\pi^3} \right)^2 - \frac{4}{3k^2} \left(1 - \frac{g}{\pi^4} \right) \geq 0,$$

whence

$$k \geq \frac{135}{134} \frac{\pi^3}{\sqrt{12}} \left(1 - \frac{g}{\pi^4} \right)^{1/2} \approx 9.04 \left(1 - \frac{g}{\pi^4} \right)^{1/2}. \quad (4.26)$$

Thus, the stability loss with respect to the asymmetric form under constant pressure takes place for $k = 9.04$ whereas under the liquid layer it appears for smaller values of curvature param-

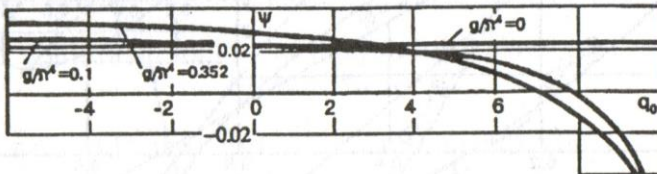


Fig. 4.17. Dependence of deflection amplitude ratio $\psi = f_3/f_1$ on the loading parameters of cylindrical panel

ter (4.26). According to (4.10), we shall have for $\nu = 0.3$

$$g/\pi^4 = 0.11n\gamma b^4/(Eh^3).$$

When, for example, $E = 2 \cdot 10^6$ kgf/cm², $b = 20$ cm, $n = 20$, $\gamma = 10^{-3}$ kgf/cm³, $b/h = 400$, then $g/\pi^4 = 0.352$ and the minimum value of curvature parameter for which stability loss is possible with respect to asymmetric form, is $k = 7.25$.

Fig. 4.15 presents the relations between q_0 and f_2 for $k=10$ and $g/\pi^4 = 0.1; 0.352$ plotted according to the equations (4.25) (dashed lines), (4.14) (dotted lines). These curves are significantly different from the curve with $k=10, g=0$. More detailed

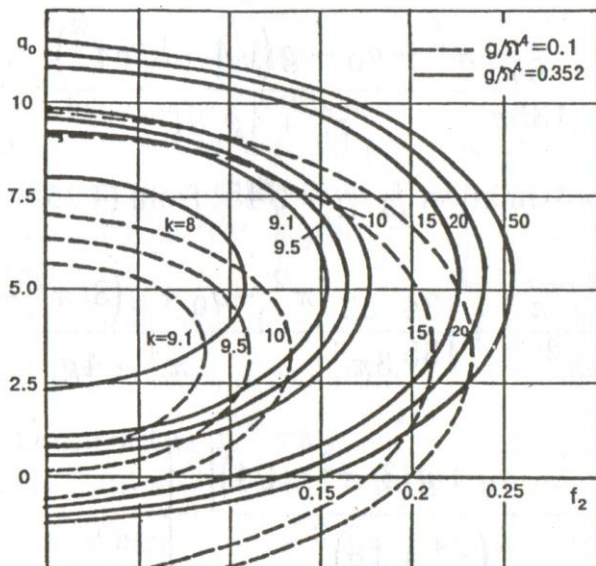


Fig. 4.18. Load versus panel deflection with respect to the asymmetric form for various curvatures

graph of function $f_2 = f_2(q_0, g, k)$ is given in Fig. 4.18.

In the case when the last term in (4.1) can be neglected ($l \gg b$), we shall have (instead of (4.7), (4.8))

$$\left[\left(\frac{\pi}{2} \right)^4 - \left(\frac{\pi}{2} \right)^2 \mu^2 - g \right] \frac{\pi}{4} f_1 = -\mu^2 + q_0 + g \left(\frac{1}{4} - \frac{4}{\pi^2} \right), \quad (4.27)$$

$$\left[\left(\frac{3\pi}{2} \right)^4 - \left(\frac{3\pi}{2} \right)^2 \mu^2 - g \right] \frac{3\pi}{4} f_3 = \mu^2 - q_0 - g \left(\frac{1}{4} - \frac{4}{9\pi^2} \right).$$

Equation (4.5) remains unchanged. From (4.27) for $\mu = \pi$ we have

$$f_1 = \frac{64}{3\pi} \frac{\pi^2 - q_0 - g(1/4 - 3/\pi^2)}{\pi^4 + 4g}, \quad (4.28)$$

$$f_3 = \frac{64}{135\pi} \frac{\pi^2 - q_0 - g(1/4 + 5/9\pi^2)}{\pi^4 + 4g/81}. \quad (4.29)$$

Using the approximation $f_3/f_1 \approx 1/45$, from (4.25) we obtain

$$f_2 = \pm \left\{ -\frac{1 - g/\pi^4}{3k^2} + \frac{134}{135} \frac{32}{3\pi^4} \frac{\pi^2 - q_0 + g(3/\pi^2 - 1/4)}{\pi^4 + 4g} - \frac{64}{9\pi^2} \frac{[\pi^2 - q_0 + g(3/\pi^2 - 1/4)]^2}{(\pi^4 + 4g)^2} \right\}^{1/2}. \quad (4.30)$$

The upper and lower critical values are found by the following formula

$$q_0^{(\pm)} = \pi^2 + g \left(\frac{3}{\pi^2} - \frac{1}{4} \right) - \left(\pi^4 + 4g \right) \frac{134}{135} \frac{3}{4\pi^2} \left\{ 1 \mp \left[1 - \left(\frac{135}{134} \right)^2 \frac{\pi^6}{12k^2} \left(1 - \frac{g}{\pi^4} \right) \right]^{1/2} \right\}.$$

The relation (4.19) can be derived from this expression. Thus, the critical value of curvature parameter remains the same as for (4.19).

§5. Stability of a cylindrical panel loaded by pressure of a compressible fluid

Stability of long shallow cylindrical panel under pressure action from its buckled side is considered. A weightless fluid is in a hermetically sealed cavity with rigid walls (Fig. 4.19). The fluid may be compressible or incompressible. The pressure in the cavity is generated by a slow fluid supply. It is assumed that in the course of rapid panel buckling the amount of the fluid in space does not change (the supply is terminated) [2].

Let p_0 , V_0 and M_0 denote the pressure, volume and mass of the fluid, respectively, at the unstressed state, m^* the mass of the fluid additionally supplied to the cavity after the panel starts buckling, v^* , p^* the corresponding changes in volume of the cavity and pressure in it, respectively.

Let the pressure p in the cavity vary in the course of loading with respect to the adiabatic law. Then, according to (0.8) from Introduction, we have

$$p = p_0 \left[\frac{1 + m/M_0}{1 + v/V_0} \right]^k, \quad (5.1)$$

when $0 \leq m \leq m^*$, $0 \leq v \leq v^*$, $p_0 \leq p \leq p^*$, and when $m = m^* + 0$, $v > v^*$, $p < p^*$.

Thus, the mass of the fluid m supplied to the cavity may be thought of as a control parameter in this problem instead of the pressure difference.

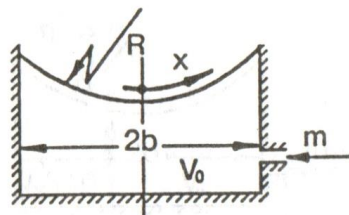


Fig. 4.19. A scheme for testing stability of cylindrical panel

Allowing for the fact that for the shallow panel

$$v \cong \int_{-b}^b w dx,$$

where $2b$ is the length, w the median surface deflection along the normal, we represent (5.1) to terms of the third order as

$$p = p_m - \frac{\kappa p_m}{V_0} \int_{-b}^b w dx \times \left[1 - \frac{\kappa + 1}{2V_0} \int_{-b}^b w dx + \frac{(\kappa + 1)(\kappa + 2)}{6V_0^2} \left(\int_{-b}^b w dx \right)^2 \right], \quad (5.2)$$

$$p_m = p_0 \left(1 + \frac{m}{M_0} \right)^\kappa.$$

In the equations describing the bending of a shallow cylindrical panel (4.2), (4.3), the external pressure is taken to be equal to the pressure in the fluid prior to panel deformation, i.e. p_0 . The membrane force N is taken with a minus sign for compression.

Let us introduce the dimensionless values

$$\xi = \frac{x}{b}, \quad f = \frac{Rw}{b^2}, \quad q_m = \frac{p_m Rb^2}{D}, \quad q_0 = \frac{p_0 Rb^2}{D},$$

$$u_0 = \frac{RV_0}{b^3}, \quad k = \frac{4b^2}{Rh}, \quad \mu^2 = -\frac{Nb^2}{D}.$$

In the case of a hinge support, we take f in the form (4.4), satisfying conditions $w = d^2 w / d\xi^2 = 0$ for $\xi = \pm 1$. Substituting

in (4.3) and satisfying conditions $u = 0$ for $\xi = \pm 1$, we obtain

$$\frac{2\pi}{k^2} \mu^2 = 3f_1 - f_3 - \frac{3\pi^2}{32} (f_1^2 + 9f_3^2 + 4f_2^2). \quad (5.4)$$

Integrating (4.2), (5.2) by Bubnov-Galerkin's method, we find

$$\begin{aligned} \frac{1}{2} \left(\frac{\pi}{2} \right)^2 \left[\left(\frac{\pi}{2} \right)^2 - \mu^2 \right] f_1 + \mu^2 &= q - q_0, \\ \frac{1}{2} \left(\frac{3\pi}{2} \right)^2 \left[\left(\frac{3\pi}{2} \right)^2 - \mu^2 \right] f_3 + \mu^2 &= q - q_0, \\ (\pi^2 - \mu^2) f_2 &= 0, \end{aligned} \quad (5.5)$$

where

$$\begin{aligned} q - q_0 &= q_m - q_0 - t_1 q_m \left(f_1 - \frac{1}{3} f_3 \right) + \\ &+ t_2 q_m \left(f_1 - \frac{1}{3} f_3 \right)^2 - t_3 q_m \left(f_1 - \frac{1}{3} f_3 \right)^3. \end{aligned} \quad (5.6)$$

Here

$$\begin{aligned} t_1 &= \frac{4\kappa}{\pi u_0}, \quad t_2 = \left(\frac{4}{\pi} \right)^2 \frac{\kappa_2}{u_0^2}, \quad t_3 = \left(\frac{4}{\pi} \right)^3 \frac{\kappa_3}{u_0^3}, \\ \kappa_2 &= \frac{1}{2} \kappa (\kappa + 1), \quad \kappa_3 = \frac{1}{6} \kappa (\kappa + 1) (\kappa + 2). \end{aligned}$$

For an arbitrary changeable smooth function $q - q_0$ and $f_2 = 0$, $\mu \neq \pi$ we come to the problem of bending and stability of the panel with respect to the symmetric form. Fig. 4.20 shows the solution of the corresponding problem for a nondimensional curvature $k = 8$. The curve 1 is plotted in coordinates $q - q_0$ and $f = f_1 + f_3$ (dimensionless deflection of the panel center).

The pressure $q - q_0$ changes according to (5.6). With an increasing supply of fluid mass m , the pressure $q - q_0$ on the rigid panel grows from zero to

$$q_m - q_0 = \frac{Rb^2}{D} \left[p_0 \left(1 + \frac{m}{M_0} \right)^\kappa - p_0 \right]. \quad (5.7)$$

The gauge pressure $q - q_0$ in the cavity with a deformed panel is increasing according to the formula (5.6). The image point moves along OA . When the pressure reaches the upper value of the critical load $(q - q_0)^*$, we have

$$q_m^* = \frac{1}{A} \left[(q - q_0)^* + q_0 \right], \quad (5.8)$$

where

$$A = 1 - t_1 \left(f_1^* - \frac{1}{3} f_3^* \right) + t_2 \left(f_1^* - \frac{1}{3} f_3^* \right)^2 - t_3 \left(f_1^* - \frac{1}{3} f_3^* \right)^3.$$

This is the limit value of q_m , which then does not change (the fluid supply during the panel stability loss is negligible). The corresponding value of m^* may be found by substituting (5.8) into (5.7). Given q_m^* , one can plot the relation between load and deflection by formula (5.6).

To plot this relation approximately, let us estimate the ratio f_3/f_1 following from the two first equations of (5.5). We obtain

$$\psi = \frac{f_3}{f_1} = \frac{1}{27} \frac{2.48 - \mu^2}{2.22 - \mu^2}. \quad (5.9)$$

The plot of (5.9) is given in Fig. 4.20 on the right. The limit value of μ is equal to π . This is the reason why the curve for $\mu > \pi$ is not graphed. For $k = 8$ the limit value is $\mu^2 \approx 7.5$. In the interval the maximum ratio of $\psi = \hat{f}_3 / \hat{f}_1$ in absolute value is 0.013. That is why the terms including \hat{f}_3 , \hat{f}_3^* are dropped in formulae (5.8) and (5.6). Moreover since \hat{f}_1^* is relatively small (as seen from Fig. 4.20, $\hat{f}_1^* \cong 0.28$ for $k = 8$) we retain in (5.8) only terms of order not higher than two. So, we have ($f \cong \hat{f}_1$)

$$q - q_0 = q_m^* - q_0 - t_1 q_m^* f + t_2 q_m^* f^2 - t_3 q_m^* f^3, \quad (5.10)$$

where

$$q_m^* = \frac{(q - q_0)^* + q_0}{1 - t_1 f^* + t_2 f^{*2}}. \quad (5.11)$$

These simplifications are valid in the case of compressible fluids.

An example. If $k = 4b^2/(Rh) = 8$, $h/b = 1/25$, $V_0 = b^2/2$, $p_0 = 1 \text{ kgf/cm}^2$, $E = 2 \cdot 10^6 \text{ kgf/cm}^2$, $\nu = 0.3$, $\kappa = 1.4$, then $b/R = 8h/4b = 0.08$, $h/R = 0.0032$, $\kappa_2 = 1.68$, $\kappa_3 = 1.9$, $q_0 = p_0 Rb^2/D = 10.9(p_0 R/Eh)(b/h)^2 = 1.06$, $u_0 = 6.25$, $t_1 = 0.285$, $t_2 = 0.070$, $t_3 = 0.016$.

Making use of tables given in [4], we find $(q - q_0)^* = 4.16$, $f^* = 0.285$. It follows from (5.11) that $q_m^* = 5.69$. The equation (5.10) gives the curve 2 in Fig. 4.20. Hence, the image point will move along the curve OAA_2 . After reaching the point A_2 , the def-

lection increase may be obtained only by additional fluid supply. The axis of ordinates is $q_m^* - q_0$.

When $\kappa = 7$, $V_0 = b^2$, and other parameters are the same, then $\kappa_2 = 28$, $\kappa_3 = 84$, $u_0 = 12.5$, $q_m^* = 6.36$, and we obtain the curve 3. With decreasing the cavity volume (or increasing κ) the load variation in f becomes closer to the curve AB and stability is lost. In further decreasing the volume V_0 , the slope of pres-

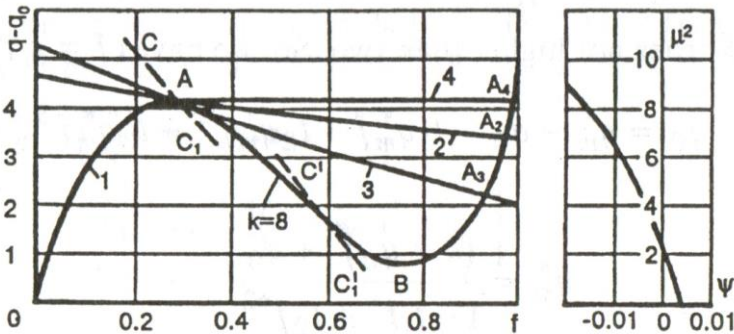


Fig. 4.20. Load versus deflection at the middle point of the span and ratio of deflection shapes as a function of panel compression parameter

sure CC_1 may be deeper than that of the curve AB . The panel slowly goes down only with additional supply ($C'C'_1$). In this case the value of the critical load is difficult to obtain experimentally. By terminating the supply the process of deformation may be stopped at any intermediate state.

Finally, when a fluid with good compressibility (for example, it has a high volume content of bubbles) is in a cavity with large volume, then deformation takes place along the way OAA_4 . And the effect of panel snap buckling is observed.

Let us consider the asymmetric form of stability loss (in equations (5.4), (5.5) $\mu = \pi$, $f_2 \neq 0$). As shown in previous

paragraph, the solution has the form

$$\begin{aligned} f_1 &= \frac{64}{3\pi^5} [\pi^2 - (q - q_0)], \quad f_3 = \frac{64}{135\pi^5} [\pi^2 - (q - q_0)], \\ f_3/f_1 &= 1/45, \\ f_2 &= \pm 4 \left[-\frac{1}{3k^2} + \frac{32}{3\pi^8} \frac{134}{135} (\pi^2 - q + q_0) - \right. \\ &\quad \left. - \frac{64}{9\pi^{10}} (\pi^2 - q + q_0)^2 \right]^{1/2}. \end{aligned} \quad (5.12)$$

The relation between $q - q_0$ and the deflection in the center $f = f_1 + f_3$ (OA_0B_0) as well as at quarter points of the panel span length (movement along OA then along the ellipse-like curve up to B) are presented in Fig. 4.21 for the nondimensional curvature $k = 15$. The latter graph is taken from the Fig. 4.16.

With loss of stability the pressure $q - q_0$ according to (5.10) and (5.11) changes along A_0A_1 (for the center) and along the ellipse-like curve from A to B_1 and then to B_2 (for the quarter points of the span). The movement upward from the point B_2 takes place only with additional fluid supply. The curve $A_0B_1B_2$ corresponds to the following data:

$$k = 15, \quad h/b = 1/25, \quad b/R = 0.15, \quad h/R = 0.006, \quad q_0 = 0.567,$$

$$(q - q_0)^* = 8.4, \quad f^* = 0.1, \quad \kappa = 7, \quad u_0 = 12.5, \quad q_m^* = 9.62.$$

In the case of a large ratio $\kappa k/u_0$, a greater number of terms should be taken in the expansion (5.2).

As in the case of symmetric deformation the stability loss is not observed if, according to the formula (5.10), the slope at point A_0 is greater than that of A_0B_0 . With additional fluid supply the panel slowly goes down and the mentioned curves intersect, for

example, at D (curve CC_1). The mean displacement of the span quarter points is determined by the position of D_1 while the amplitudes of deflection with respect to the asymmetric form are equal to the lengths D_1D_2 and D_1D_3 . Thus, after the pressure

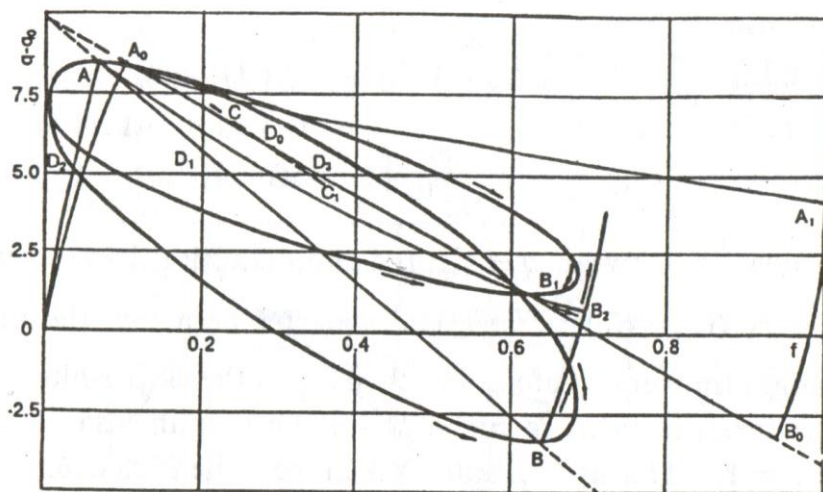


Fig. 4.21. Load versus deflection for panel

reaches the value $(q - q_0)^*$, a modest change in fluid supply may cause small deflection with respect to the symmetric form but a significant deflection with respect to the asymmetric form.

According to equations (5.12) and (5.10), the slopes are determined by

$$\operatorname{tg} \varphi \cong \frac{3\pi^5}{64q_m^*}, \quad \operatorname{tg} \varphi_1 \cong (t_1 - t_2 f^*).$$

When the pressure reaches the value $(q - q_0)^*$ the buckling takes place if $\operatorname{tg} \varphi_1 < \operatorname{tg} \varphi$ or if

$$t_1 - t_2 f^* < 3\pi^5 / (64q_m^*). \quad (5.13)$$

Allowing for (5.11), inequality (5.13) may be rewritten in the form

$$\frac{\kappa}{u_0} \left[1 - \frac{2(\kappa + 1)}{\pi u_0} f^* \right] < \frac{3\pi^6}{256} \left[(q - q_0)^* + q_0 + \frac{3\pi^5}{64} f^* \right]^{-1}. \quad (5.14)$$

It follows that the critical value of $[\kappa/u_0]$ may be found on exceeding which the stability loss in the sense mentioned above does not take place. In the example considered above the second term of the left side of (5.13) and (5.14) is small so that the critical parameter is determined by the following simple formula

$$[\kappa/u_0] \cong 3\pi^6 / (256q_m^*) \cong 1.17.$$

When panel is loaded by an incompressible fluid supply, the condition (4.5) from the Chapter III should be met. The panel may buckle with respect to asymmetric form if the fluid is supplied even after reaching the point A_0 in Fig. 4.21. Buckling with respect to the symmetric form does not occur.

In the case of cylinder completely submerged in fluid the solution has the form [1].

$$\theta_0 = \pi s, \quad x_0 = \frac{1}{\pi} \sin \pi s, \quad z_0 = \frac{1}{\pi} (1 - \cos \pi s),$$

$$u_0 = \frac{1}{\pi^2} \sin \pi s - \frac{1}{4\pi^2} \sin 2\pi s - \frac{1}{2\pi} s, \quad t_0 = \frac{\mu}{\pi}, \quad \frac{P}{\tau} = \frac{1}{2\pi}.$$

In the case of partial submersion of a cylinder in a fluid the solution is

$$\theta_0 = \pi s, \quad x_0 = \frac{1}{\pi} \sin \pi s, \quad z_0 = \frac{1}{\pi} (1 - \cos \pi s),$$

$$u_0 = \begin{cases} 0 & \text{for } 0 \leq s \leq s^* \\ \frac{\sin \pi s - \sin \pi s^*}{\pi^2} - \frac{\sin 2\pi s - \sin 2\pi s^*}{4\pi^2} - \frac{s - s^*}{2\pi} & \text{for } s^* < s \leq 1, \end{cases}$$

$$t_0 = 0.$$

2. A long cylindrical shell containing fluid rests on rigid foundation. The weight of the shell is assumed to be small as compared with the weight of fluid contained in it, and is neglected. Only one cross-section (or ring) may be considered, as shown in Fig. 4.22a. Since the system is symmetric about the vertical axis AC we determine the force factors only in half the shell (Fig. 4.22b). An undeformed shell equilibrium is the zero approximation in the corresponding problem of hydroelasticity. Moreover, determination of circular, transverse and bending moments for an undeformed cylinder is of independent interest in the case of large bending stiffness [7].

There is no vertical force at point A while it is equal to the linear fluid weight $\pi\gamma R^2/2$ at point C . The sum of forces T_A and

T_C is equal to the total hydrostatic pressure along the length AC

$$T_A + T_C = 2\gamma R^2. \quad (6.1)$$

The gravity center of half-circle area is away from the vertical AC by the distance $4R/(3\pi)$. Hence the moment of the liquid weight about point C is equal to $(2/3)\gamma R^3$. Moment of the

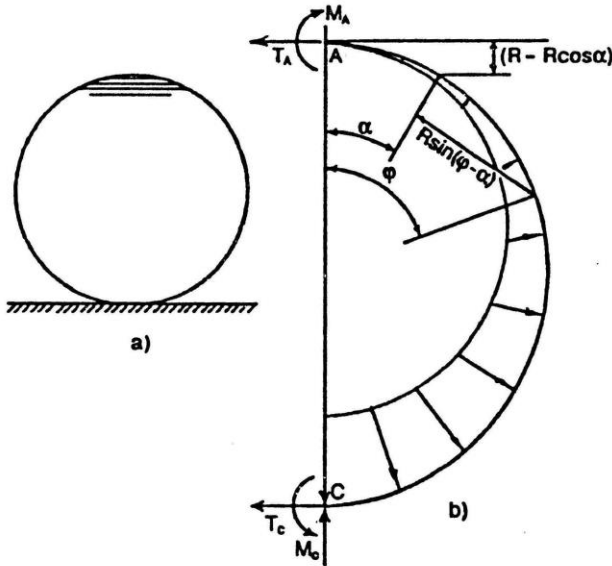


Fig. 4.22. Rigid cylindrical shell with fluid on horizontal surface (a) and notations (b)

hydrostatic pressure is equal to $(4/3)\gamma R^3$. Equating the sum of all moments to zero, we obtain

$$M_A - 2T_A R - M_C + 2\gamma R^3 = 0. \quad (6.2)$$

The total moment of all forces about the shell point with the central angle φ is

$$M = M_A - T_A R(1 - \cos \varphi) + \gamma R^2 \left(1 - \cos \varphi - \frac{\varphi}{2} \sin \varphi \right). \quad (6.3)$$

Making use of (6.3), we have

$$\int_0^{\pi} M d\varphi = \pi \left(M_A - T_A R + \frac{1}{2} \gamma R^3 \right) = 0, \quad (6.4)$$

$$\int_0^{\pi} M(1 - \cos \varphi) d\varphi = \frac{1}{2} \pi R \left(T_A - \frac{3}{4} \gamma R^2 \right) = 0.$$

It follows that

$$T_A = \frac{3}{4} \gamma R^2, \quad M_A = \frac{1}{4} \gamma R^3. \quad (6.5)$$

From (6.5), (6.1), (6.2), we find

$$T_C = \frac{5}{4} \gamma R^2, \quad M_C = \frac{3}{4} \gamma R^3. \quad (6.6)$$

Thus, the membrane force and bending moment at point C are greater than that at the upper point A by factors of 1.66 and 3, respectively.

Substituting (6.5) into (6.3), we determine the bending moment as

$$M = \frac{1}{2} \gamma R^3 \left(1 - \frac{1}{2} \cos \varphi - \varphi \sin \varphi \right),$$

which is shown in Fig. 4.23. The maximum stress at point C is

$$\sigma_{\varphi\varphi} = \frac{\gamma R^2}{4h} \left(5 + 18 \frac{R}{h} \right),$$

where h is the shell thickness. For the usual values of various dimensions, the stress due to the membrane force T_C (the first term) is negligible as compared with that caused by the bending moment.

When the shell weight $2\pi R h \gamma_0$ is taken into account together with the fluid weight $\pi R^2 \gamma$, the bending moment is

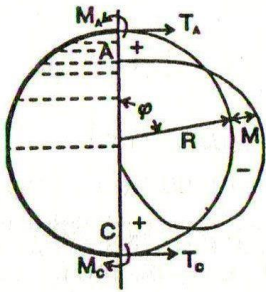


Fig. 4.23. Diagram of bending moments in cylindrical shell containing fluid

$$M = \left(\frac{1}{2} \gamma R^3 + \gamma_0 R^2 h \right) \left(1 - \frac{1}{2} \cos \varphi - \varphi \sin \varphi \right).$$

If the shell is partially filled with fluid (Fig.4.24.) the bending moment is [7]

$$M_{AB} = \frac{\gamma R^3}{\pi} \left[\frac{\pi - \varphi^*}{2} - (\pi - \varphi^*) \cos \varphi^* - \sin \varphi^* + \frac{1}{4} \sin 2\varphi^* + \left(\frac{\pi}{4} - \frac{\varphi^*}{2} + \frac{3}{8} \sin 2\varphi^* + \frac{\pi}{2} \cos^2 \varphi^* - \frac{\varphi^*}{4} \cos 2\varphi^* \right) \cos \varphi \right],$$

$$M_{BC} = M_{AB} + \frac{\gamma R^3}{\pi} \left[2 \cos \varphi^* - \cos \varphi^* \cos (\varphi - \varphi^*) - (\varphi - \varphi^*) \sin \varphi - \cos \varphi \right].$$

When the shell is half-filled with fluid ($\varphi^* = \pi/2$) we have

$$M_{AB} = \frac{\gamma R^3}{\pi} \left(\frac{\pi}{4} - 1 + \frac{\pi}{8} \cos \varphi \right),$$

$$M_{BC} = \frac{\gamma R^3}{\pi} \left[\frac{\pi}{4} - 1 - \frac{3\pi}{8} \cos \varphi + \frac{\pi}{2} \left(\frac{\pi}{2} - \varphi \right) \sin \varphi \right].$$

The bending moment distribution in this case is shown in

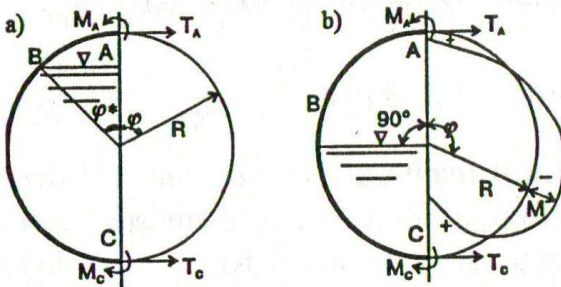


Fig. 4.24. Bending moment diagram for cylindrical shell partially filled with fluid

Fig. 4.24b. The maximum bending moment (for $\varphi = \pi$) is here less than that in the case of a totally filled shell by a factor of 2.45.

CHAPTER V

EQUILIBRIUM OF MEMBRANE SHELLS CONTACTING LIQUIDS IN CONTAINERS

§1. A long cylindrical shell containing liquid

Because of the large length of the cylinder only one its sections need be considered. Moreover we may consider a membrane instead of a shell. Assume the weight of the membrane to be negligible. So, a flexible closed membrane of length L is on a rigid surface and subjected only to the hydrostatic load of the inner liquid (Fig. 5.1). The origin of the coordinates x, z is placed at the up-

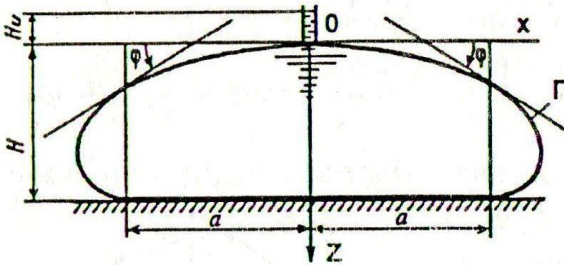


Fig. 5.1. Long cylindrical soft shell containing fluid on the horizontal surface

permost point of the membrane. Notations are given in Fig. 5.1.

Note that investigations of form changes of soft shells are performed taking into account their deformations including large deformations (for example, [9,10]). But throughout this chapter the shell is considered to be inextensible.

As is shown in §4 of Chapter II, the deformed shape of the membrane depends on values of constant p_0 and variable γH

portions of the hydrostatic pressure. The same is true for the shape of soft and flexible containers for storing and transporting fluids. In the idealized example (Fig. 5.1) the membrane shape, the height of water column H_u in the flexible branch pipe (through which the liquid is fed) and the height H are interrelated. When $H_u/H \gg 1$ the constant portion of hydrostatic pressure in container predominates. The membrane tends to take the form of a circle with a small piece bearing against the rigid surface $2a$. If $H_u/H \ll 1$ a shallow form appears with a large bearing area.

In this paragraph, the equilibrium of a shallow system membrane-liquid is considered. That is $H_u = 0$ is assumed. This assumption allows one to put the curvature equal to zero at the uppermost point of the curve Γ .

In this case, as follows from previous chapters, $p_* = \gamma z$ and the equilibrium equation may be written in the form

$$T\tilde{k} = \gamma z, \quad (1.1)$$

where T , \tilde{k} are the tension and curvature of a membrane, respectively, γ is the specific weight of the liquid.

As is known from the previous chapter, dx , dz , ds and an angle φ generated by the tangent to the curve Γ and the axis x are related to each other as follows

$$dx = \cos \varphi ds, \quad dz = \sin \varphi ds, \quad d\varphi = \tilde{k} ds. \quad (1.2)$$

Taking into account (1.2) and the fact that T and γ are constant, we find by differentiation that

$$\tilde{k} \frac{d\tilde{k}}{d\varphi} = \frac{\gamma}{T} \sin \varphi.$$

Integration with respect to φ gives $\tilde{k}^2 = 2(C - \cos \varphi)\gamma/T$, where C is constant.

Further consideration of the problem is given following [1]. The curvature is taken to be $\tilde{k} = 0$ for $\varphi = 0$ and for convenience a new angle is introduced, $\theta = \varphi/2$.

Then $C = 1$ and $\tilde{k} = 2\sqrt{\gamma/T} \sin \theta$. Comparison with equation (1.1) gives

$$z = 2\sqrt{\gamma/T} \sin \theta. \quad (1.3)$$

Putting $\theta = \pi/2$, we obtain the value of the height of the upmost point of the membrane

$$H = 2\sqrt{T/\gamma}, \quad z = H \sin \theta. \quad (1.4)$$

Thus the system height and the membrane tension are inter-related. From these expressions together with (1.2) it follows that

$$\tilde{k} = (4/H) \sin \theta, \quad ds = (H/2 \sin \theta) d\theta, \quad (1.5)$$

$$ds - dx = H \sin \theta d\theta.$$

Integrating the last expression between the limits from the uppermost point of Γ ($s = 0$, $x = 0$, $\theta = 0$) to the point of contact between membrane and horizontal foundation ($s = l$, $x = a$, $\theta = \pi/2$), we find the relation $l - a = H$, where l is the length of the membrane element between upmost and contact points. Since $L = 2a + 2l$ then

$$4a + 2H = L. \quad (1.6)$$

Consequently, the perimeter of the rectangle with base $2a$ and height H is equal to perimeter of the membrane L . This rectangle also has one more curious feature [1].

Integrating the expression

$$z dx = \left(H^2/4\right) \cos \varphi d\varphi$$

obtained from (1.2) with respect to φ from 0 to π , we find that the area S_1 is equal to S_2 (Fig. 5.2a). Consequently, the area of

the above rectangle is equal to the area S bounded by the membrane. So

$$2aH = S. \tag{1.7}$$

This rectangle with base $2a$ and height H may be referred to as equivalent since its perimeter and area are equal to perimeter of

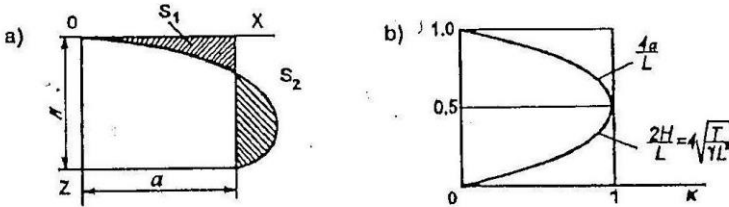


Fig. 5.2. Equivalent cross-sectional areas (a) and dependence of the shell lift height and the length of contact with horizontal surface on the filling coefficient (b)

the membrane L and to the area bounded by it, respectively.

Elimination of a from (1.6) and (1.7) gives a quadratic equation in H/L whence

$$\frac{H}{L} = \frac{1}{4} \left(1 \pm \sqrt{1 - \kappa} \right) \quad \left(\kappa = 16 \frac{S}{L^2} \right).$$

The lower sign should be taken here because $H = 0$ for $S = 0$. Parameter κ may be referred to as a coefficient of filling of the long cylindrical container. Using (1.4), we have

$$\sqrt{\frac{T}{\gamma L^2}} = \frac{H}{2L} = \frac{1}{8} \left(1 - \sqrt{1 - \kappa} \right).$$

These functions are presented in Fig. 5.2b. They are valid when $\kappa \leq 1$ or $16S \leq L^2$.

The curve Γ may be presented as an elastic line in the problem of bending a rod (Euler's elastica) (Fig. 5.3a). This will be discussed in more details in §3. Now we only consider its most characteristic features.

At the most remote point N (Fig. 5.3b) $\theta = \pi/4$ and from (1.4) it follows that $Z_N = (\sqrt{2}/2)H$. To find the overall dimension A we integrate (1.5) with respect to θ from zero to $\pi/4$. Let l_1 denote the arc length OMN . Then we can write

$$l_1 - A = (1 - \sqrt{2}/2)H.$$

Now integrating (1.5) between $\theta = \pi/4$ and $\theta = \pi/2$, we obtain the expression for the arc length NP in the form

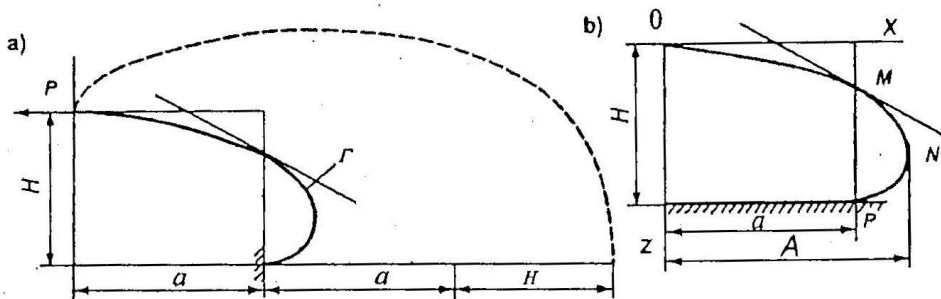


Fig. 5.3. Features of shape of membrane shell containing liquid

$l_2 = -(H/2) \ln \operatorname{tg}(\pi/8)$. Since $l_1 + l_2 = l$ and, as was shown above, $l = a + H$, we can write

$$A = a + \left(\frac{1}{\sqrt{2}} + \frac{1}{2} \ln \operatorname{tg} \frac{\pi}{8} \right) H = a + 0.266H. \quad (1.8)$$

To find the angle θ_M at point M we first evaluate the length l_3 of the arc MNP . By integrating (1.5) between θ_M and $\pi/2$ we get both $l_3 = H \cos \theta$ and $l_3 = -(H/2) \ln \operatorname{tg}(\theta_M/2)$. It follows that $\cos \theta_M = -(1/2) \ln \operatorname{tg}(\theta_M/2)$. Using the notation $\operatorname{tg}(\theta_M/2) = e^{-v}$, we shall have $v = 2 \operatorname{tg} v$. The unique positive root of the last equation is $v = 1.915$ so that $\theta_M = 0.293$.

The ordinate of M is determined from (1.4) to be $z_M = 0.288H$. Note that the tangent at the point M cuts the base ($z = H$) at a distance of $1.074H$ from the contact point P .

§2. Volume of liquid in a rectangular cushion-shaped container

Suppose again that the shell of a "cushion" is flexible, nontensile and weightless. The cushion may be made in a variety of ways. Consider the case when two unstrained quadratic sheets with sides $L/2$ are fastened along their edges. By feeding liquid into the volume between the sheets, the cushion is formed. Let it rest on the horizontal foundation.

For the hydrostatic pressure we take the same assumptions as in previous paragraph ($H_u \ll H$, $p_0 \ll \gamma H$). In such a formulation in [1] the volume of the liquid contained in the cushion is found approximately. The results of this work are given below.

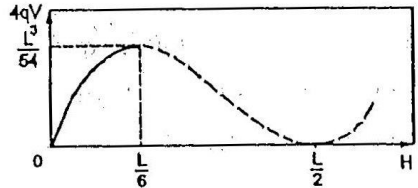


Fig. 5.4. Volume of a liquid in a shell as a function of its lift height

The pressure force on the foundation is equal to $\gamma Ha^2 c$, where a is the distance between the center of contact area and its boundary measured in that plane of symmetry which does not contain cushion angles, c is the coefficient of the completeness of contact spot area. The latter depends on the volume V of liquid in shell. If there is no liquid inside ($V = 0$) the area is equal to $4a^2$ and $c = 4$. For a maximum volume V of a nontensile shell, the contact spot tends to take the form of a circle with vanishing

radius a . And $c \rightarrow \pi$. Thus $\pi < c \leq 4$. Actually the coefficient c is closer to 4 than to π .

Since the liquid weight is γV the condition for equilibrium of the whole system is

$$\gamma V = \gamma H a^2 c. \quad (2.1)$$

To make approximate calculations, suppose that the curves of intersection of shell and planes of symmetry which do not contain the angles of the cushion, coincide with the cross-sections of long cylindrical shell with perimeter L (§1). This hypothesis is purely geometrical and does not use any assumptions about the acting forces. According to this hypothesis the equality (1.6) holds. It may be rewritten in the form

$$4qV = H(L/2 - H)^2, \quad (2.2)$$

where $q = 1/c$ ($1/4 \leq q \leq 1/\pi$).

The cubic corresponding to (2.2) is shown in Fig. 5.4. The maximum value of $4qV$ takes place for $H = L/6$ and is equal to $L^3/54$. Only one part of the curve, from $H = 0$ to $H = L/6$, makes sense. It is marked in the figure.

Introducing as before in the previous paragraph, the coefficient of filling of the container, $\kappa = 216qV/L^3$, we have by definition $0 \leq \kappa \leq 1$.

The tension T is determined from the assumption that a section of the cushion is a section of a long cylindrical shell. Since the fabric and film materials have greater strength in an uniaxial stressed state than in the biaxial one, the least strong point of the cushion is its uppermost point where its stressed state is biaxial.

The overall dimension A is found by formula (1.8). As to the stressed state of the cushion angles and their influence upon the value of the volume, they cannot be determined within the limits of the given approximate solution.

In conclusion, utilizing the same approximation, we give the generalization for rectangular cushion with the perimeter of middle lines L_1, L_2 ($L_1 \geq L_2$). The area of contact spot is equal to ca_1a_2 , where a_1, a_2 are the dimensions of contact spot with base in both planes of symmetry, c is the coefficient of completeness of the contact spot area. As before for the square we have $\pi < c \leq 4$. Instead of (2.2) we have

$$4qV = H(L_2/2 - H)(L_1/2 - H). \tag{2.3}$$

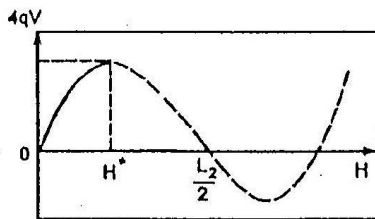


Fig. 5.5. Volume of a fluid in a cushion as a function of its lift

The cubic of (2.3) is shown in Fig. 5.5. The extremum points of $4qV$ are obtained from the following expression

$$H = \frac{1}{6}(L_1 + L_2)(1 \pm m), \quad m = \sqrt{1 - 3L_1 L_2 / (L_1 + L_2)^2}.$$

Since $0 < L_2/L_1 \leq 1$ then $0 < m \leq 1/2$. In the expression for H the lower sign should be chosen. And the extremum of $4qV$ is defined by

$$864qV / (L_1 + L_2)^3 = (1 - m)^2(1 + 2m).$$

Only that part of curve in Fig. 5.5 makes sense which corresponds to $0 \leq H \leq H^*$, where $H^* = (L_1 + L_2)(1 - m)/6$.

For given L_1 and L_2 the limit value of system height H^* may be found. Then the volume of cushion V is determined from (2.3) for any intermediate value H .

§3. Equilibrium of a cylindrical shell under total hydrostatic pressure

In previous paragraphs of this chapter the simplified formulation of the problem of equilibrium of long cylindrical shell and its solution for approximate analysis of cushion-like container have been considered. Clear results have been obtained. Now we shall consider the problem in a more general statement, namely we remove the restriction, taken in the beginning of §1, assuming the absence of a constant part of the hydrostatic pressure. Consequently, arbitrary values of both the liquid column height H_u in the branch pipe and the shell height H are allowed (Fig. 5.1).

The total pressure on the contour is

$$p_* = \gamma (z + H_u). \quad (3.1)$$

Values γ , H_u are given. Coordinates of the membrane points x , z and the tension T are unknown. But the latter is assumed to be constant along all the contour.

Many papers are devoted to solving this problem. Reviews may be found by the interested reader, for example, in [4,8]. Following [7], we give here only a brief summary of some results.

The angle α is introduced in accordance with the Fig. 5.6a. For the membrane point of the corresponding angle α the coordinates are

$$\begin{aligned} x &= -\sqrt{T k^2 / \gamma} \delta A, \\ z &= \sqrt{H_u^2 + 2(T/\gamma)(\sin \alpha_0 - \sin \alpha)} - H_u \end{aligned} \quad (3.2)$$

and the arc length L counting off from the point O is

$$L = -\sqrt{T k^2 / \gamma} \delta F. \quad (3.3)$$

The following notations are used

$$k^2 = \frac{4T/\gamma}{H_u^2 + (4T/\gamma)\sin^2 \alpha_0}, \quad \varphi = \frac{\pi}{4} + \frac{\alpha}{2}, \quad \varphi_0 = \varphi \quad (\alpha = \alpha_0),$$

$$A(\varphi, k) = \frac{2 - k^2}{k^2} F(\varphi, k) - \frac{2}{k^2} E(\varphi, k),$$

$$\delta A = A(\varphi, k) - A(\varphi_0, k), \quad \delta F = F(\varphi, k) - F(\varphi_0, k),$$

where φ is the amplitude (this angle differs from the angle φ of §1), k is the modulus of the elliptic integrals, $F(\varphi, k)$, $E(\varphi, k)$

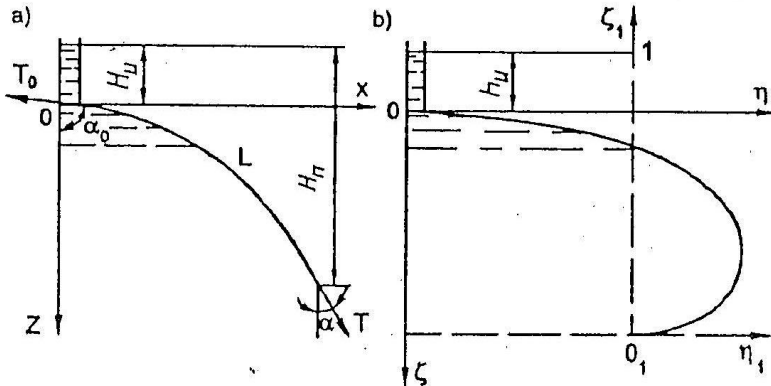


Fig. 5.6. To determining the shape of a membrane shell contacting a liquid

are incomplete elliptic integrals of the first and second kind, respectively.

The area S bounded by curve L and axis z is

$$S = \frac{T}{\gamma} \left(\sin 2\varphi_0 - \sin 2\varphi - 2\delta A \sqrt{1 - k^2 \sin^2 \varphi} \right). \quad (3.4)$$

A linear dimension d is introduced which, depending on the problem under consideration, may be perimeter, height, square root of the area occupied by fluid, etc.

In nondimensional parameters

$$\xi = z/d, \quad \eta = x/d, \quad l = L/d, \quad h_u = H_u/d, \quad t = T/(\gamma d^2)$$

formulae (3.2) and (3.3) take the form

$$\eta = -\sqrt{tk^2} \delta A, \quad l = -\sqrt{tk^2} \delta F, \quad (3.5)$$

$$\xi = \sqrt{h_u^2 + 2t(\cos 2\varphi - \cos 2\varphi_0)} - h_u.$$

Moreover

$$k^2 = \frac{4t}{(h_u^2 + 4t \sin^2 \varphi_0)}.$$

It has already been mentioned in §1 that the form of the field of the hydrostatic load is the curve of elastic rod bending, the Euler's elastica. The curves of the more general equation (3.5) are also elasticas. Reducing them to standard form, the origin of coordinates is placed at the point where $\alpha = -\pi/2$, $\varphi = 0$ (Fig. 5.6b). Axes η_1 , ξ_1 are introduced, the second one being directed upwards. The distance between the plane of hydrostatic pressure (free

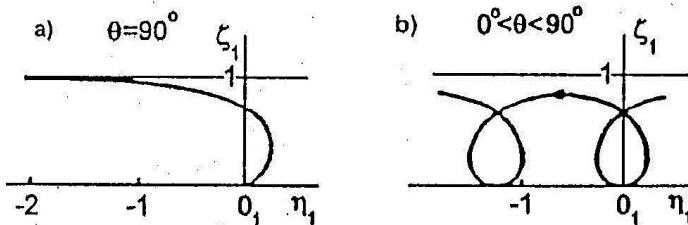


Fig. 5.7. Determining the shape of a membrane shell under the action of hydrostatic pressure

fluid surface) and the axis η_1 along the vertical line is taken as a reference linear dimension. Then the equation of these elasticas are

$$\eta_1 = -\left(k^2/2\right) A(\varphi, k), \quad \xi_1 = 1 - \sqrt{1 - k^2 \sin^2 \varphi}.$$

In Fig. 5.7 the elasticas are presented for θ by the formula $k = \sin \theta$. If $k^2 < 1$ the elasticas are periodic non-inflectional curves (Fig. 5.7a). If $k^2 = 1$ there is one curve asymptotic to the plane of hydrostatic pressure $\xi_1 = 1$ (Fig. 5.7a).

In tables, elliptic integrals are given for $k^2 \leq 1$. When $k^2 > 1$ the new modulus \bar{k} and the new angle $\bar{\varphi}$ are taken in accordance with the following relations

$$\sin \bar{\varphi} = k \sin \varphi, \quad F(\varphi, k) = \bar{k} F(\bar{\varphi}, \bar{k}),$$

$$\bar{k} = \frac{1}{k}, \quad E(\varphi, k) = \frac{1}{k} E(\bar{\varphi}, \bar{k}) + \frac{(\bar{k}^2 - 1)}{\bar{k}} F(\bar{\varphi}, \bar{k}).$$

The ordinary equations of elasticas in this case are

$$\eta_1 = \frac{1}{2\bar{k}} [2E(\bar{\varphi}, \bar{k}) - F(\bar{\varphi}, \bar{k})], \quad \xi_1 = 1 - \cos \bar{\varphi}.$$

The formulae (3.2)–(3.5) also change their form. This is the reason why in literature there are several forms. Moreover, the formulae are presented in terms of Jacobi's elliptic functions, Weierstrasse functions.

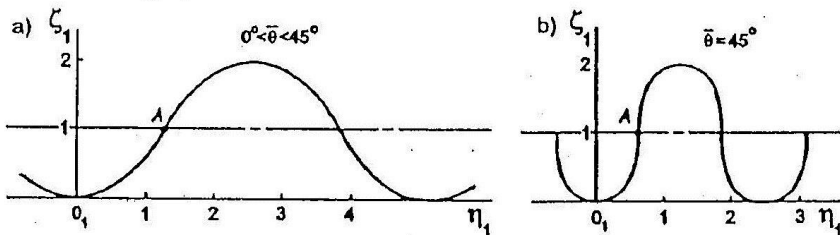


Fig. 5.8. T_0 determining the shape of a membrane shell under the action of a hydrostatic pressure

When $k^2 > 1$ ($\bar{k} < 1$) the elasticas are periodic inflectional curves with an inflection point at the level of hydrostatic pressure ($\xi_1 = 1$). Below the inflection point ($\xi_1 < 1$) the shell has an internal positive pressure, above it ($\xi_1 > 1$) an external one. Some elasticas are presented in Fig. 5.8.

The data of this paragraph will be used in the following paragraphs of this Chapter.

§4. Analysis of partitions separating compartments with liquid

Compartments with soft partitions for fluid are used, for example, on small fishing vessels. Fig. 5.9 shows the notations and coordinate systems.

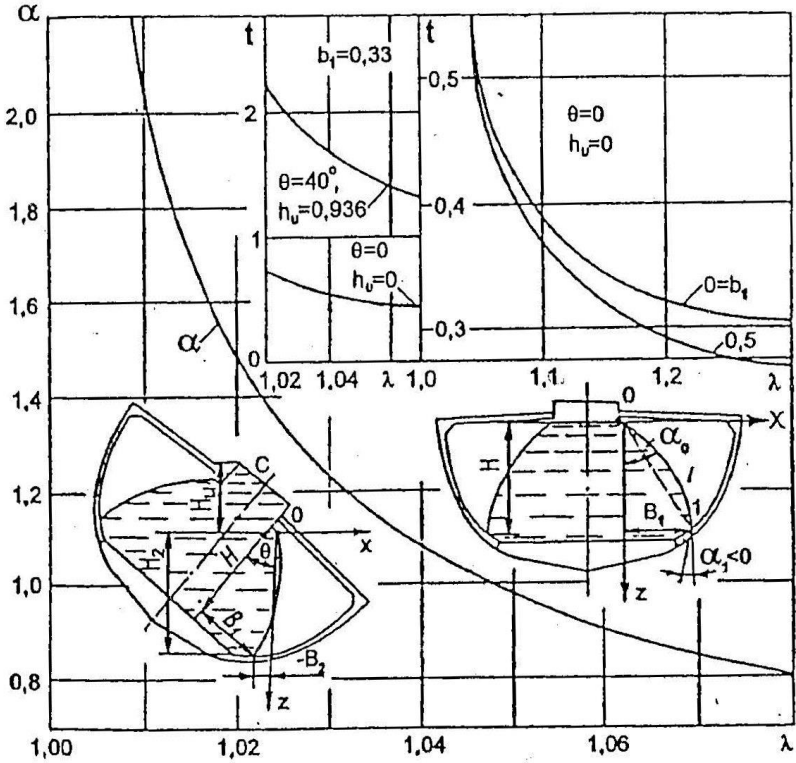


Fig. 5.9. Cross-section of a soft container for liquid transport and calculational parameters

Taking, for reference, the fluid depth H in the vessel without list, we introduce, similarly to §3, the nondimensional parameters

$$\eta = x/H, \quad \xi = z/H, \quad h_u = H_u/H,$$

$$t = T/\gamma H^2, \quad \lambda_1 = L/H, \quad b_1 = B_1/H.$$

The following set of equations is derived [7] for the vessel without list

$$h_u = \frac{\Delta_0}{\Delta_1 - \Delta_0}, \quad -\lambda_1 = \frac{k^2 \delta F(\varphi, k)}{2(\Delta_1 - \Delta_0)}, \quad -b_1 = \frac{k^2 \delta A(\varphi, k)}{2(\Delta_1 - \Delta_0)}, \quad (4.1)$$

where

$$\Delta_1 = \sqrt{1 - k^2 \sin^2 \varphi_1}, \quad \Delta_0 = \sqrt{1 - k^2 \sin^2 \varphi_0}, \quad (4.2)$$

$$\delta A(\varphi, k) = A(\varphi_1, k) - A(\varphi_0, k),$$

$$\delta F(\varphi, k) = F(\varphi_1, k) - F(\varphi_0, k).$$

These functions introduced in the previous paragraph are taken for angles φ_0 , φ_1 at points 0 and 1, respectively. These points are shown in Fig. 5.9. Nondimensional tension is calculated by the formula

$$t = \frac{k^2}{4(\Delta_1 - \Delta_0)^2}. \quad (4.3)$$

Numerical solution gives φ_0 , φ_1 , k .

For small positive pressure $k^2 > 1$, it is more convenient (see previous paragraph) to use other variables $\bar{k} = 1/k$ etc. Then instead of system (4.1)–(4.3), we shall have

$$h_u = \frac{\cos \bar{\varphi}_0}{\cos \bar{\varphi}_1 - \cos \bar{\varphi}_0}, \quad -\lambda_1 = \frac{\delta F(\bar{\varphi}, \bar{k})}{2\bar{k}(\Delta_1 - \Delta_0)}, \quad (4.4)$$

$$-b_1 = \frac{\delta F(\bar{\varphi}, \bar{k}) - 2\delta E(\bar{\varphi}, \bar{k})}{2\bar{k}(\cos \bar{\varphi}_1 - \cos \bar{\varphi}_0)}, \quad t = \frac{1}{4\bar{k}^2(\cos \bar{\varphi}_1 - \cos \bar{\varphi}_0)^2}.$$

These formulae are valid if the partition does not adjoin the second bottom, that is if

$$\lambda_1 \leq -\frac{k^2 F(\bar{\varphi}_0, \bar{k})}{2\Delta_0}, \quad \lambda \leq -\frac{F(\bar{\varphi}_0, \bar{k})}{2\bar{k} \cos \bar{\varphi}_0}.$$

Function $t(\lambda)$ is given for $\theta = 0$, $h_u = 0$ in the upper right corner of Fig. 5.9. Parameter $\lambda = \lambda_1 / \sqrt{1 + b_1^2}$ is used instead of λ_1 .

For the vessel with list θ (Fig. 5.9) the positive pressure is calculated graphically. The dimensions B_2 , H_2 ($b_2 = B_2/H$, $h_2 = H_2/H$) may be also readily found from the figure. The resolving system of equations is

$$\frac{\Delta_1}{\Delta_0} - 1 = \frac{h_2}{h_u}, \quad \frac{k^2 \delta A(\varphi, k)}{2\Delta_0} = -\frac{b_2}{h_u},$$

$$\frac{k^2 \delta F(\varphi, k)}{2\Delta_0} = -\frac{\lambda_1}{h_u}, \quad t = \left(\frac{kh_u}{2\Delta_0} \right)^2.$$

Numerical solution of the system is presented on the left side of Fig. 5.9.

For any list angles, sufficient accuracy is provided by the formula [7]

$$t = \left(\frac{1}{2} + h_u \right) \left(1 + b_1^2 \right)^{1/2} a(\lambda_1),$$

where $a(\lambda_1)$ is found from the following equations

$$a = \frac{1}{2 \sin \beta}, \quad \frac{\beta}{\sin \beta} = \lambda_1 = \frac{\lambda}{\sqrt{1 + b_1^2}}.$$

The values of shell tension $T = \gamma H^2 t$, which have been found here, are not, of course, determinant since in practice their maximum values appear during the vessel's rolling. But dynamic problems are beyond the scope of this work.

§5. Freely lying containers

An example of freely lying container is a cushion (Fig. 5.10), the equilibrium of which was considered in §2 of this chapter. Besides the cushion-like containers the collapsible tube-like containers are widely used, which are made by fastening two rectangular sheets along their edges. A large number of other forms are also known.

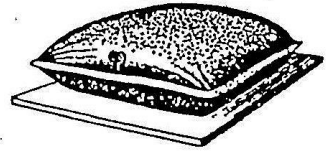


Fig. 5.10. Freely lying container for fluid

To avoid fluid oscillations (in other words, in order to increase the stiffness of the whole system), the vessel's containers are filled so that they have rather large positive pressure. That is why they are made out of strong materials. Volumes of transporting containers usually vary from 1 m^3 to 15 m^3 .

There is a large variety of such containers for ground storage of fluids. Their volumes exceed 200 m^3 . Features of such containers are small positive pressure and therefore shallow forms. That is why these containers are usually made out of relatively weak materials.

A great amount of literature is devoted to static and dynamic analysis of freely lying containers (see for example [4, 5, 7, 9]). This analysis is based on the deformation model with a cylindrical form. Thus this approach is the same as was used in §2 of this Chapter.

Now, following [7], we give, without derivations, the solution of the problem of equilibrium of a container on a horizontal rigid foundation. The notations to be used are: S the area of container

section, d the diameter of circular shell section, T , T_n the annular (transverse) and longitudinal shell tensions, respectively. The other notations are shown in Fig. 5.11 a).

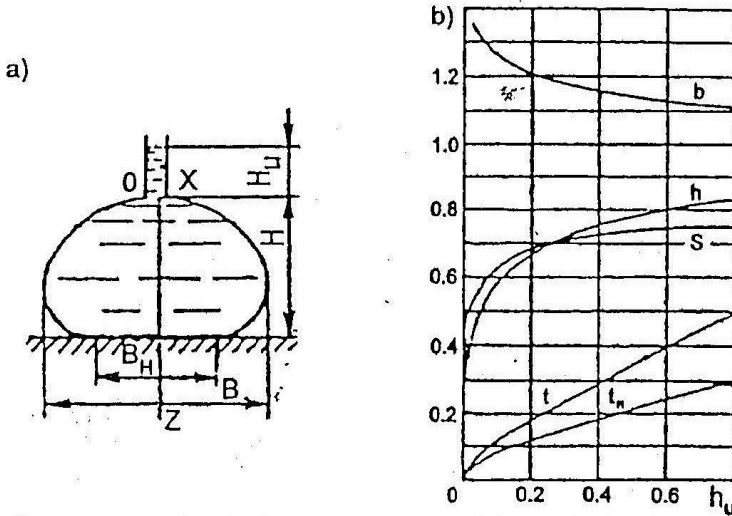


Fig. 5.11. Section of a freely lying container (a) and the desired parameters as functions of relative fluid height in a branch pipe (b)

Using the nondimensional parameters

$$h = \frac{H}{d}, \quad h_u = \frac{H_u}{d}, \quad b = \frac{B}{d}, \quad b_H = \frac{B_H}{d},$$

$$s = \frac{S}{d^2}, \quad t = \frac{T}{\gamma d^2}, \quad t_n = \frac{T_n}{\gamma d^2}$$

the calculational formulae take the form

$$h_u = 2 \sqrt{\frac{1-k^2}{k^2}} t, \quad t = \left(\frac{\pi}{4}\right)^2 \frac{k^2}{[K(k) - E(k)]^2},$$

$$s = 4tA(k), \quad h = 2 \left(1 - \sqrt{1-k^2}\right) \sqrt{t/k^2},$$

$$b = 2 \sqrt{tk^2} [A(k) - A(\pi/4, k)], \quad b_H = 2 \sqrt{tk^2} A(k).$$

Here $K(k)$ is the total elliptic integral of the first kind. The functions A , E are given in §3 of this Chapter.

Curves plotted by these formulae are presented in Fig. 5.11 *b*. It is seen that with increasing fluid height in the branch pipe, the nondimensional values of tensions t , t_n , height of the container h , and area of its cross-section s increase and the rate of this increase is greater for smaller values of h . As to overall dimension B (Fig. 5.11 *a*), it decreases with increasing fluid height in the branch pipe. Note that the tensions keep on growing to the right exceeding the boundary of the figure, while for $h_u > 0.6$ the value of section area remains constant.

If the foundation is inclined the container rolls over. When there is a wall the shell leans on it (Fig. 5.12 *a*). Let θ denote the

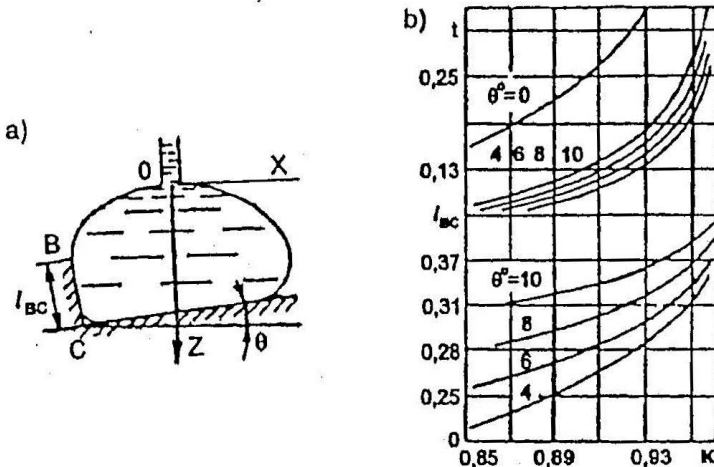


Fig. 5.12. Section of an inclined container (*a*) and the desired parameters as functions of the coefficient of filling for different angles of inclinations (*b*)

angle of inclination of foundation, and $L_{BC} = l_{BC}d$ the height of shell contact with the wall. The filling coefficient κ of the container may be introduced here as earlier in §1 so that $\kappa = 4S/\pi d^2$.

Fig. 5.12*b* shows the nondimensional values of tension t and contact height l_{BC} versus the filling coefficient for different angles of inclination. These parameters grow rapidly as the filling coefficient increases. When the inclination angle of the foundation increases, the nondimensional values of tension go down while the contact size, clearly, goes up.

§ 6. Insertable vessel containers

Among the insertable vessel containers, the following three types may be noted: 1) the close-filling, all surfaces of which closely adjoin walls, bottom and upper partition of compartment, 2) the tensioned, the upper surface of which does not have contact

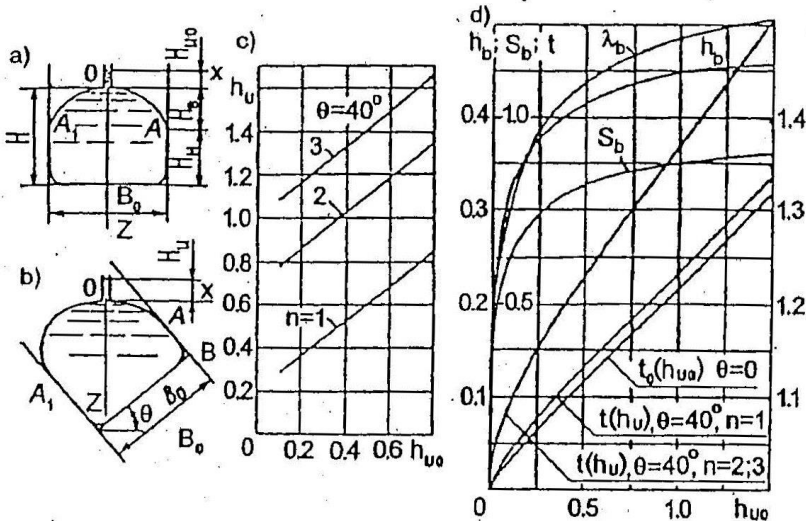


Fig. 5.13. Cross-section of insertable containers (a, b) and the desired parameters versus positive pressure (c, d)

with a compartment and is tensioned by positive fluid pressure (Fig. 5.13*a, b*), 3) the close-fitting-tensioned, which have at the top both zones free and adjoining to partition. The containers may be combined with soft and rigid elements:

Now consider the analysis of stressed insertable containers [7]. Consider the results obtained for the straight vessel position (Fig. 5.13*a*). Let L denote the full perimeter of the shell cross-section, L the perimeter of the upper part, A_1OA and S_0 , S_B the areas of sections of the whole container and the upper part, respectively. As a reference linear dimension we take the base width B_0 and introduce common nondimensional parameters

$$\lambda = \frac{L}{B_0}, \quad \lambda_{B0} = \frac{L_{B0}}{B_0}, \quad h_{u0} = \frac{H_{u0}}{B_0}, \quad h = \frac{H}{B_0}, \quad h_B = \frac{H_B}{B_0},$$

$$h_H = \frac{H_H}{B_0}, \quad t = \frac{T}{\gamma B_0^2}, \quad s_{B0} = \frac{S_B}{B_0^2}, \quad s_0 = \frac{S_0}{B_0^2}.$$

Then for the planar problem

$$t = \frac{1}{4k^2 [A(k) - A(\pi/4, k)]^2}, \quad h_{u0} = 2 \sqrt{\frac{1-k^2}{k^2}} t,$$

$$h_B = h_{u0} \left(\sqrt{\frac{2-k^2}{2(1-k^2)}} - 1 \right), \quad s_B = \sqrt{\frac{2(2-k^2)}{k^2}} t - 2t,$$

$$h_{B0} = 2k \sqrt{t} [K(k) - F(\pi/4, k)], \quad h_H \approx \frac{1}{2} (\lambda - \lambda_{B0} - 1),$$

$$s_0 \approx s_B + h_H = h.$$

Graphic relations plotted using these formulae are given in Fig. 5.13*d*. For $0 \leq h_{u0} < 1/2$ the parameters λ_B , h_B , s_B strongly depend on h_{u0} . When $h_{u0} > 1/2$ the dependence becomes slight. As in the previous paragraph, the function $t(h_{u0})$ is nearly linear:

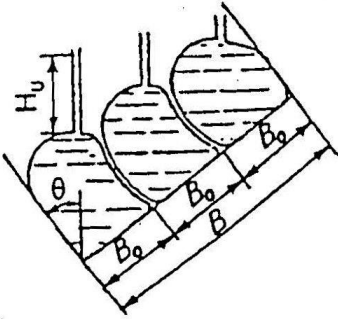


Fig. 5.14. Cross-section of a group of insertable containers

When the vessel has a list θ , the nondimensional tension t against the actual positive pressure h_u is, as for $\theta = 0$, close to a linear function (Fig. 5.13*d*). The difference between h_u and h_{u0} consists in that the first parameter corresponds to the shell in inclined position. This curve is shown by $t(h_u)$ for $\theta = 40^\circ$, $n = 1$ (n denotes the number of containers).

It is clear that h_u depends on h_{u0}, θ . Such dependence may be found from consideration of the problem taking into account the fluid incompressibility. An experimental function $h_u(h_{u0})$ may also be recommended. Such a function is shown in Fig. 5.13*c* for index $n = 1$.

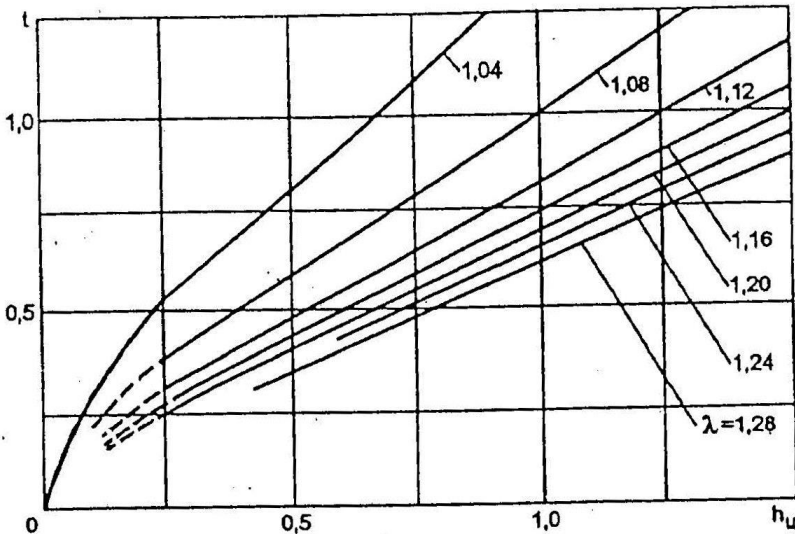


Fig. 5.15. Dependence of tension on positive pressure in shell of insertable containers with longitudinal diaphragms

In the case of several containers in one compartment (Fig. 5.14) the approximate calculations are made in the same way as for the single container. B_0 may be taken as the compartment width divided by the number of containers n . Containers adjoin along the circular cylindrical surfaces. For list the function $t(h_u)$ may be obtained by an experimental curve. In Fig. 5.13d these functions are shown for angle $\theta = 40^\circ$ (container number $n = 2, n = 3$).

For containers with longitudinal diaphragms the nondimensional tension t as a function of pressure h_u and parameter λ is presented in Fig. 5.15. It is characteristic that for $h_u > 1/4$ the function $t(h_u)$ is linear.

§7. Soft floating containers

Floating containers are used as storage and tow transport. Tow containers of cigar-shaped form (Fig. 5.16) are used for transport of petroleum products and fresh water [3,6]. Floating is due to a difference between specific weights of fluid inside and outside the shell as well as to arrangement of air-balloons and air-tubes inside the container (Fig. 5.17).

The analysis of equilibrium of the floating container in a three-dimensional formulation is extremely complicated. The difficulties increase significantly in a dynamic formulation simulating real operating conditions, particularly the behavior on sea waves. We shall give below, following [3,6,7], only the simplest static analysis of the cross-section of the long soft container.

Some notations to be used are: γ, γ_e the specific weight of fluids inside and outside the shell, respectively, d the diameter of the shell when it takes the circular form, S_0 the area of cross-

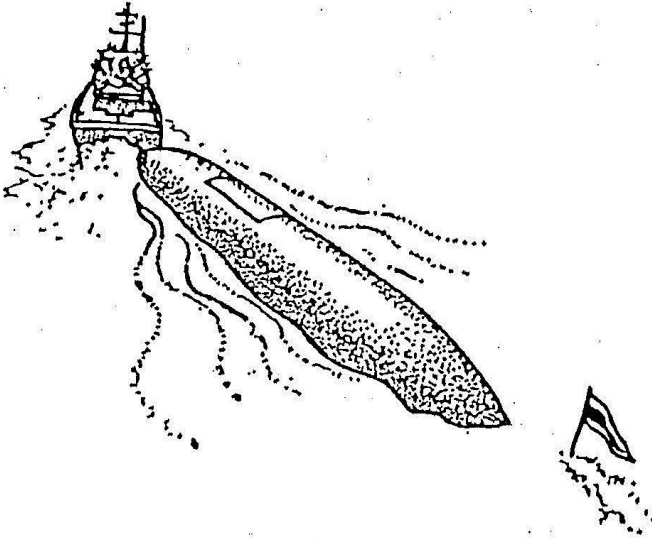


Fig. 5.16. Floating tow container

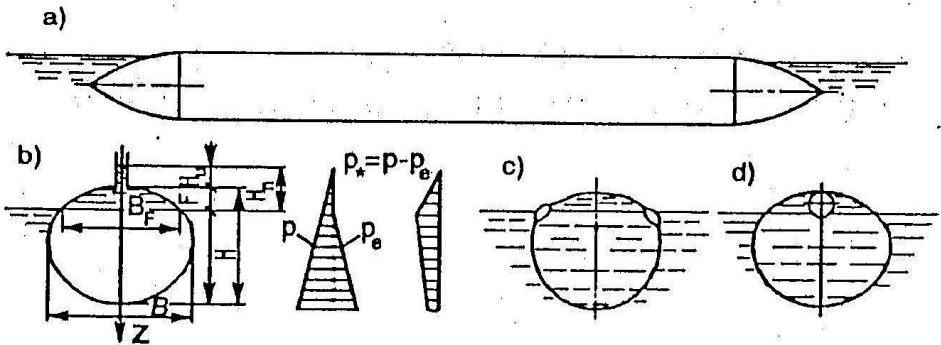


Fig. 5.17. Longitudinal and cross-sections of a floating container

tion of the container with cargo. We shall also utilize the following nondimensional parameters

$$h_u = \frac{H_u}{d}, \quad h = \frac{H}{d}, \quad b = \frac{B}{d}, \quad b_F = \frac{B_F}{d},$$

$$f = \frac{F}{d}, \quad h_n = \frac{H_n}{d}, \quad s_0 = \frac{S_0}{d^2}, \quad t = \frac{T}{\gamma d^2}.$$

Let us introduce the ratio of specific weights of fluids and coefficient of container filling

$$\nu = \frac{\gamma}{\gamma_e}, \quad \kappa = \frac{4S_0}{\pi d^2}.$$

Given positive pressure h_u , the parameters φ_1 , k , k_H are determined from the following system of equations

$$\frac{k}{k_H} \sqrt{\frac{1-\nu}{\nu}} \frac{A(k) - A(\varphi_1, k)}{A(k_H) - A(\varphi_1, k)} = 1,$$

$$\psi_1 = \frac{\pi}{2} - \varphi_1, \quad \sin^2 \varphi_1 = (1-\nu) \left(1 - \frac{1}{k_H^2}\right) + \frac{\nu}{k^2},$$

$$k [K(k) - F(\varphi_1, k)] +$$

$$+ k_H \sqrt{\frac{\nu}{1-\nu}} [K(k_H) - F(\psi_1, k_H)] = \pi h_u \sqrt{\frac{1-k^2}{k^2}}.$$

Using known values of parameters φ_1 , k , k_H , the other variables may be found by the formulae

$$t = \frac{h_u^2 k^2}{4(1-k^2)}, \quad f = \frac{2\sqrt{t}}{k} \left(\sqrt{1-k^2 \sin^2 \varphi_1} - \sqrt{1-k^2} \right),$$

$$h = f + \frac{2\sqrt{t}}{k_H} \sqrt{\frac{\nu}{1-\nu}} \left(\sqrt{1-k_H^2 \sin^2 \psi_1} - \sqrt{1-k_H^2} \right),$$

$$b = 2 \sqrt{\frac{\nu t}{1-\nu}} k_H^2 [A(k_H) - A(\pi/4, k_H)],$$

$$s_0 = \frac{h_u + f}{1-\nu} 2 \sqrt{t k^2} [A(k) - A(\varphi_1, k)] - \frac{2t}{1-\nu} \sin 2\varphi_1.$$

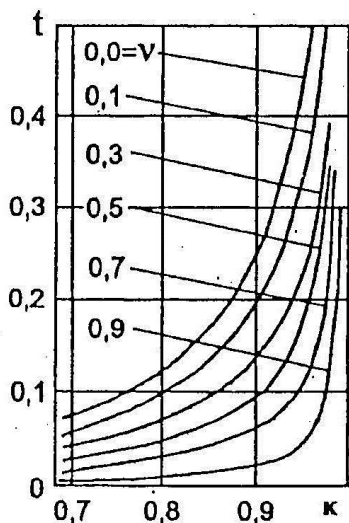


Fig. 5.18. Tension as a function of coefficient of container filling for different ratios of specific weights of internal fluid to those of external fluid

Corresponding plots may be found in literature [7]. For example, nondimensional annular tension t as a function of filling coefficient and ratio of specific weights is presented in Fig. 5.18. Parameter $\nu = 0$ may be thought of as a filling of the container with gas. In this case the tension is a maximum. With increasing specific weight of inner fluid, t decreases. When $\nu = 1$ the shell does not acquire tension.

If the values of container filling coefficient are small ($\kappa < 1/3$), t tends to zero for all ν . In approaching $\kappa = 1$ the tension values rapidly go up.

§ 8. Containers for load lifting

Consider the equilibrium of a soft spherical container submerged in water, filled with air and held by a load. Assume that holding ropes are continuously fastened to the shell and represent a conical surface (Fig. 5.19a). Let φ_0 denote the meridional angle of the ropes fastened to the shell, L_0 be the distance between the lower point of the sphere and the joint point of the ropes.

The container shell is subjected to internal pressure of air and external pressure of fluid. Depending on the value of this pressure difference, the stressed state of different parts of the shell may be of several types. But here we shall consider such system equilibrium in which at every point of the shell only the biaxial tensioned

state is realized. In this case the shape and volume variations of the sphere are small. It allows one to consider only the stressed state of the shell under load, assuming the shell shape to be known. In such a formulation the problem has been considered in [2].

Note that the problem will not change if the container being in air is filled with fluid and is suspended by the same ropes (Fig. 5.19b). The pressure produced by the water column in the

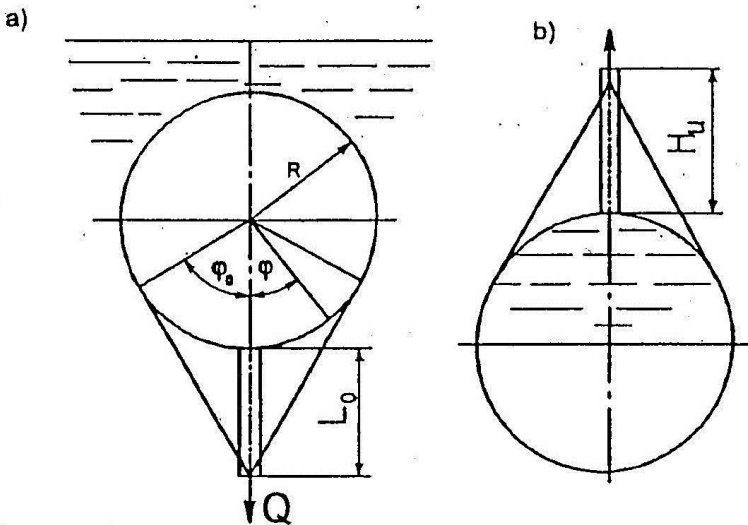


Fig. 5.19. Spherical container for load lifting in fluid (a) and container of fluid (b)

branch pipe corresponds to the constant part of the pressure difference of the problem shown in Fig. 5.19a.

For the case of a spherical membrane shell under axisymmetrical load, the following formulae for meridional and annular tensions may be written

$$T_\varphi = \frac{R}{\sin^2 \varphi} \left(\int p \cos \varphi d\varphi + C \right), \quad T_\theta = pR - T_\varphi. \quad (8.1)$$

Here φ, θ are the angular coordinates of the meridian and parallel, respectively, C is the constant of integration.

If the pressure difference on the shell changes in such a way that it is zero at its lower point and is equal to $2\gamma R$ at the upper one, we may write

$$p = \gamma R(1 - \cos \varphi). \quad (8.2)$$

From (8.1), (8.2) it follows that

$$T_\varphi = \frac{\gamma R^2}{6 \sin^2 \varphi} \left[(2 \cos \varphi - 3) \cos^2 \varphi + 6C \right],$$

where for $\varphi = 0$ the denominator vanishes. For the tension values to be finite, the expression in brackets has to be zero. Therefore $C = 1/6$.

For the zone lower than the line of fastening ropes to shell, formulae (8.1) take the form

$$\begin{aligned} T_\varphi &= \frac{\gamma R^2}{6} \left(1 - \frac{2 \cos^2 \varphi}{1 + \cos \varphi} \right), \\ T_\theta &= \frac{\gamma R^2}{6} \left(5 - 6 \cos \varphi + \frac{2 \cos^2 \varphi}{1 + \cos \varphi} \right) \\ &\quad (0 \leq \varphi \leq \varphi_0). \end{aligned} \quad (8.3)$$

For the upper shell part ($\varphi_0 \leq \varphi \leq \pi$) the constant C is found from the condition that for $\varphi = \pi$ the shell tension must have finite values. This gives $C = 5/6$. Consequently,

$$\begin{aligned} T_\varphi &= \frac{\gamma R^2}{6} \left(5 + \frac{2 \cos^2 \varphi}{1 - \cos \varphi} \right), \\ T_\theta &= \frac{\gamma R^2}{6} \left(1 - 6 \cos \varphi - \frac{2 \cos^2 \varphi}{1 - \cos \varphi} \right) \\ &\quad (\varphi_0 \leq \varphi \leq \pi). \end{aligned} \quad (8.4)$$

In the linear problem the tensions caused in the sphere by the constant pressure difference

$$T_\varphi = T_\theta = T_0 = p_0 R/2 \quad (8.5)$$

are added together with the values (8.3), (8.4).

For the scheme in Fig. 5.19b the constant difference and

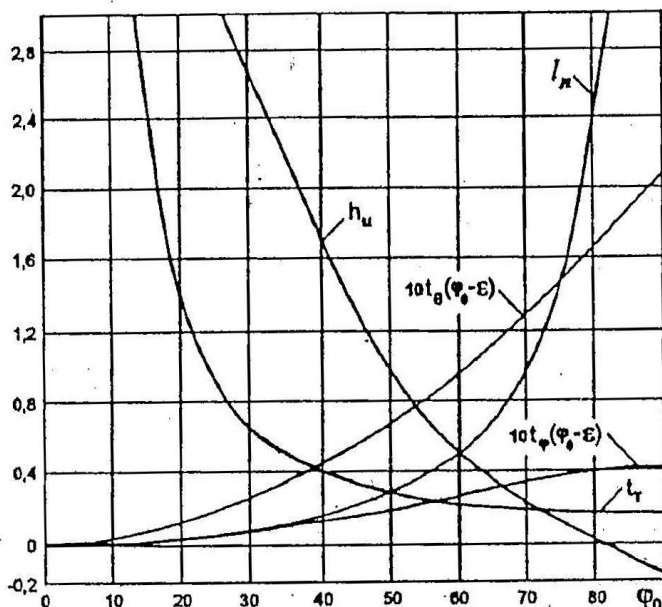


Fig. 5.20. Desired parameters of spherical container for load lifting as functions of rope fastening angle

uniform tension are respectively $p_0 = \gamma H_0$, $T_0 = \gamma H_0 R/2$.

The tension in the ropes per unit length of line of their fastening is

$$T_T = \frac{2\gamma R^2}{3 \sin^2 \varphi_0}$$

If the ropes are directed tangentially to the spherical surface at an angle φ_0 (in this case the rope length is equal to

$(L_0 + R)/\sin \varphi_0$), the tensions are related to each other as follows

$$T_\varphi(\varphi_0 + \varepsilon) = T_\varphi(\varphi_0 - \varepsilon) + T_T,$$

where the small meridional angle ε points out the different sides of parallel with angle φ_0 . Here the maximum tensions in the shell may appear. Their values depend on the angle φ_0 .

Fig. 5.20 shows the nondimensional values of tensions

$$t_\varphi = \frac{T_\varphi}{4\gamma R^2}, \quad t_\theta = \frac{T_\theta}{4\gamma R^2}$$

on the lower side from rope fastening line ($\varphi = \varphi_0 - \varepsilon$).

As is seen, with an increase of fastening angle φ_0 these tensions go up. Nondimensional distance $l_n = L_n/(2R)$ also increases since the ropes are assumed to be fastened to the shell tangentially. Nondimensional values of rope tension $t_T = T_T/(4\gamma R^2)$ and equivalent liquid level in branch pipe $h_n = H_n/(2R)$ decrease with increasing angle φ_0 . These values of h_u are found from the condition that folds do not arise in shell, i.e. $T_\theta(\varphi_0 + \varepsilon) + T_0 = 0$.

For the zero positive pressure at the lower point of the container, the compressive forces in the shell where the ropes are fastened are zero for $\varphi_0 = 81^\circ$. If $\varphi_0 > 81^\circ$ folds will not appear in the shell.

As an example, a container with $\varphi_0 = 60^\circ$ is considered. In this case the shell tensions are not so large and the length L_n is

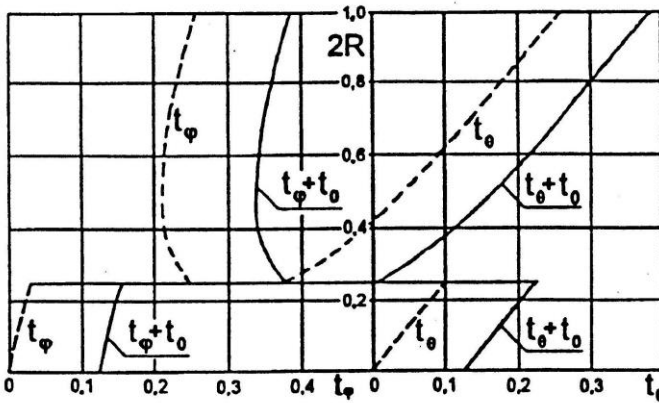


Fig. 5.21. Meridional and annular tensions in an undeformed spherical shell equal to the radius R . To exclude folds, a nondimensional tension greater than $t_0 = T_0 / (4\gamma R^2) = 0.125$ is necessary. Meridional and annular tensions in this case are presented in Fig. 5.21. Solid and dotted curves show total tensions (together with positive pressure) and tensions for $t_0 = 0$, respectively, as functions of height. These plots may be useful for estimating the state of spherical container in its submerged static state.

CHAPTER VI

EQUILIBRIUM OF FILMS CONTACTING A LIQUID IN DISPLACING DEVICES

§1. Plane problem of film equilibrium

A device for liquid displacement out of vessel by means of movement of a separating membrane or film may be such as shown schematically in Fig. 2.5*b* or 2.6*a*. The space above the film is filled with a gas under pressure p_e , which may serve as control parameter. Under the action of this pressure the film displaces liquid from the lower space (where the presence of removal pipe is assumed). The gravitation force may be directed both downward (as the usual gravity force) and upward (or, under common conditions, liquid is in the upper space while gas in the lower one). Correspondingly, the overload factor, used in §4 of Chapter IV, is $n > 0$ and $n < 0$, respectively.

As in previous chapter, we assume the film to be a flexible and nontensile surface. In a plane formulation of the problem it may be considered as a thread. Tensility of the membrane is taken into account only in the last paragraph. And its large deformations are allowed.

As will be seen from the following, there is a lot in common in behavior of the systems under consideration and those examined in Chapter II and V. In presenting the material of this chapter, we shall follow [2–6].

Points of film attachment to the walls are at the same level, the distance between these points being $2L$. The length of the film \tilde{L} is greater than the distance $2L$ so that there are nontensile, folded states. The film does not touch the walls at points different from those of its attachment. This problem was considered for the first time in [6].

The origin of the coordinate system x, z is taken in the middle of the interval $2L$ with the x -axis directed horizontally (through the fastening points) and the z -axis upward. The hydrostatic pressure is $p = p_0 - n\gamma z$, the pressure on the film is $p^* = p_e - p_0 + n\gamma z$.

The equilibrium equation has the form of (1.1) from Chapter V with the right side equal to p^* . Thus

$$T\tilde{k} = p_e - p_0 + n\gamma z, \quad (1.1)$$

where T is the tension constant along the film, and \tilde{k} the curvature expressed by the formula

$$\tilde{k} = \frac{d^2z}{dx^2} \left[1 + \left(\frac{dz}{dx} \right)^2 \right]^{-\frac{3}{2}}.$$

The condition of nontensility for the film

$$\int_{-L}^L \left[1 + \left(\frac{dz}{dx} \right)^2 \right]^{\frac{1}{2}} dx = \tilde{L}, \quad \tilde{L} \geq 2L \quad (1.2)$$

and the condition of incompressibility for the liquid

$$\int_{-L}^L z dx = V \quad (1.3)$$

together with the fastening conditions ($z = 0$ for $x = \pm L$) and with (1.1) are the problem statement.

The constant V is the difference between the volume of liquid layer of unit thickness and the corresponding volume of the vessel with rigid diaphragm $z = 0$. Therefore, V cannot exceed the area of segment with chord $2L$ and arc length \tilde{L} , Hence, it follows that

$$|V| \leq \frac{L^2 (2\beta - \sin 2\beta)}{2 \sin^2 \beta}, \quad (1.4)$$

where the auxiliary parameter β is determined as a root of the equation

$$\frac{\sin \beta}{\beta} = \frac{2L}{\tilde{L}},$$

lying in the first quarter.

Consider the linear problem for a small difference between the film length \tilde{L} and the distance $2L$ between the fastening points

$$\tilde{L} = 2L + \delta, \quad 0 \leq \delta/L \ll 1. \quad (1.5)$$

Then the deflection from the horizontal line will be small. Therefore, $\tilde{k} \approx d^2 z / dx^2$, and the equation (1.1) takes the form

$$\frac{d^2 z}{dx^2} + \alpha^2 z = \frac{p_e - p_0}{T}, \quad \alpha^2 = -\frac{n\gamma}{T}, \quad (1.6)$$

which has several times been used in Chapter II.

Condition (1.2) together with (1.5) give

$$\int_{-L}^L (dz/dx)^2 dx = 2\delta. \quad (1.7)$$

Inequality (1.4) reduces to

$$v \equiv V^2 / (8L^3 \delta) \leq 1/6. \quad (1.8)$$

Now we consider the case when the gravity force is directed upward, along the positive direction of z -axis. Similar problem for initially stretched membrane was examined in Chapter II. The overload factor is $n < 0$. Hence $\alpha^2 > 0$ and solution (1.6) has the form

$$z = A \cos \alpha x + B \sin \alpha x - (p_e - p_0)/(n\gamma). \quad (1.9)$$

In the case of shape symmetrical about z -axis, according to (1.3) and fastening conditions for $x = \pm L$, we obtain from (1.9) that

$$z = \frac{\alpha V (\cos \alpha x - \cos \alpha L)}{2(\sin \alpha L - \alpha L \cos \alpha L)}. \quad (1.10)$$

Relations (1.7), (1.8) and (1.10) give the following equation

$$v = \frac{(\alpha L \cos \alpha L - \sin \alpha L)^2}{(\alpha L)^3 (\alpha L - \sin \alpha L \cos \alpha L)}, \quad (1.11)$$

to determine αL . For given L , V , δ which satisfy condition (1.8) there exists at least one solution to equation (1.11). The number of solutions is finite for any $v > 0$ and grows from one to infinity as v decreases from $1/6$ to zero. After determining αL , the film shape and tension force T are found by (1.10) and (1.6). Thus $T = -n\gamma/\alpha^2$ (as is mentioned above, in this problem $n < 0$).

In a similar way the linear behavior of the system with respect to asymmetric shape deflection is considered [6]. It was found that for $v > \pi^{-2} \approx 0.1$ the asymmetrical solutions do not exist at all, while for $0 < v \leq \pi^{-2}$ there are a finite number of such solutions.

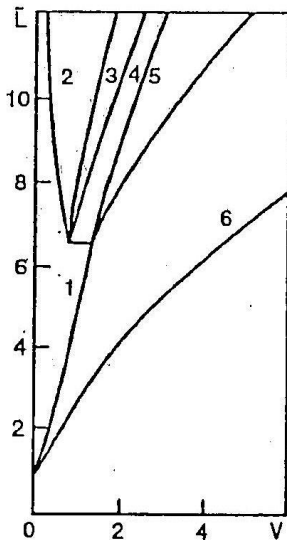


Fig. 6.1. Domains of different shapes of film equilibrium in terms of film length and liquid volume exceeding the volume of vessel with rigid wall $z=0$ (\bar{L} has the dimensions of length, V the dimension of length cubed)

Since for $n < 0$ the equilibrium shapes are not unique their stability has to be considered [5,6]. To this end, the principle of potential energy minimum and sufficient conditions for weak minimum were used. For $n < 0$ and $0.1 \leq v \leq 1/6$ there exists a unique stable shape of film equilibrium. It is determined by equations (1.10) and (1.11). For $0 \leq v \leq 0.1$ there exists a stable asymmetric shape when $\alpha L = \pi$. All other shapes are not stable. Similar consideration for $n > 0$ shows that for $0 \leq v \leq 1/6$ there exists a unique and stable equilibrium shape.

As is known from §3 of Chapter V, the nonlinear behavior of nontensioned membrane shell under action of hydrostatic pressure is found in the form of elliptic integrals of the first $F(\varphi, k)$ and second $E(\varphi, k)$ kind where φ is the amplitude, k the modulus of elliptic integrals. The shape of film equilibrium in problem (1.1)–(1.4) is described in parametric form by the functions

$$x = \sqrt{m} [F(\varphi, k) - 2E(\varphi, k)] + x_0,$$

$$z = d + 2k \sqrt{m} \cos \varphi.$$

Constants k , m , d , x_0 are found from conditions of film fastening, constancy of length \bar{L} and liquid volume V .

In [5,6] the equilibrium is considered in the nonlinear case when the acceleration is directed in the negative direction of z -axis when the liquid is under the film. As in the linear case, for $V = 0$ there exists a countable number of equilibrium shapes for the film and liquid. When $V \neq 0$ the number of such shapes is finite.

It was found [5,6] that there are six types of equilibrium shape. Fig. 6.1 shows various domains corresponding to the type of equilibrium. Given \tilde{L} and V , the shape with least potential energy was chosen.

The fields 1–4 correspond to asymmetric shapes of equilibrium. In the domain 4, the different portions of the curve representing film shape touch each other. This section of touch (or stick) forms the straight line along the vertical. In the area 3 such a section includes the fastening point and shows a bend at this point. In the area 2 the shapes also have a bend while the touch section degenerates into a point coincident with the point of film fastening. The area 1 corresponds to the shapes without sections of touch or bends.

In the areas 5 and 6 symmetrical shapes are realized. They do not have touch sections in the area 6 while in the area 5 the touch takes place in the axis of symmetry.

When the liquid is under the film, nonunique solutions also exist and the shapes of film equilibrium can contain touch sections and a corner point.

§2. Equilibrium of a spherical and semispherical film

Film in an undeformed state is a sphere of radius R and touches the walls of spherical vessel of the same radius. Two points of film attachment to the walls are located at the opposite ends of the vertical diameter (Fig. 6.2). In the deformed state the volume V between the film and vessel walls is filled with incompressible fluid

while inside the film there is a gas under the pressure p_e . Gravity force acts along the vertical. Now we present the results of [3].

Since there is an axial symmetry we can consider only the vertical plane passing through the axis of symmetry. Axes r , z are shown in Fig. 6.2. Position of the film is determined by equation $r = r(z)$.

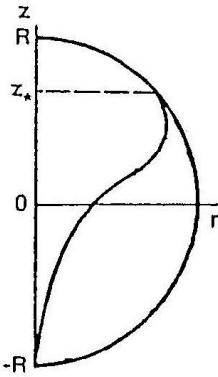


Fig. 6.2. Spherical film in vessel dividing liquid and gas

On the film surface there are folds located in meridional planes along the curves $r = r(z)$. The assumption is used that each fold is infinitely small and that the number of the folds is large.

According to the problem statement, in the area tightly fitting against the spherical wall, both tension components (T_1 and T_2 are forces acting on the unit length of the parallel and meridian, respectively) are taken to be zero. In the one-axial zone where there are folds, $T_2 \equiv 0$, T_1 is found from the solution.

The equilibrium conditions have the form

$$T_1 r \equiv F = \text{const},$$

$$F \frac{d^2 r}{dz^2} + (n\gamma z - p_0 + p_e) \left[1 + \left(\frac{dr}{dz} \right)^2 \right]^{3/2} r = 0. \quad (2.1)$$

For the film sections attaching to the vessel walls we have (instead of equation (2.1))

$$r(z) = (R^2 - z^2)^{1/2}.$$

For these sections the mating conditions are posed. Moreover, there are fastening conditions

$$r(-R) = 0; \quad r(R) = 0 \quad (2.2)$$

and conditions of film nontensility and liquid incompressibility

$$\int_{-R}^R \left[1 + \left(\frac{dr}{dz} \right)^2 \right]^{1/2} dz = \pi R, \quad \pi \int_{-R}^R r^2 dz = \frac{4}{3} \pi R^3 - V, \quad (2.3)$$

where V is the volume between the film and spherical wall of vessel.

It may be shown [3,5] that there exists no more than one section of film attachment to the vessel walls. This section $[z_*, R]$ may be only at the end of the interval $[-R, R]$ (Fig. 6.2). In the presence of attachment section we can use, instead of conditions (2.2), the following

$$r(-R) = 0, \quad r(z_*) = (R^2 - z_*^2)^{1/2}, \quad (2.4)$$

$$\left(\frac{dr}{dz} \right)_{z_*} = -z_* (R^2 - z_*^2)^{-1/2}, \quad z_* > 0.$$

Solution $r(z)$ has to satisfy the inequality

$$r(z) \leq R \sin \frac{s(z)}{R} \quad (-R \leq z \leq z_*), \quad (2.5)$$

where $s(z)$ is the arc length of the curve $r = r(z)$ measured from the point $z = -R$. This inequality expresses the fact that the radius of circumference in horizontal section of the film is less than the radius of circumference generated by the same points of the film in its undeformed state.

The case $F = 0$ corresponds to the non-tensile state of the film. Therefore, the liquid has free horizontal surface $z = z_0$. The film, in this case, consists of three parts: the vertical bundle $r = 0$ for $-R \leq z \leq z_0$, the part floating on the surface $z = z_0$ and the part attaching to the vessel walls, $z_0 \leq z \leq R$. Such a

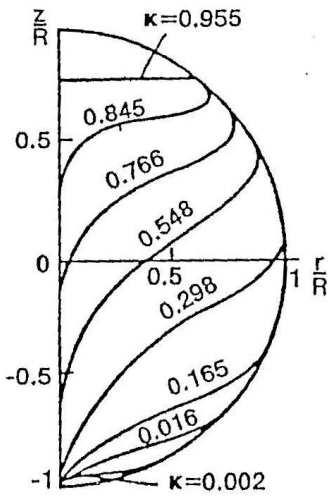


Fig. 6.3. Position of film and liquid in the volume under the film for different values of filling factor (coordinates z and r are referred to the radius of sphere R)

the maximum tension of the film takes place when thirty percent of the vessel volume is filled with liquid.

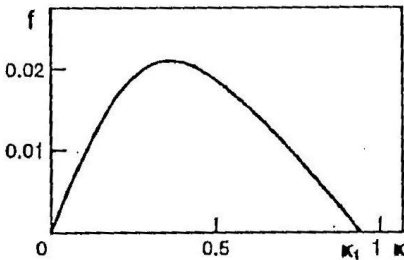


Fig. 6.4. Nondimensional force of tension in one-axial zone (the corresponding shapes are shown in Fig. 6.3 for different κ) as a function of filling factor

solution is realized if the filling factor $\kappa = 3V/(4\pi R^3)$ satisfies the inequality $\kappa \geq \kappa_1 = 0.956$ (about the filling factor see Chapter V). When $\kappa < \kappa_1$ the film is stretched and the value F is greater than zero and is determined in the course of the problem solution.

Problem (2.1)–(2.5) was solved numerically [3]. Fig. 6.3 shows the film shapes corresponding to different values of the filling factor κ .

Fig. 6.4 shows the dependence of nondimensional force of tension $f = F/(n\gamma R^3)$ on the coefficient κ . The function $f(\kappa)$ has its maximum, which is $f \approx 0.022$, at $\kappa \approx 0.3$. Thus

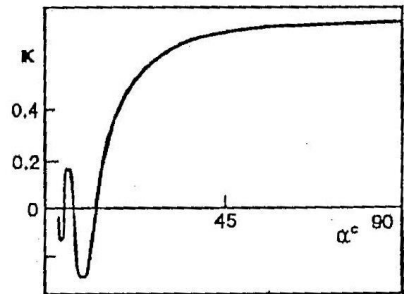


Fig. 6.5. Relation between the filling factor of semispherical film and the angle of spherical segment

ilibrium, are those with maximum value of α° . The maximum tension force arises at the top of spherical segment.

When the liquid is under the film the required surface of equilibrium consists of a two-axial area in the form of spherical belt and of an unstressed area which is a circle in horizontal plane. In this case maximum forces occur on the film contour.

§3. Equilibrium of a cylindrical film

Nontensile film in an undeformed state is a circular cylindrical shell of radius R and height \bar{L} . Its edges are fastened in horizontal planes $z = 0$ and $z = -L$. It is assumed that $L < \bar{L}$. The axis of symmetry z is directed oppositely to the gravity force.

Position of the film is determined by the function $r(z)$. All lengths are referred to the radius R .

Inside the cylindrical film there is a liquid while outside a gas. The film is assumed not to have common point with the axis of cylinder and not to be in touch with vessel walls. In such a statement this problem was considered in [4]. Now our consideration will follow [4,5].

As in the case of semispherical film examined in previous paragraph, the equilibrium shape of cylindrical

film may consist of two-axial and one-axial zones. The former corresponds to the cylindrical shape of equilibrium. In one-axial zone ($T_2 = 0$) the film equilibrium is determined from the solution of a nonlinear problem for an equation like (6.1) using con-

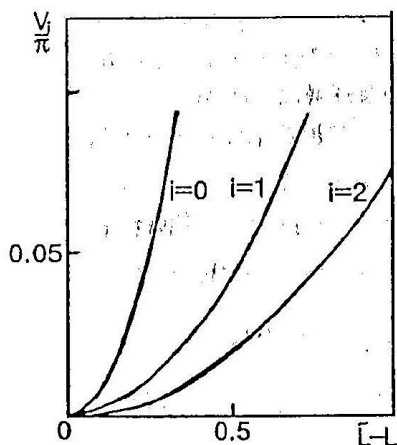


Fig. 6.7. Critical volumes of liquid determining the type of membrane equilibrium

ditions of fastening, smoothness, nontensility of the film, and incompressibility of the liquid.

Four types of film equilibrium have been found numerically. Their realization is determined by parameters \tilde{L} , L and V , where V is the liquid volume.

For each value of \tilde{L} and L there exist five critical liquid volumes which are denoted further by V_0, V_1, V_2, V_3, V_4 . The type of film equilibrium corresponding to these volumes is determined as follows. For $V_3 < V < V_4$ the whole film is in one-axial state. Equilibrium with one one-axial and one two-axial areas corresponds to the case $V_2 < V < V_3$. If $V_1 < V < V_2$ the film has two two-axial and one one-axial areas. When $V_0 < V < V_1$ there are two two-axial and two one-axial areas.

Liquid volumes V_3 and V_4 depend on \tilde{L} and L in a complex way while V_0, V_1, V_2 are determined only by the difference of lengths $\tilde{L} - L$. Fig. 6.7 shows these functions V_i/π ($i = 0, 1, 2$) versus parameter $\tilde{L} - L$.

Fig. 6.8 shows the first three shapes of film equilibrium. Curves 1, 2, 3 correspond to equilibrium shapes of the film when the liquid volume is in intervals (V_1, V_2) , (V_2, V_3) , (V_3, V_4) , respectively. In all variants it was taken that $L = 1.5$, $\tilde{L} = 1.8$.

Equilibrium shapes of the fourth type ($V_0 < V < V_1$) which are not presented here, contain one more one-axial area near the upper edge. When $V = V_0$ generators of two one-axial areas touch each other at one point. For $V < V_0$ the segment of this touch enlarges.

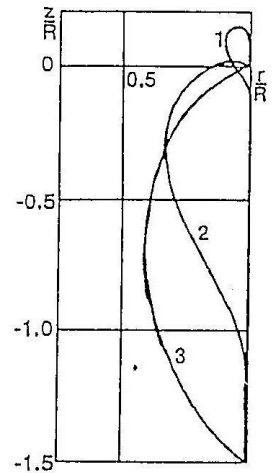


Fig. 6.8. Shapes of membrane equilibrium corresponding to the different volumes of liquid

§4. Finite strains of a membrane

In conclusion of the Chapter we consider deformation of a circular membrane accompanied by significant displacements and shape changes. Material of the membrane is assumed to be incompressible, deformation to be described by elastic potential in the form of Mooney [1]. Tension of the membrane occurs at the expense of changes in its thickness. Significant shape changes of membrane are encountered, for example, in various sensitive elements of hydrosystems, displacing devices, etc.

A circular membrane of ribbon-like material is fastened along the outline of radius R , being subjected to a gas pressure p_e from below, from above by hydrostatic liquid pressure so that the pressure difference (positive direction of z -axis downward) is

$$p_* = p_0 + \gamma z - p_e. \quad (4.1)$$

Further we put the origin of coordinate system z, r into the center of the deformed membrane.

Following [2] the solution of the problem will be presented for the case when the elongation factors λ_r and λ_θ in radial and annular directions, respectively, are expressed in terms of deformations $\varepsilon_r, \varepsilon_\theta$ by linear function

$$\lambda_r = 1 + \varepsilon_r, \quad \lambda_\theta = 1 + \varepsilon_\theta.$$

For an incompressible material $\lambda_n = (\lambda_r \lambda_\theta)^{-1} = h/h_0$ where h_0, h are the thicknesses of membrane in undeformed and deformed states, respectively. Let us take

$$\sigma_r = 8(C_1 + C_2) \left(\varepsilon_r + \frac{1}{2} \varepsilon_\theta \right), \quad \sigma_\theta = 8(C_1 + C_2) \left(\varepsilon_\theta + \frac{1}{2} \varepsilon_r \right).$$

Then the forces in radial and annular directions are expressed as follows $T_r = \sigma_r h, T_\theta = \sigma_\theta h$.

Physical constants of material C_1 and C_2 are related to the elasticity modulus E by the expression $E = 6(C_1 + C_2)$. Let us use the notation Γ for C_2/C_1 and introduce functions ψ and w by the formulae

$$r\sigma_r = -\frac{3}{2}(1 + \Gamma)\psi, \quad z = w + \frac{p_0 - p_e}{\gamma}. \quad (4.2)$$

The equations of membrane equilibrium take the form [2]

$$r \frac{d^2\psi}{dr^2} + \frac{d\psi}{dr} - \frac{1}{r}\psi = 2C_1 \left(\frac{dw}{dr} \right)^2, \quad (4.3)$$

$$\frac{d\psi}{dr} \frac{dw}{dr} + \psi \frac{d^2w}{dr^2} = -\frac{2}{3} \frac{\gamma}{1 + \Gamma} r.$$

In the center of strained membrane

$$w = -(p_0 - p_e)/\gamma, \quad \psi = 0 \quad (r = 0). \quad (4.4)$$

Moreover, it follows from the conditions of axial symmetry that

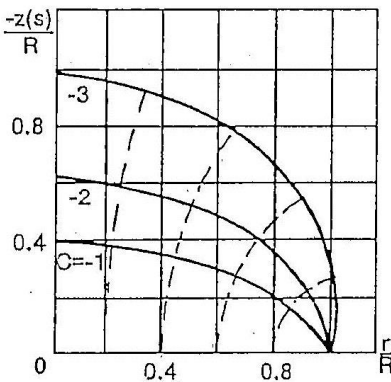


Fig. 6.9. Equilibrium shapes of stretched circular membrane under various differences of pressure in gas and liquid

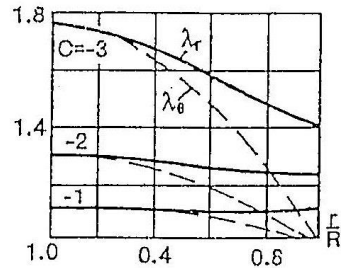


Fig. 6.10. Main elongation factors for different pressure difference of gas and liquid

$d\psi/dr = 0$ ($r = 0$). At the fastened edge $\varepsilon_\theta = 0$ or

$$\frac{d\psi}{dr} - \frac{1}{2r}\psi = 0 \quad (r = R). \quad (4.5)$$

Not going into the details of the solution of (4.3)–(4.5), we note only that, given stress, one can determine the displacement of membrane points and then the value of volume ΔV of liquid displaced. The problem has been solved by an analytical method (r/R power series) as well as by a finite-difference method [2].

Fig. 6.9 shows the meridional sections of strained membrane for different values of load parameters

$$C = (p_0 - p_e)R / (2C_1h_0), \quad D = -\gamma R^2 / (2C_1h_0).$$

In the figure $\Gamma = 0.1$, $D = 1$ were used. Dashed lines correspond to the trajectories of transition of undeformed membrane points into points of deformed surface.

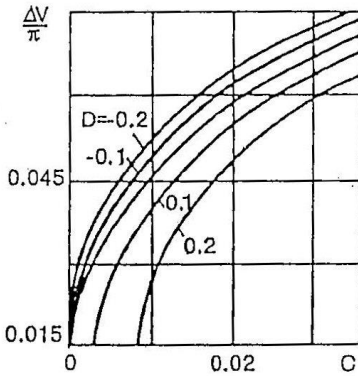


Fig. 6.11. Volume of displaced liquid as a function of determining parameters

Dependences of main elongation factors λ_r , λ_θ on the distance r/R are presented in Fig. 6.10 for some parameters of hydrostatic load. One can see that in the neighborhood of the center of stretched membrane there is an area where the elongation factors λ_r , λ_θ are equal to each other.

Volume of liquid displaced by membrane is defined by the parameter $\Delta V/\pi$. This volume is presented in Fig. 6.11 as a function of the parameter C for different values of intensity of the gravity field. We note that the parameter $\Delta V/\pi$ is equal to $\Delta V' / (\pi R^3)$ where $\Delta V'$ corresponds to a dimensional volume.

CONCLUSION

This book represents an effort to collect some characteristic static problems of hydroelasticity and to describe them from their common foundations. Remarkable is the fact that the mechanical behavior of objects different in their construction and dimensions (sometimes by several orders of magnitude) are often described by closely similar models. To determine the behavior of a cellular membrane (see, for example, the book by E.A.Evans, R.Skalak, Mechanics and Thermodynamics of Biomembranes, RCR Press, Inc., 1980), the same equilibrium equations of a soft shell and medium contained in it are used as for huge aerostatic objects such as dirigibles, balloons and air-supported building constructions.

Not all problems relevant to the subject of this book are covered. First, each of the six chapters may be enlarged. For the most part three-dimensional problems are neglected as well as some nonlinear effects. Secondly, not all classes of static problems of hydroelasticity are touched upon.

An example of the last statement is the problem of interaction which arises when plastic deformations appear in the solid body and during the transition of the liquid from a liquid phase into a rigid one (ice). These phenomena are widely known in nature and engineering. Water freezing in a pipe-line causes large and plastic deformations. The flaring of the cylindrical walls of a vertically standing barrel and a rather significant buckling of its bottom are observed. All this also depends on the water level.

In this and other examples, the number of which is very large, the formulations of the problems of hydroelasticity change. Hydrostatic forces in the fluid may not dominate but rather volume

expansion is significant (the specific volume of water at 4°C is equal to $1\text{ cm}^3/\text{g}$ and of ice at 0°C to $1.09\text{ cm}^3/\text{g}$). With phase transition the conditions on the contact surface change. Conditions of equality for not only the normal components of deflection and forces (as everywhere in the book), but also their tangent components are needed.

An expanded treatment of the subject of hydroelasticity might also include some technological techniques of plastic formation of thin-walled parts using not only fluids, but also granular media. For example, to produce a bent tube for some measuring instruments, first the crystalline salt is pressed in the space of a straight tube. In the course of further bending of the tube on a matrix it ensures the conservation of the circular shape of its cross-section (without such a filler it becomes flat). The mathematical formulation of this problem has to involve the equilibrium equations of granular media. Conditions on the contact surface should take into account the possibility of some mutual slip of the media and the dependence of the slip on the pressure on this surface.

Note that many problems of such a kind have not been formulated yet and their solutions have not been found. They may become a subject of future research.

REFERENCES

INTRODUCTION

1. *Bisplinghoff R.L., Ashley H., Halfman R.L.* Aeroelasticity. Cambridge (Mass.). 1955. 860 p.
2. *Fung Y.C.B.* An Introduction to the Theory of Aeroelasticity. New York: Wiley. 1955. 490 p.
3. *Dowell E.H., Ilgamov M.A.* Studies in Nonlinear Aeroelasticity. New York – Tokyo: Springer Verlag. 1988. 456 p.
4. *Ilgamov M.A.* Introduction to Nonlinear Hydroelasticity. Moscow: Nauka. 1991. 200 p. (in Russian).
5. *Dowell E.N., Crawley E.F., Curtiss H.C., Peters D.A., Scanlan R.H. and Sisto F.* A Modern Course in Aeroelasticity. Third Edition: Kluwer Publishing, The Netherlands. 1995. 699 p.

CHAPTER I

1. *Bernitsas M.M., Kokkinis T.* Buckling of risers in tension due to internal pressure: motionless boundaries. J. Energy Resources Technology. 1983. Vol.105. № 3. P. 277–281.
2. *Bernitsas M.M., Kokkinis T.* Buckling of columns with movable boundaries. J. Structural Mechanics. 1983. Vol.11. № 3. P. 351–370.
3. *Bernitsas M.M., Kokkinis T.* Buckling of columns with nonmovable boundaries. J. Structural Engineering. 1983. Vol.105. P. 2113–2128.
4. *Bernitsas M.M., Kokkinis T.* Global static instability of risers. J. Ship Research. 1984. Vol.28. № 4. P. 261–271.
5. *Bernitsas M.M., Kokkinis T.* Asymptotic behavior of heavy column and riser stability boundaries. J. Applied Mechanics. 1984. Vol.51. № 2. P. 1–6.

6. *Biezeno C.B., Koch J.J.* Note on the buckling of a vertically submerged tube. *Appl. Sci. Res. Sec. A.* 1948. 1(2). P. 131–138.
7. *Bolotin V.V.* Nonconservative Problems Theory of Elastic Stability. London: Pergamon Press. 1963. 340 p.
8. *Feodosyev V.I.* Selected Problems and Questions in Strength of Materials. Moscow: Mir Publishers. 1977. 430 p.
9. *Goodman T.R., Breslin J.S.* Statics and dynamics of anchoring cables in wakes. *J. Hydronautics.* 1976. Vol.10. №4. P. 113–120.
10. *Handelman G.H.* Buckling under locally hydrostatic pressure. *J. Applied Mechanics.* 1946. Vol.13. P. 198–200.
11. *Huang T., Dareing D.W.* Buckling and frequency of long vertical pipes. *J. Engineering Mechanics Division.* 1967. Vol.95. P. 167–181.
12. *Ilgamov M.A.* Oscillations of Elastic Shells Containing Liquid and Gas. Moscow: Nauka, 1969. 182 p. (in Russian)
13. *Ishlinsky A.Ju.* Investigation of stability of elastic systems from the point of view of mathematical theory of elasticity. *Ukrainsky matematichesky jurnal* 1954. V.6. №2. P. 140–146 (in Russian)
14. *Kerr A.D., Tang S.* The effect of lateral hydrostatic pressure on the instability of elastic solids, particularly beams and plates. *J. Applied Mechanics.* 1966. Vol.33. P. 617–622.
15. *Link H.* Über den geraden Druckstab in Flüssigkeit. *Ingenieur-Archiv.* 1962. B.31. S. 149–167.
16. *Lubinski A.* A study of the buckling of rotary drilling strings. *Drilling and Production Practice.* API. New York. 1950. P. 178–214.
17. *Peterson J.P.* Axially loaded column subjected to lateral pressure. *AIAA J.* 1963. Vol.1. №6. P. 1458–1459.
18. *Pflüger A.* Stabilitätsprobleme der Elastostatik. Berlin: Springer-Verlag, 1950. 217 s.
19. *Sugiyama Y., Ashida K.* Buckling of long columns under their own weight. *Trans. Japan Soc. Mech. Eng.* 1978. 21(158). P. 1228–1235.
20. *Svetlitsky V.A.* Mechanics of Pipelines and Hoses. Moscow: Mashinostroenie, 1982. 280 p. (in Russian)
21. *Timoshenko S.P., Gere J.M.* The Theory of Elastic Stability. New York: McCraw-Hill, 1961. 400 p.

22. *Yasinsky F.S.* Selected Proceedings on Beam Stability. Moscow: Fizmatgiz, 1962. 200 p. (in Russian)

CHAPTER II

1. *Dinnik A.N.* Application of Bessel's functions to problems of elasticity theory. Part I. *Izvestia Donskogo Politekhnikeskogo Instituta*. V.II, 1913. 156 p. (in Russian)
2. *Dinnik A.N.* Selected Proceedings, Vol.II. Kiev: Izd. AN Ukrainskoi SSR, 1955. 223 p. (in Russian)
3. *Ilgamov M.A.* On stability of shallow panel under the liquid layer. Proceedings of Seminar on Shell Theory. Kazan, Kaz. fiz.-tekh. inst. 1973. № 3. P. 241–255. (in Russian)
4. *Ilgamov M.A.* Equilibrium of a membrane contacting a liquid. *Mechanics of Solids*. 1997. № 5. P. 134–141.
5. *Lavrentyev M.A., Shabat B.V.* Problems of Hydrodynamics and Their Mathematical Models. Moscow: Nauka. 1973. 280 p. (in Russian)
6. *Kerr A.D.* On plates sealing an incompressible liquid. *Int. J. Mech. Sci.* 1966. Vol.8. P. 295–304.
7. *Kerr A.D., Coffin D.W.* On membrane and plate problems for which the linear theories are not admissible. *J. Appl. Mech.* 1990, Vol.57. № 1. P. 128–133.
8. *Otto F., Trostel R.* Zugbeanspruchte Konstruktionen. Frankfurt-Berlin: Ullstein Fachverlag. 1962. 320 p.
9. *Wang C.Y.* Nonlinear deflection of a thin elastic sheet on a liquid foundation. *Quarterly of Appl. Math.* 1984. Vol.41. P. 433–442.

CHAPTER III

1. *Dinnik A.N.* Selected Proceedings Vol.II. Kiev: Izd. AN Ukrainskoi SSR. 1955. 223 p. (in Russian)
2. *Feodosyev V.I.* Selected Problems and Questions in Strength of Materials. Moscow: Mir Publishers. 1977. 430 p.

3. *Hertz H.* Über das Gleichgewicht Schwimmender Elastischer Platten. Wiedemann's Ann. 1884. Bd22. S. 35–45.
4. *Ilgamov M.A.* Bending and stability of a plate covering a space with liquid. Proceedings of Seminar on Shell Theory. Kazan, Kaz. fiz.-tekh. inst. 1973. № 3. P. 232–240 (in Russian)
5. *Ilgamov M.A., Sakhabutdinov J.M.* On stability of elastic plate between liquids of different density. Selected Problems of Applied Mechanics. Moscow: Nauka, 1974. P. 341–346. (in Russian)
6. *Kerr A.D.* On the instability of circular plates. J. Aerospace Sci. 1962. Vol.29. P. 486–487.
7. *Kerr A.D.* Bending of circular plates sealing an incompressible liquid. J. Appl. Mech. 1965. Vol.32. P. 704–707.
8. *Kerr A.D.* On plates sealing an incompressible liquid. Int. J. Mech. Sci. 1966. Vol.8. P. 295–304.
9. *Korenev B.G.* Some Problems of Theory of Elasticity and Thermoconductivity Solved in Bessel's Functions. Moscow: Fizmagiz, 1960. 459 p. (in Russian)
10. *Rjanitsyn A.R.* Stability of Equilibrium of Elastic Systems. Moscow: Gostekhizdat, 1955. 280 p. (in Russian)

CHAPTER IV

1. *Elgindi M.B.M., Yen D.H.Y., Wang C.Y.* Deformation of a thin-walled cylindrical tube submerged in a liquid. Quarterly J. Mechanics and Applied Mathematics. 1992. Vol.45. P. 250–268.
2. *Ilgamov M.A.* On stability of cylindrical panel loaded by liquid pressure. Proceedings of Seminar on Shell Theory. Kazan, Kaz. fiz.-tekh. inst. 1973. № 3. P. 220–230 (in Russian)
3. *Ilgamov M.A.* On stability of shallow panel under the liquid layer. Proceedings of Seminar on Shell Theory. Kazan, Kaz. fiz.-tekh. inst. 1973. № 3. P. 241–255 (in Russian)
4. *Kornishin M.S., Isanbaeva F.S.* Flexible Plates and Panels. Moscow: Nauka, 1968. 260 p. (in Russian)
5. *Kornishin M.S., Mushtary Kh.M.* Stability of infinitely long shallow

- cylindrical panel under the action of normal uniform pressure. Izvestia Kazanskogo Filiala AN SSSR. 1955. №7. P.36–50 (in Russian)
6. *Mushtary Kh.M.* Nonlinear Shell Theory. Moscow: Nauka, 1990. 223p. (in Russian)
 7. *Van Den Broek J.A.* Elastic Energy Theory. London: John Wiley and Sons. 1950. 298 p.
 8. *Wang C.Y.* Nonlinear deflection of a thin elastic sheet on a liquid foundation. Quarterly J. Applied Mathematics. 1984. Vol.41. P.433–442.
 9. *Wang C.Y.* Load capacities of floating elastic sheets of finite width. Quarterly J. Mechanics and Applied Mathematics. 1985. Vol.38. P.257–266.
 10. *Volmir A.S.* Flexible Plates and Shells. Moscow: Gostekhizdat, 1956. 450p. (in Russian)

CHAPTER V

1. *Alekseev S.A.* Calculation of cushion-like containers. Statics and Dynamics of Flexible Systems. Moscow: Nauka. 1987. P.34–43 (in Russian)
2. *Druzz I.B., Druzz B.I.* Load lifting by emerging spherical soft container. Symposium "Design and Exploitation of Constructions out of Soft Shells". Vladivostok. 1990. P.53–64 (in Russian)
3. *Golod B.I., Koshevoy A.A.* Elastic Containers for Transportation and Storing Liquid Loads. Leningrad: Sudpromgiz. 1963. 91 p. (in Russian)
4. *Ermolov V.V. etc.* Pneumatic Constructions of Airsupporting Type. Moscow: Stroyizdat. 1973. 288 p. (in Russian)
5. *Khubernyan K.M.* Rational Shapes of Pipelines, Containers and Pressure Spans. Moscow: Gosstroyizdat. 1956. 254p. (in Russian)
6. *Knoring S.D., Pavlinova E.A., Filippov V.V.* Floating Elastic Containers for Petroleum Transportation. Leningrad: Sudostroenie. 1965. 224p. (in Russian)

7. *Magula V.E.* Ship's Elastic Constructions. Leningrad: Sudostroenie. 1978. 263 p. (in Russian)
8. *Magula V.E., Druzz. B.I., Kulagin V.D.* Ship's Soft Containers. Leningrad: Sudostroenie, 1966. 287 p. (in Russian)
9. *Otto F., Trostel R.* Zugbeanspruchte Konstruktionen. Frankfurt-Berlin: Ullstein Fachverlag. 1962. 320 p.
10. *Usyukin V.I.* On equations of theory of large deformations of soft shells. Izvestia AN SSSR. MTT. 1976. №1. P. 70-75 (in Russian)

CHAPTER VI

1. *Green A.E., Zerna W.* Theoretical Elasticity. Oxford: Clarendon Press. 1954. 457 p.
2. *Lukovsky I.A., Trotsenko V.A., Usyukin V.I.* Interaction of Thin-walled Elastic Elements with Liquid in Moving Spaces. Kiev: Naukova dumka, 1989. 240 p. (in Russian)
3. *Kuzmina R.P.* Axisymmetric problem of equilibrium of a hemispherical film under hydrostatic pressure. Izvestia AN SSSR. MTT. 1972. №1. P. 125-130 (in Russian)
4. *Kuzmina R.P.* Axisymmetric problem of equilibrium of a cylindrical film under hydrostatic pressure. Izvestia AN SSSR. MTT. 1972. №4. P. 183-188 (in Russian)
5. *Kuzmina R.P., Petrov V.M., Chernousko F.L.* Problems of mechanics of flexible films containing liquid masses. Advances of Mechanics of Deformable Media. Moscow: Nauka, 1975. P. 324-339 (in Russian)
6. *Petrov V.M., Chernousko F.L.* Equilibrium of a fluid bounded by a flexible film. Izvestia AN SSSR. MTT. 1971. №4. P. 131-142 (in Russian)

The layout of the book was prepared for printing
in the Institute of Mechanics KSC RAS
Computer design by *E. T. Smirnova*
Editor *Mirtova D. A.*

Publishing Company «Fiziko-matematicheskaja literatura»
Akademizdatcentre «Nauka» RAS,
117071, Moscow, Leninsky prospect, 15.

Printed from the layout in Printing House
Ufinsky polygrafkombinat,
450001, Ufa, prospect Oktyabrya, 2.

Оригинал-макет подготовлен к печати в Институте механики
и машиностроения КИЦ РАН
Редактор *Миртова Д. А.*

ЛР № 020297 от 23.06.97. Подписано к печати 27.01.97. Формат 60 × 90^{1/16}.
Бумага офсетная № 1. Усл. печ. л. 13,5. Уч.-изд. л. 12,73. Тираж 400 экз.
Тип. заказ № 1018.

Издательская фирма «Физико-математическая литература»
Академиздатцентра «Наука» РАН,
117071, Москва, Ленинский проспект, 15.

Отпечатано с оригинал-макета в Уфимском полиграфкомбинате.
450001 г. Уфа, проспект Октября, 2.